Traffic signal optimisation in disrupted networks

By

DANA HANI ABUDAYYEH

Department of Civil and Natural Resources Engineering
UNIVERSITY OF CANTERBURY, CHRISTCHURCH, NEW ZEALAND

A dissertation submitted to the University of Canterbury
in accordance with the requirements of the degree of
DOCTOR OF PHILOSOPHY in the Faculty of Engineering.

SEPTEMBER, 2019

Abstract

Transport has a critical role in economic development; an efficient transport system can enable economic growth and enhance social well-being. Road networks, as a part of a transport system, are among the most important lifeline systems. Urban road networks experience serious congestion because of infrequent major disruptions. Due to these disruptions the traffic system performance is reduced and the travel time and emissions in a road network are increased. This thesis describes a method for optimising traffic signal settings (i.e. green times and offsets) to assist drivers to avoid partial or complete blockages, to minimise the travel time or carbon dioxide emissions in the case of disruptions in road networks. This involves different capacity degradations (i.e. 25%, 50%, 75%, and 100%) with various durations (4 minutes, 20 minutes, 36 minutes, and 60 minutes). The Cross-Entropy optimisation method is applied, along with a static then a semi-dynamic approach, to optimise traffic signal control in disrupted road networks. This includes investigating two objective functions: minimising the travel time or minimising carbon dioxide emissions. The results for minimising the travel time, on the Cambridge (UK) network, show that applying the proposed method reduces the travel time by almost 6% in the case of a complete capacity reduction at the most congested node in that network, compared to not applying this approach. In terms of minimising carbon dioxide emissions, applying the proposed approach can result in almost an 8% reduction in the carbon dioxide emissions, in the case of a complete capacity reduction compared to not applying the proposed approach. An implication of these findings is that signal optimisation could be used as a means of reducing the travel time and CO_2 emissions in disrupted networks. This thesis comprises two main parts divided into seven chapters. Part one provides an introduction chapter and literature review of the resilience of urban road networks, modelling disrupted road networks, traffic signals optimisation, and emissions modelling. Part two presents the formulation of the problem and solution methods, to optimise traffic signal control in disrupted road network.

ACKNOWLEDGEMENTS

I am thankful to **Professor Alan Nicholson**, my primary supervisor, for all his support throughout my journey in New Zealand. Prof Alan is an example not only of how a scientific researcher could be, but also an example of commitment and integrity. Thank you, Prof Alan, for your encouragement, knowledge and motivation all of which have helped me to accomplish this thesis. Thank you for caring about my work, and responding to my emails so promptly. Thank you for helping me to broaden my horizon and think beyond the limits.

I also would like to thank those wonderful people:

- **Dr Dong Ngoduy**, my co-supervisor, for his technical support and insightful comments. Dr Dong has always a worthy comment to consider.
- **Dr Diana Kusumastuti**, my associate supervisor, for her support and encouragement; her amazing character and kindness helped me to survive in difficult times during my PhD studies.
- **Dr Glen Koorey** from Viastrada, **Tim Wright** from QTP, **Dr Dirck van Vliet** from the University of Leeds, **Dr Rua Murray** from the Mathematics and Statistics Department at UC, **Dr Matthew Hughes** from the Civil Engineering Department at UC, and **Dr Angela Curl** from Geography Department at UC for their technical support.
- **Olive Dalton**, **Joost Stenfert Kroese**, **Anthony FitzPatrick**, **Francois Rene Pierre Bissey**, and **Khalid Salah** for their computer support. Without this support my complicated simulation would not have finished.
- **Dr Jan-Dirk Schmoecker** for his support during my visit to Kyoto University.
- **Lisa Carter** for all the support and wise wording I received when I needed to hear them most. I am still practising her exercise: “Remind yourself of three positive things in the morning.”
- **Dr Ricardo Bello Mendoza**, **Prof Mark Davidson**, **Elizabeth Ackermann**, **Dr Mofreh Saleh**, and **Leigh Davidson**, from the Civil Department at UC for their support to get through a critical stage in my research!

- **Dr Mehdi Keyvan-Ekbatani** for his input at some stages of this research.
- **Professor Khair Jadaan** for supporting me in so many ways to pursue my PhD studies. Prof Khair has been a great influence on my personal character and career, which I deeply appreciate.
- **Rana Obaid** for making my stay in Christchurch comfortable with her support, from the very first moment when she picked me up from the airport until her last day in Christchurch. Rana made my days blossom even in my worst times!
- **Walter Raymond** and **Dr Kim Parent** for patiently proofreading the thesis.
- All my colleagues in the Civil Engineering Department for their kindness, short talks, as well as their souvenirs. It always brings a smile on my face to see chocolate on my desk.

Also, I would like to acknowledge Engineering NZ Transportation Group for partially funding this research through the 2018 Tertiary Study Grant.

Last but not least, I would like to thank my beloved mum, who has supported me with all the strength in her at each stage of my life, and my lovely dad for sharing his wisdom just at the right time, his words always help me to pick myself up. My parents have taught me a lesson in dignity and hard work. A thank you also goes to my sisters who never feel bored with my complaints; my younger sister always cares, always understands; my older sister texts me every single day to make sure that I am okay! A thank you also goes to my brothers for their warm gestures: it always makes me smile to see their thoughtful gifts in my mail. I should admit that without their endless love, blessings, and support throughout the years, I would not be able to make this dream a reality!

I could not have done this without you all! Thank you for helping me to add something to make our society perform better and to be more resilient!

DEDICATION

To my beloved mum and dad who taught me how to colour the world with kindness!

To HaNdeel!

TABLE OF CONTENTS

List of Tables

List of Figures

Figure **Page**

Part I

Introduction and Literature Reviews

CHAPTER 1

INTRODUCTION

1.1 Background and context

To ensure operational continuity of urban road networks, the resilience of a transportation system has become an important issue. Over the last two decades, there has been extensive discussion about the need for robust networks to minimise the economic and social impacts of disruptions. Detailed reviews of the literature related to degraded networks have been conducted, e.g. Berdica (2002*a*) and Mattsson and Jenelius (2015).

Koorey et al. (2015) explored the scope for dynamic traffic signal control to reduce the impact of disruptions associated with non-recurrent congestion (e.g. traffic incidents). It has been suggested that reducing the causes of non-recurrent congestion will have a great effect on network reliability, as about half the congestion delay is caused by non-recurring events (Pearce, 2000; Schrank et al., 2009).

Several studies of infrastructure resilience have proposed a disruption profile to capture the phases of any significant disruption before, during, and after the disruption. For example, Asbjornslett (1999) proposed three phases, namely, a stable situation before a disruptive event, disruption time, and a new stable situation after the disruption time has passed (Fig. 1.1). The new stable situation may be better or worse than the one before the disruption. Sheffi (2005) identified five typical phases of the disruption profile (Fig. 1.2): the preparation phase, the disruptive event, the first response, the recovery preparation, and the recovery. Both authors indicated that the severity of a disruptive event dictates the initial network performance reduction and the recovery time.

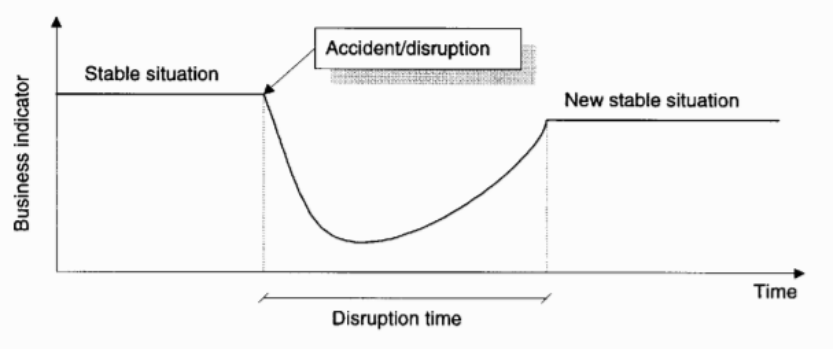

Figure 1.1: Regaining stability after an incident/disruption (Asbjornslett, 1999)

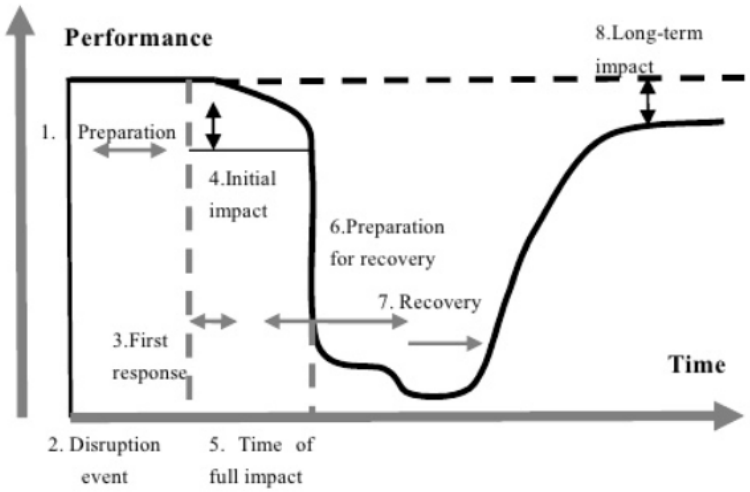

Figure 1.2: Sheffi's disruption profile (Sheffi, 2005)

Additionally, Bruneau et al. (2003) have proposed a resilience triangle (Fig. 1.3), where t_0 denotes the event starting time, and t_1 denotes the time when the recovery is completed (the new stable condition), suggesting that the smaller the area of the triangle the greater the resilience. More recently, Taylor (2017) presented another representation to reflect the dynamic performance of an infrastructure system (Fig. 1.4). This distinguishes between frequent minor variations in performance and infrequent major disruptions.

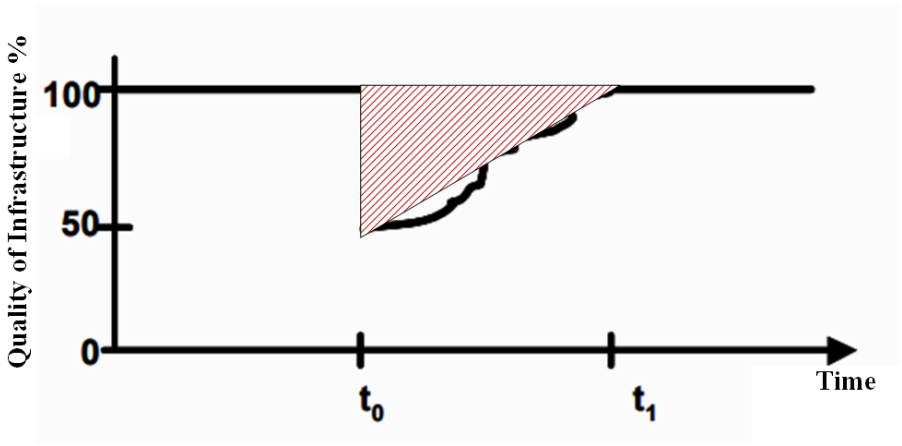

Figure 1.3: The concept of the resilience triangle (Bruneau et al., 2003)

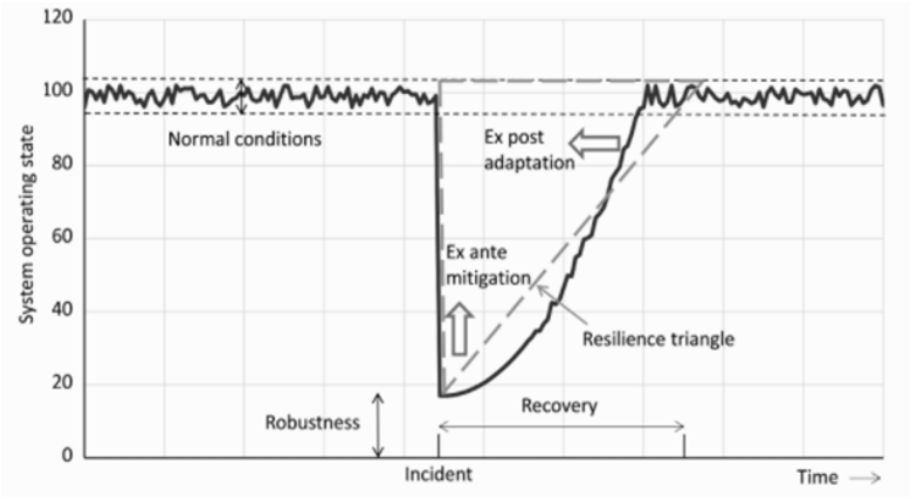

Figure 1.4: The resilience triangle in traffic (Taylor, 2017)

This research seeks to improve the resilience by reducing the area of the resilience triangle by reducing its height (i.e. reducing the reduction in system performance when the incident occurs), and/or its base (i.e. the recovery time). There are various options to achieve this, including constructing or improving parallel routes between given pairs of nodes. Another option is to use traffic signal control, and the aim of this study is to reduce the impact of a disruptive event using traffic signal control.

Traffic signal control can be used to influence drivers' decision in choosing routes to avoid partial or complete blockages and to use other routes to minimise delays. Various optimisation algorithms have been implemented to find the optimal set of signal timings,

taking into account the impact of re-routing. These include Hill Climbing (Cantarella et al., 2006), the Genetic Algorithm (Ceylan and Bell, 2004; Teklu et al., 2007), and the Cross-Entropy method (Ngoduy and Maher, 2011), among others.

The Cross-Entropy (CE) method has proved more efficient, compared to the Genetic Algorithm (GA) as reported by Ngoduy and Maher (2011) who applied the CE method on Cambridge network (the UK). In their paper, they concluded that the CE method performs better than the GA method in terms of computational time and producing near global optimum solution. Maher (2008) introduced the CE algorithm to optimise the signal settings on a six-arm signalised roundabout. Ngoduy and Maher (2011) and Maher et al. (2013) further explored the CE method to optimise traffic signals in urban networks. The results of applying the CE method showed encouraging advantages for computational efficiency and convergence, with its more formal mathematical and statistical basis, and making it simpler to apply (Maher, 2008), as was also found by Zhong et al. (2016), who used the CE method to calibrate microscopic traffic models.

While some research has been devoted to studying traffic signal optimisation, optimising traffic signal control to improve road network resilience has received little attention. This research adopts and extends a bi-level optimisation approach to minimise the impact of disruption (i.e. to minimise the travel time in a network by optimising the signal settings (i.e. the green times and offsets), in order to influence drivers re-routing around a partial or complete blockage of various severities and durations.

It is important to note that one can argue (Elmqvist et al., 2019) that improving the resilience of a system (i.e. a road network), could decrease the environmental sustainability in this system. For instance, providing more alternative routes in a road network, could result in improving the resilience (i.e. decrease the impact of disruption), but decreasing the environmental sustainability (i.e. more emissions). To this end, in this thesis, traffic signal optimisation will be used as a means to minimise the travel time in disrupted networks (to improve the resilience), and then to minimise carbon dioxide emissions (to improve the environmental sustainability). In addition, the interaction of minimising the travel time and minimising carbon dioxide emissions will be evaluated.

1.2 Knowledge gaps and problem statement

The introductory section highlights the need for a robust and practical management tool to be used to facilitate traffic diversion away from blocked intersections and to minimise the impact of the blockage without increasing carbon dioxide emissions. This means there is a need to review what has been done in the following areas: robustness and resilience of road networks, modelling disrupted networks, including the assignment and simulation models, traffic signal optimisation, and modelling carbon dioxide emissions. This leads to a broad range of literature review that is detailed in Chapter 2. However, a summary of key gaps based on the detailed literature review is provided below.

The review of the literature on optimising traffic signal control has revealed that a wide range of signal optimisation algorithms have been implemented to optimise traffic signals in 'normal" conditions (i.e. without network disruption). However, optimising traffic signals to improve the resiliency of road networks has received little attention, if any. Therefore, this thesis investigates the use of traffic signal control to improve the resiliency of road networks.

The reviewed literature has revealed that a number of indices and methods have been proposed to improve road networks resiliency. These methods focused on complete link capacity reductions or partial link capacity reductions. Little literature has focused on varying the level of capacity reductions along with varying the reduction durations, thus, to have a better understanding of the impact of the level of disruption and the duration of the disruption, this study considers different capacity degradations (i.e. 25%, 50%, 75%, and 100%) along with varying durations (4 minutes, 20 minutes, 36 minutes, and 60 minutes).

In terms of the simulation and assignment methods, the semi-dynamic assignment approach is considered a reasonable midpoint between the static and dynamic assignment models, as it combines the computational efficiency of static assignment models and much of the realism of traffic flow in dynamic assignment models. However, little has been done to investigate the semi-dynamic approach in simulating disrupted road networks. It therefore seems reasonable to investigate the semi-dynamic approach to simulate disrupted networks (as proposed in this thesis) since this approach approximates the dynamic assignment with less computational effort.

In terms of emissions modelling, road traffic is a significant source of emissions and CO_2 emissions are one of the largest contributors to global warming. For instance, CO_2 emissions contribute 81% of the UK total of GHG (DBEIS, 2018) and around 80% of the

EU total of the greenhouse emissions (Eurostat, 2018). Thus, in this thesis minimising CO_2 emissions in disrupted road networks is investigated to improve environmental sustainability.

Based on these gaps, the research method and objectives are determined as detailed in the next section.

1.3 Motivation and objectives

The primary objective of this thesis is to use traffic signals to assist drivers diverting around partial or complete blockages, to improve the resilience and reduce carbon dioxide emissions of disrupted road networks. This includes minimising the travel time and mitigating carbon dioxide emissions. To achieve this objective, four tasks are carried out:

- to evaluate the application of the Cross-Entropy method and the static assignment (CEM-static) bi-level framework, to optimise traffic signal control in disrupted networks as described in Chapter 4.

  This research applies a bi-level framework; the lower level estimates the travel time in a disrupted network for the combinations of signal settings specified by the upper level.

- to evaluate the application of the Cross-Entropy and the semi-dynamic assignment (CEM-semi) bi-level framework, to optimise traffic signal control in disrupted networks, as described in Chapter 5.

  The bi-level framework is applied again, but using the semi-dynamic approach instead of the static assignment approach. In this task, the semi-dynamic approach is used to estimate the travel time in disrupted networks for the combinations of signal settings specified by the CE algorithm. This task also includes a comparison between the static and semi-dynamic approaches to evaluate which approach gives better results in terms of minimising the travel time and convergence of the signal settings (i.e. green times and offsets).

- to evaluate the minimisation of carbon dioxide emissions in disrupted networks, applying the CEM-semi bi-level framework, as described in Chapter 6.

  Based on the comparison that is carried out between the static and semi-dynamic approaches, the CEM-semi approach is applied again, but with minimising the carbon dioxide emissions instead of travel time in disrupted networks.

- to evaluate the interaction between minimising the travel time and carbon dioxide emissions in disrupted networks, applying the CEM-semi bi-level framework described in Chapter 6. This includes comparing the results of travel time and carbon dioxide emissions when minimising the travel time and then when minimising the carbon dioxide emissions.

  It is worth noting that each task is published or accepted for publication as listed in Appendix F.

This thesis has impacts at the theoretical, strategic, and operation levels as summarised below:

- the theoretical level: connecting different methods (i.e. heuristic optimisation and simulation based techniques) to estimate the impacts of blockages with different levels of disruption severity and duration on urban road networks.
- strategic level: suggesting a policy to improve the robustness and resilience of urban road networks, without decreasing the environmental sustainability.
- operation level: suggesting a tool to facilitate traffic diversion using traffic signal control to minimise the total travel time and/or carbon dioxide emissions in disrupted networks. This also means minimising the time cost of travel and air pollution.

1.4 Scope and Limitations

Simulating road networks is a complex task. This research has involved some simplifications. The limitations of this study are addressed below:

- the driver will divert around partial or complete blockages based on the set of signal settings (i.e. green times and offsets); however, roadside guidance (i.e. Variable Message Signs) has not been taken into consideration.
- the signal settings in terms of green times and offsets are optimised; however, the cycle time is assumed to be fixed and not included in the optimisation framework.
- capacity reduction and incident duration are the two main factors that this study focused on. The effect of other factors (e.g. weather conditions) are not investigated.

- the Cambridge network was coded, calibrated, and validated by Atkins (a British engineering company based in London, the UK); however, the process of calibration and validation could not be documented in this thesis as these reports are confidential documents and unavailable to public. Calibration involves ensuring that the model results match observed data (flows, delays, etc.). Such data are available only for the non-disrupted situation. Validation of the model; however, involves ensuring that the model accurately predicts the flows, delays, etc. during disruption. Flows, delays, etc. have not been observed for the disruption scenarios, and creating a disruption to observe flows, delays, etc. during the disruption, so the model can be validated, is very unlikely to be permitted. Hence, validation of the model (as a predictor of what will happen to flows, delays, etc. during a disruption) is not practical. Therefore, the Cambridge network which is used in this thesis is a generic test of an algorithm rather than reflecting absolute reality on the ground.

- the research focuses on non-recurring short-term degradations (i.e. less than one hour); however the approach presented in this study, can be extended to cover long-term events.

- this research does not consider the potential for multiple disruptions. The presence of multiple disruptions could increase the running time and there might be some difficulty in finding the optimal set of offsets.

- it is worth noting that in this research the OD matrix is assumed to be fixed. This assumption is realistic when modelling a dense network where there are a number of alternative routes and the trip durations are short. However, in case of a sparse network, this assumption is not realistic and elastic demand (i.e. an indication of how much demand changes) can be implemented to give a more realistic estimate of the number of trips.

- the results of this research are based on the topology of the Cambridge network (i.e. the arrangement of the nodes and links). Other different network topologies could be considered.

- the emissions part of this research focuses on carbon dioxide emissions. It is noteworthy that while estimates of the other emissions (e.g. nitrogen oxides) are very low, they are still significantly harmful to health and the environment. The model could be extended to include carbon monoxide, nitrogen oxides, lead compounds, and hydrocarbons.

- in this study, the emission model embedded in SATURN is used to calculate carbon dioxide emissions, for the reason that the semi-dynamic assignment embedded in SATURN package is used in this study. However, it is important to note that 1. the SATURN trip assignment model output is based on a standard trip-assignment model algorithm that minimises travel times and does not consider emissions as part of the assignment; 2. the parameters which are used in SATURN emissions model were determined based on Matzoros and van Vliet (1992); another study could be done to improve these parameters. It is worth noting that changing the parameters of the SATURN emissions model could affect the estimates of emissions in this study.
- this research considers minimising the travel time or CO_2 emissions as an objective functions. To minimise the travel time and CO_2 emissions, a multi-objective framework is needed. More details are given in Section 7.3.

1.5 Thesis outline

This thesis comprises 7 chapters. Chapter 2 reviews the literature related to resilience of road networks, traffic signal optimisation, along with modelling carbon dioxide emissions in disrupted road networks. The aim of this detailed literature review is to define the gaps and to determine the research objectives and methods. Chapter 3 presents the formulation of the problem and solution methods, the simulation-based scenarios and assumptions to apply the proposed approach, along with a description of the test network. Chapter 4 then presents the results of applying the Cross-Entropy optimisation method, along with static approach in a bi-level framework to minimise the travel time in disrupted road networks. Chapter 5 explains the results of applying the Cross-Entropy optimisation method, along with the semi-dynamic approach in a bi-level approach. After that, compares the results of the static approach to the semi-dynamic approach. Chapter 6 presents results of applying the Cross-Entropy optimisation method, along with semi-dynamic approach to minimise carbon dioxide emissions and evaluates the interaction between minimising the travel time and CO_2 emissions. Each chapter discusses the main findings and concludes with a short summary. Chapter 7 concludes the thesis and discusses future directions.

CHAPTER 2

LITERATURE REVIEW

2.1 The resilience of urban road networks

The need for a robust network and durable infrastructure in order to decrease the socioeconomic impact of disruptions is frequently discussed in the literature. Various terms have been proposed to describe network reliability within different contexts. For example, the term "resilience" has been applied to the following: 1. the ability of materials to accommodate shock and return them to their previous form; 2. the ability of ecosystems to tolerate extreme climatic conditions; 3. the ability of adults and children to cope with traumatic conditions. The focus of this section is on defining the terms related to network reliability (i.e. vulnerability, reliability, robustness, risk, and resilience, among other terms) in the road transportation system. The works most similar to what is discussed in this section are the review papers by Berdica (2002*a*), Mattsson and Jenelius (2015), and Calvert and Snelder (2018), among others.

2.1.1 Reliability, resilience, and robustness of urban road networks

The literature of road networks reliability embraces a broad range of studies that focus on improving the performance of road networks subjected to disruptive events. It has been more than six decades since the concept of travel time reliability (i.e. the probability that traffic can reach a given destination within a specified time period) was introduced. For example, see the early work of Turner and Wardrop (1951), Herman and Lam (1974), and Richardson and Taylor (1978), among others. The increasing awareness of the importance of reliable road networks has led to increased efforts to define and model disrupted road networks to reduce the impact of disruptions on those networks. Starting in the 1990s, Nicholson and Du (1994) proposed the concept of a "degradable transportation system". This concept assumed that "transportation systems are subject to degradation as a result of a wide variety of events (e.g. earthquakes, floods, traffic accidents, adverse weather, industrial action, and inadequate maintenance) for a period of time varying from a few hours to a few years". During the 1990s, travel time reliability and road network connectivity (i.e. to find a path between an origin and a destination) were the main two dimensions which discussed in the literature. See, for example, Bell and Iida (1997). During the 2000s, definitions of five common terms were intensively discussed in the literature to describe degradable transportation systems, namely, vulnerability, reliability, robustness, risk, and resilience, as discussed later in this section. In addition, a number of measures and models have been introduced and tested on real networks to quantify the impact of disruptive events. For example, see Bell and Iida (2003). During the 2010s, the applications of Intelligent Transportation Systems (ITS) were introduced to model and simulate degraded road networks in order to improve the resilience of road networks, see, for example, Ganin et al. (2019).

It is important to distinguish between the terms used to describe a degraded road network: vulnerability, reliability, robustness, risk, and resilience. Then the discussion proceeds with reviewing the resilience measures of degraded road networks.

- **Vulnerability**

  The concept of vulnerability was defined by Berdica (2002*a*) as, " the susceptibility to incidents that can result in considerable reductions in road network serviceability". This concept is related to the function of the system rather than the physical network. In this sense, the vulnerability depends on: 1. the accessibility: the ease of reaching (Jones, 1981); 2. the mobility: the ability to move by private or public

means; 3. the demand. D'este et al. (2003) defined vulnerability by relating it to the network topology and network operating conditions as also discussed in Taylor (2017). Thus, it is argued (Faturechi and Miller-Hooks, 2014) that the concept of vulnerability can be considered vague.

- **Reliability**

  Berdica (2002*a*) defined reliability as, "the possibility of successfully travelling from one place to another". Wakabayashi and Iida (1992) defined it as "the probability of a system performing within a satisfactory level of service under a disruption event".

- **Robustness**

  Robustness is defined by Bruneau et al. (2003) as "the strength of a system and its elements to withstand a disruption". This definition has been widely used in transportation systems, and is consistent with Snelder et al. (2012): "a network is able to maintain the function for which it was originally designed". In this sense, robustness is a measure of strength rather than loss. Berdica (2002*a*) connects the robustness to vulnerability, as "less vulnerable systems can be regarded as more robust". This means that vulnerability is the complement of robustness (Berdica, 2002*a*). On the other hand, Faturechi and Miller-Hooks (2014) distinguished between robustness and reliability as "reliability considers probability of meeting a given level-of-service; whereas, robustness assesses remaining functionality for a given event". Based on this definition, robustness is not a synonymous with reliability.

- **Risk**

  Berdica (2002*a*) defined risk as "a composite of the probability for an incident to occur and the resulting consequences". Nicholson and Dalziell (2003) introduced the use of risk analysis for assessing the reliability of transportation road networks.

- **Resilience**

  Bruneau et al. (2003) defined the term resilience as, "a system's ability to resist and absorb the impact of disruptions". This means that resilience concept focuses on describing the reduction in system performance and recovery after a disruptive event. Fig. 1.3 in Chapter 1 suggests that this concept is based on the robustness (the physical characteristics of the road network dimension) and recovery (the time

dimension). This suggests that the term resilience includes the robustness and recovery. In this thesis, the term 'resilience' will be used; however, the definition of this term will be "a system's ability to accommodate the impact of disruptions".

2.1.2 Road network reliability indices and measures

It has been said, "what gets measured gets managed " (Gill and Zuccollo, 2012). A number of indices were proposed to measure the reliability of road networks. Some literature focused on developing indices to measure network reliability. For instance, Rashidy and Hassan (2014) developed a composite resilience index for road transport networks. This index employs a number of characteristics, namely, redundancy, vulnerability, and mobility, which measures resilience at junctions, links and origin-destination levels. Moreover, Liao et al. (2018) proposed a resilience index to improve the resilience of transport networks subjected to long-term disasters (e.g. floods and man-made disasters). This index includes three system performance measures: coping capacity (i.e. the probability of completing a trip between an origin and a destination), robustness, and flexibility (i.e. a system's response to disruptions). Mattsson and Jenelius (2015) proposed what is called the importance index. This index is based upon the increases in travel cost as a result of disruptions, so one needs to estimate those travel cost increases to get the importance index for the link. Snelder and Calvert (2016) presented the Link Performance Index for Resilience, which evaluates the resilience level of individual road sections in relation to a wider road network. Recently, the literature focuses on how the topological and geometrical characteristics affect performance and robustness of road networks. For instance, Calvert and Snelder (2018) investigated the effects of topological and geometrical roadway designs (e.g. hard shoulders, the number of lanes, parallel structures, and weaving sections) on the robustness of road networks. They found that there is a need to consider the use of a hard shoulder as a spare capacity in the case of disruption. The work of Faturechi and Miller-Hooks (2014) and more recently Zhou et al. (2019) provided a summary of the road network reliability measures.

2.1.3 Intelligent transportation systems in degraded networks

The last decade has seen the emergence of ITS which include a wide range of methods to manage road networks. The ITS literature contains little material on the resilience and robustness of smart road networks. In this context, there is a need to answer three questions:

- how could a failure in a disrupted smart network be assessed or measured?
- is there a need to define new reliability measures considering ITS applications?
- how could ITS applications be used to improve degraded networks?

Most literature has focused on finding answers to the last question: How could ITS applications be used to improve degraded networks? Koorey et al. (2014) investigated the possibility of using adaptive signal control and Variable Message Signs to manage road networks in the case of traffic accidents. Ganin et al. (2019) investigated targeted disruptions on smart road networks. Kaviani et al. (2017) sought the optimal locations of roadside guidance devices across a regional road network for improving total travel time within a network during long-term closures caused by natural disasters.

Overall, much has been done to improve the reliability of road networks; however, there is still scope for more improvements. This study goes one step further to improve the resilience of road networks by optimising traffic signal control for various disruption levels and durations.

The following sections review the literature related to modelling disrupted road networks, traffic signal optimisation, and modelling carbon dioxide emissions. Based on this review, the method used in this study is determined.

2.2 Modelling disrupted road networks

Traffic assignment models are concerned with assigning trips to routes through the road network. These models are divided into three broad types: static, dynamic, and semi-dynamic traffic assignment models. Semi-dynamic assignment models might be considered as a reasonable 'midpoint' between static and dynamic assignment models. The characteristics of these assignment models raises the question of which assignment model is appropriate for different circumstances? The answer is case-specific; however, a better understanding of assignment models helps in deciding which model should be used in which circumstances, as some simulation models are better than others in dealing with congested and disrupted road networks.

2.2.1 Traffic simulation models

In this section, different traffic representation levels: macroscopic, microscopic, mesoscopic, and hybrid simulation models are discussed.

2.2.1.1 Macroscopic models

Macroscopic models of traffic flow attempt to classify the average traffic behaviour on a link, instead of the behaviour of each specific vehicle. Typically, macroscopic models are based on a four-step model, involving trip generation, trip distribution, mode split, and trip assignment. These types of models accept a coarse level of input data such as link configuration (i.e. number of lanes, intersection form etc.). Data may be aggregated at the zonal level or at the household level.

According to Burghout and Wahlstedt (2007), macroscopic model applications usually have fewer parameters to calibrate and are less sensitive to small changes in network description, which means the model running time is shorter than in microscopic models. However, they are limited to the cases where the interaction of vehicles is not crucial to the results of the simulation (Burghout and Wahlstedt, 2007).

2.2.1.2 Microscopic models

In microscopic models, the interactions of individual vehicles are represented by vehicle acceleration and deceleration, lane changing behaviour and gap acceptance. They produce space-time trajectories of vehicles as they move through the network (Jeannotte et al., 2004). Microscopic traffic flow models require, in addition to the parameters required by macroscopic models, fine-detailed information about vehicle and driver behaviour performance parameters, and road geometry and layout.

There are a number of concerns related to applying microsimulation models, summarised by Akçelik and Besley (2007) and Zhang et al. (2010) as follows:

- the large amount of detail needed when modelling a road network;
- the slowness of input data preparation, and running time for large scale applications;
- the large effort needed to calibrate the model with a large number of parameters.

As a result, this makes developing microscopic models for large networks very challenging, especially if there is a very large number of vehicles in a network, when it may not be possible for the software to keep track of every vehicle.

In the presence of Intelligent Transportation Systems (ITS) applications (e.g. ramp controls, or adaptive traffic signal control systems), it has been noticed (Barceló et al., 2005; Burghout and Wahlstedt, 2007) that microscopic simulation models are suited to modelling both vehicle interactions and drivers' reactions when exposed to such applications. The possibility of modelling route choice in microsimulation models is important when evaluating an ITS application that helps drivers decide their routes via en-route messages.

2.2.1.3 Mesoscopic models

Mesoscopic models fit within the gap between macroscopic and microscopic models, and their properties are a mixture of the properties of both microscopic and macroscopic models (Hadi et al., 2007). For example, they can simulate the routing of individual vehicles equipped with in-vehicle, real-time travel information systems. The travel times are determined from the simulated average speeds on the network links and nodes. The average speeds are, in turn, calculated from the speed-flow relationship. Mesoscopic models deal with platoon dispersion and queuing, in which the vehicle departure profile, arrival pattern, and the average travel time in the link are estimated. SATURN is an example of software packages that implement the mesoscopic approach. In this study, SATURN software package is used, thus the following paragraphs gave more detail about SATURN.

In SATURN, two distinct forms of input data are required: an OD trip matrix representing zone to zone trip demands for the period of interest, and a network description (e.g. junction type, lane arrangements, and saturation flows). Both the trip matrix and network data are put into a "route-choice" model, which allocates trips to routes, using an equilibrium approach. SATURN provides two levels of detail: a "simulation" network, which is used to describe a traffic management scheme where the impacts of traffic are crucial and large, and a "buffer" network, which is used where the traffic impact management scheme is less critical. The buffer network, which normally surrounds the simulation network, is coded in less detail. SATURN simulation structure is based on Cyclic Flow Profiles (CFPs). Hall and Willumsen (1980) defined the CFP as "the flow of traffic past a certain point as a function of time over a single cycle of the traffic signals in the network", as illustrated in Fig. 2.1.

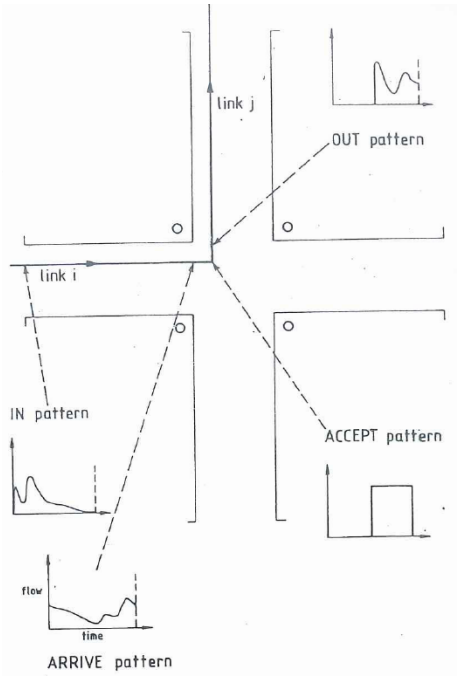

Figure 2.1: The four basic CFPs for the turning movement from link "i" to link "j" (Hall and Willumsen, 1980)

The figure proposed by Hall and Willumsen (1980) represents a single node within a network, and each turn has associated with it four CFPs which are as follows: the IN pattern (the flow profile at the upstream end of link i); the ARRIVE pattern (the profile at the downstream end of i); the ACCEPT pattern of traffic which can actually make the turn; and the OUT pattern (the flow at the upstream end of link j).

These profiles are related, as the ARRIVE pattern is derived from the IN pattern by the process of platoon dispersion and arrival flow profiles of conflicting movements. The ACCEPT pattern is independently derived (de Dios Ortuzar and Willumsen, 2011) and is based on junction capacities, signal timings and offsets, and the arrival flow profiles of conflicting movements. Finally, the OUT pattern is derived from both the ARRIVE and ACCEPT patterns.

SATURN assigns travel demands between discrete geographical areas (zones) to the most likely routes, and then simulates travel times on roads and through intersections. The complete model is based on an iterative loop between the assignment and simulation phases. Thus, the simulation determines flow-delay curves, based on a given set of turning movements and feeds them to the assignment. The assignment in turn uses these curves to determine route choice and updated turning movements. These iterations continue until the turning movements reach reasonably stable values (de Dios Ortuzar

and Willumsen, 2011).

One feature of interest in SATURN is what is called "time-slicing", with the traffic conditions at the end of a time-slice being the starting conditions for the subsequent time-slice. For example, if a network is modelled from 9:00 am - 10:00 am (Fig. 2.2), small intervals (say 15 minutes) could be used to estimate the flows and travel times in each interval, taking into consideration the residual queues from the previous time-slice (PASSQ). This means, short-term degradation can be simulated applying the semi-dynamic approach (i.e. time-slicing), since the traffic conditions for short intervals can be captured. It should be noted that the time-slice interval is user-set and the duration of the time-slice is directly related to the simulation running time. For instance, for a one-hour simulation interval, using a 1-minute time-slice will need more running time than a 15 minute time-slice, as SATURN will develop 60 scenarios versus only 4 for 15-minute time-slices.

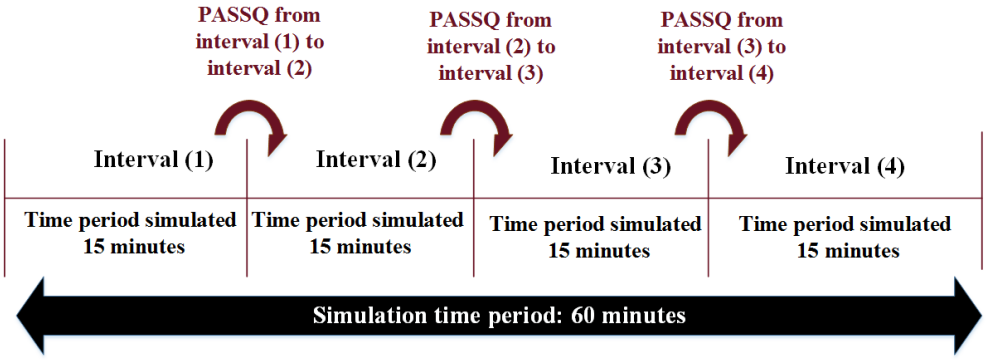

Figure 2.2: The time-slice method

To activate the time-slicing facility in SATURN, the Length of the Time Period (LTP) parameter or time-slice should be specified. SATURN generates a file for each time period or time-slice. For instance, in this study 4- minute time-slices were used to simulate one hour. Thus, SATURN generates and simulates 15 separate files to represents 15 time-slices. After that, SATURN combines the 15 files into one to represent one time period (i.e. one hour in this case).

In terms of optimising signal control, there is a simple signal optimisation within SATURN (van Vliet, 2018). However, in this thesis the Cross-Entropy method will be used to optimise the signal settings, as described in Section 2.3.

2.2.2 Traffic assignment models

Since the 1950s, researchers have endeavoured to develop methods and techniques to represent the interaction between the network supply (i.e. the physical characteristics of road networks) and demand (i.e. the number of trips on routes between an origin and a destination). This is a difficult problem due to its dimensions and complexity. For instance, the number of trips generated between origins and destinations could be numerous according to a driver's behaviour and preferences to reduce their travel time or cost, which vary considerably. This study will investigate two approaches to assigning traffic to networks: static and semi-dynamic assignment models. A brief discussion is presented in this section; however, for a full review and discussion of those models, see Bliemer et al. (2017).

These assignment models are simulated at different representation levels: macroscopic, mesoscopic, and microscopic models. Simulation models, as with virtually all models for predicting traffic flows on networks, are based on the User Equilibrium (UE) principle. According to Barceló (2010), "the concept of user equilibrium assumes that travellers try to minimize their individual travel times, that is, travellers choose the routes that they perceive to be the shortest under the prevailing conditions". This is consistent with Wardrop's first principle (Wardrop, 1952) that "the journey times on all the routes actually used are equal, and less than those which would be experienced by a single vehicle on any unused route".

Wardrop's first principle is used differently in different types of models. For instance, to reduce the delay in microscopic simulation models, optimal paths are recalculated periodically and vehicles re-assigned to new optimal paths to allow for route changes after a trip has begun if there is a blockage. In the absence of disruption or congestion, no re-assignment will occur. This regular "updating" is appropriate for studying short-term capacity reductions (Berdica et al., 2003). In contrast, macroscopic and mesoscopic models do not allow for re-assignment of traffic after a trip has commenced. This may result in inaccurate estimates of delays. After a blockage and congestion occurs, traffic generally diverts around the blockage to reduce the delay, so if a model does not allow for such diversion, it might over-estimate the impact of the blockage, making it unsuitable for assessing the impact of short-term congestion reductions. However, the semi-dynamic approach updates the traffic state at the beginning of each time-slice, with the traffic conditions at the end of a time-slice being the starting conditions for the subsequent time-slice (as described in Section 2.2.1.3, Fig. 2.2). This allows for simulating the residual queue (i.e. vehicles in the queue from the previous time-slice). In the following

paragraphs, a discussion about the static, dynamic, and semi-dynamic assignments is presented.

2.2.2.1 Static assignment models

Static Traffic Assignment (STA) models include the following constituents: Static User Equilibrium (UE), System Optimal (SO), and Stochastic User Equilibrium (SUE). The UE model has been the most widely adopted in assignment models for ease of use and computational convenience, along with the alignment with real driver behaviour as drivers tend to choose the route with the least cost or time. This model was defined by Wardrop (1952) and mathematically formulated by Beckmann et al. (1956). The UE mathematical equation to minimise the objective function Z to find the link flows is as follows:

$$min\, Z_{UE}(q) = \sum_{a \in A}^{L} \int_{0}^{q_a} q_a\, t_a(x)\, dx \tag{2.1}$$

where q_a is the flow on link a; t_a is the average travel time for the link flow; and L is the set of links. This objective function is subject to the following flow constraints:

- the flows are conservative and no trips are lost, as follows:

$$\sum_{p \in P} f_{ijp} = OD_{ij} \qquad \forall i \in O;\, j \in D \tag{2.2}$$

  where O and D are the set of origins and destinations; P is the set of possible paths; i, j are the origin index and destination index; p is the path index; f_{ijp} is the path flow between origin i and destination j using path p.

- the flows are not negative, as follows:

$$f_{ijp} \geq 0 \qquad \forall i \in O\; j \in D;\, p \in P \tag{2.3}$$

- the incidence relationships express the link flows in terms of the path flows, as follows:

$$q_a = \sum_{i \in O} \sum_{j \in D} \sum_{p \in P} f_{ijp}\, \delta_{aijp} \qquad \forall a \in L \tag{2.4}$$

where a equals one if the link a is on path p between i and j, and zero otherwise; δ_{aijp} is an indicator variable, which equals one if the link a is on path p between i and j, or zero otherwise.

- the link flow is less than or equal to the capacity of the link, as follows:

$$q_a \leq q_a^0 \qquad \forall a \in L \tag{2.5}$$

where q_a^0 is the link capacity.

The second Wardrop principle, on the other hand, minimises the total cost of travel in a network and not the individual cost of each individual driver as the UE method does. The SO can be formulated as follows:

$$min\, Z_{SO}(q) = \sum_{a \in A} q_a\, c_a\,(q_a) \tag{2.6}$$

where Z_{SO} is the 'marginal cost' of travel for each individual driver when link costs/times are strict 'separable ' functions of link volumes, and c_a is the cost of travel on link a.

The applications of the SO models are highlighted in the literature on managing traffic, minimising travel costs, and congestion pricing (Tajtehranifard, 2017). However, (van Vliet, 2004) recommended using this model as a research tool, rather than a practical tool, as this model is not based on logical behavioural principals.

The third family member is the SUE model, which is defined as, "traffic arranges itself on congested networks such that the routes chosen by individual drivers are those with the minimum 'perceived' cost; routes with perceived costs in excess of the minima are not used" (van Vliet, 2018). This means that SUE allows different users to have different perceptions of what actually constitutes a travel cost to them. For a full description of the SUE and the differences between this model and the UE, one can refer to Sheffi and Powell (1981).

STA models are still widely used for strategic transport planning for their ease of use and computational convenience (Bliemer et al., 2014). On one side of the spectrum, these models provide sufficient approximation for traffic flows, along with the ability to model

large-scale networks. On the other side of the spectrum, these models assume that travel demand and link cost functions remain constant during the simulation time horizon. This makes them inappropriate for real-time traffic modelling, especially in congested networks, as these models cannot indicate the locations and extents of queues associated with them (Jayakrishnan and Mahmassani, 1991). In the light of the above deficiencies, there is a need for more realistic models to capture the 'dynamic' nature of traffic flows.

2.2.2.2 Dynamic assignment models

Since the 1990s, Dynamic Traffic Assignment (DTA) models have been developed to replicate the dynamic traffic states for recurrent and non-recurrent congestion. Unlike static models, there is a lack of a unified modelling framework for the DTA models. Ran et al. (1996) formulated the dynamic version of Wardrop's UE: "If, for each OD pair at each instant of time, the actual travel times experienced by travellers departing at the same time are equal and minimal, the dynamic traffic flow over the network is in a travel time-based dynamic user equilibrium state".

Significant research has been undertaken to model DTA using mathematical programmes and/or simulation-based approaches: for example, Papageorgiou (1990); Janson (1991); Astarita (1996); Florian et al. (2001), among others. Taale and Pel (2015) classified the DTA models into deterministic dynamic (user equilibrium) traffic assignment (DDUE) and stochastic dynamic (user equilibrium) traffic assignment (SDUE). The DDUE assumes travellers have prior knowledge of the traffic conditions. The SDUE, on the other hand, is defined such that for each OD pair, any road user travelling between the OD pair, and departing during a specific time interval cannot improve his perceived route travel costs unilaterally by changing routes during that time interval.

DTA models are able to simulate highly congested urban networks using DTA algorithms and parallel DTA simulation (Ben-Akiva et al., 2012). In the context of ITS, ITS applications are beyond the modelling capabilities of static assignment models, as these applications require regular time updating. This makes DTA models more appropriate to be used, as these models are capable of updating the network status based on real time data (Chiu et al., 2011). However, these models require a high detail level of data, which makes them complex and data-hungry. This stems from the fact that these models provide detailed dynamics of the flows which are not always needed (e.g. in strategic planning). Moreover, DTA models require complicated calibration techniques (Bliemer et al., 2014; Taale and Pel, 2015; Lu et al., 2015), which need considerable computational effort. In the light of this, the semi-dynamic models might be considered as a reasonable

midpoint between the static and dynamic assignment models. DTA models are out of scope in this study.

2.2.2.3 Semi-dynamic assignment models

Because of the complexity of DTA models and the simplicity of the STA models, researchers have developed semi-dynamic models. This approach was proposed by van Vliet (1982), using the simulation and assignment procedures in SATURN software package. The semi-dynamic approach involves dividing the simulated time horizon into short time-slices, with the traffic conditions at the end of a time-slice becoming the starting conditions for the subsequent time-slice. This approach is referred to as quasi-dynamic by van Vliet (1982) and semi-dynamic by Bliemer et al. (2017). The latter term will be used in this thesis to refer to the time-slices approach.

Transport researchers have subsequently modelled residual queues using link capacity constraints (Kheifits and Gur, 1997; Schmöcker et al., 2008; Fusco et al., 2012; Bliemer et al., 2014; Tajtehranifard, 2017). These studies showed that this approach is considered a reasonable 'midpoint' between the static and dynamic assignment models as it combines the computational efficiency of static assignment models and the realism of traffic flow in dynamic assignment models. However, little has been done, to investigate the time-slices approach to simulate disrupted road networks. It therefore seems reasonable to investigate the semi-dynamic approach to simulate disrupted networks (as proposed in this thesis) since this approach approximates the dynamic assignment with less computational effort.

2.2.3 Application to modelling disrupted road networks

A number of attempts to model disrupted road networks have been conducted applying various levels of disruption. For instance, a study with a congested network was presented in Berdica (2002*b*) for the city of Stockholm, Sweden. Twelve scenarios to simulate complete and partial link closure were applied to investigate the effects of capacity reductions and the traffic demand variations considering route choice under equilibrium conditions. She concluded that a microsimulation model is more appropriate to model link closures after the trip has been commenced. This is in line with Berdica et al. (2003) who investigated the implications of model choice in detail using a small road network in Christchurch (New Zealand) as a study case. In their model, complete closures of 10, 20, 30 and 40 minutes were simulated for one link, with the mid-point of each closure

scenario being 8:30 am. The average time spent travelling on the road network for different closure durations, as estimated using microsimulation, can be seen in Fig. 2.3.

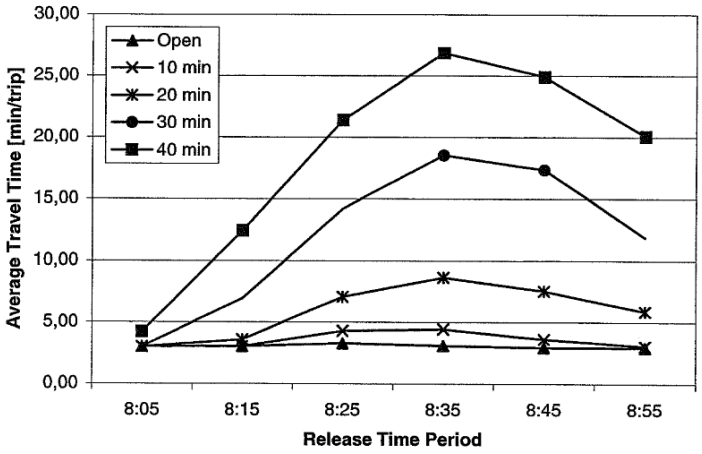

Figure 2.3: The average travel time for different closure durations using microsimulation (Berdica et al., 2003)

It is interesting to notice the average travel time between closure intervals. If the midpoint of the closure is taken as a base to compare, it is clear that the difference in average travel time between the 20 minute and 30 minute closures is almost twice the difference between the 10 minute and 20 minute closure intervals. One might therefore expect a larger difference between the 30 minute and 40 minute closures, but this seems not to be the case: in fact the difference decreased. Moreover, the results of Berdica's study showed that a microscopic model is more sensitive to disturbances and disturbances duration than macroscopic and microscopic models, indicating that microsimulation is able to better simulate short-term disturbances in the road transportation system.

It is worth noting that the size of the network should depend upon the level and duration of the degradation and the subsequent spatial distribution of re-routed traffic. For a small and short capacity reduction, a small sized network might give good simulation results, as not many drivers will divert far from their usual route to avoid congestion. However, in the case of a large and long capacity reduction, more drivers will divert further from their usual routes, to avoid congestion and decrease their travel time, and the new path could be outside the boundaries of the simulated network, resulting in inaccurate estimates of the effect of the degradation.

Recently, another study conducted in Christchurch, New Zealand by Wilmshurst (2015) who applied macroscopic, mesoscopic, and microscopic models respectively, to

estimate the impact of a blockage in the northern corridor into and out of Christchurch.

The studied area is well covered by a Bluetooth journey time data system and permanent traffic count sites. Bluetooth data was investigated for both directions of travel. The traffic count data was used to determine the flow rates in key locations and to factor up the flow rates sample. The study concluded that the microscopic model was able to give a more robust estimate of the actual impacts compared with mesoscopic and macroscopic models. However, mesoscopic and macroscopic models were city-wide models and, unlike the microsimulation model, were not calibrated for traffic data from Christchurch's northern corridor network. This could well explain in part the different estimates of actual impacts using different models.

Other studies have focused on applying road network reliability measures to identify the most vulnerable links in the network. For instance, Jenelius et al. (2006) implemented two measures: the importance index (a measure of the consequences to the overall network of a selected location having a failing link or group of links and the exposure index (a measure of the consequences at a selected location of an incident resulting in a failing link somewhere in the network (Jenelius et al., 2006) to a road network in Sweden, consisting of 42, 956 links and 19,392 nodes. In their study, the importance of each individual link with respect to the whole network was measured. Similar analysis was carried out by Freeman et al. (2008) who applied the importance and exposure measures to the city of Adelaide, Australia using macroscopic and mesoscopic models. In their model, nine scenarios were implemented to simulate complete link closures by deleting the links (in both directions) and considering no capacity for the vehicle flow. The results of their model were consistent with Jenelius et al. (2006), they found that the user exposure (i.e. consequences of the event in a particular place as defined by Jenelius et al. (2006) could be worse in sparse networks where the travel times are long compared to dense networks. This means the total travel time has a greater influence on total exposure than the availability of alternative routes.

Overall, none of the above mentioned studies investigated applying various levels of disruptions and durations of the capacity reductions to improve the reliability of road networks.

2.3 Traffic signals optimisation

Akcelik (1998) proposed setting signal timings so as to minimise a weighted sum of the delays (travel time) and stops (fuel consumption). In this thesis, traffic signals are optimised to minimise travel time or CO_2 emissions.

This section reviews traffic signal optimisation algorithms with a focus on the Cross-Entropy optimisation, then describes a bi-level algorithm to optimise traffic signals in urban road networks applying the Cross-Entropy method.

2.3.1 Traffic signals optimisation methods

Traffic signals are used to control traffic flow at one junction or a network of junctions in road networks. The way that traffic signals are set up can help in optimising the traffic flow rate (e.g. facilitate traffic flows to pass through intersections) and minimising the congestion, with resulting reductions in fuel cost and pollution. Signal timing optimisation has been studied using a variety of methods, which fall into two main groups: analytical and heuristic. The analytical approach was developed for one junction by Webster (1958), then for a network of junctions by Little (1966) and Allsop (1972). Due to the complexity of the problem, in terms of having numerous different combinations of the set of parameters, meta-heuristic optimisation methods have been applied for large scale problems to find near optimal solutions. Some of the meta-heuristic optimisation methods are Hill Climbing, Simulated Annealing, Tabu Search, Genetic Algorithms, and Cross-Entropy. These methods are briefly described in the paragraphs below. However, until now it is debatable whether an algorithm computes a global optimum due to the computational complexity.

The Simulated Annealing (SA) algorithm

The SA algorithm was first introduced by Kirkpatrick et al. (1983) and Černỳ (1985). This method imitates some thermodynamic principles of producing an ideal crystal, to achieve a global optimal solution (Zhilinskas et al., 2002; Sharda et al., 2003). The algorithm is used for simulating the thermal moves of molecules at a particular temperature, and this temperature influences the efficiency of finding the global optimal. The algorithm starts with a random solution to determine the initial value of the temperature. For each iteration, the algorithm calculates a random neighbouring solution and compares it to the initial solution to decide which one is accepted or not. Hadi and Wallace (1994) implemented the SA algorithm to optimise cycle length, phase sequences,

and offsets simultaneously on road networks. Their results suggested that the algorithm has potential for optimising signal phasing and timing for arterial streets as well as multi-arterial networks. However, the selection of neighbouring solutions and the way of reducing the initial guess might significantly affect the effectiveness of finding the optimal solution as reported by Kontorinaki et al. (2015).

The Hill Climbing (HC) method

The HC method starts from a given solution, then improves this solution by making an incremental change to the solution, and stops when the value of the objective function cannot be further improved. Cantarella et al. (2006) applied the HC method to find the optimal set of signal timings (i.e. optimising green times and offsets), taking into account the impact of re-routing. However, the HC algorithm depends on the initial solutions (Hadi and Wallace, 1994).

The Tabu Search (TS) method

The TS algorithm was introduced by Glover (1986). This algorithm is basically a gradient-descent search. The method is based on a memory that keeps a Tabu list of the moves of the previous iterations that might considered unwanted. The typical procedure is to assign a random initial solution, evaluate this solution based on a particular criterion, then put the current solution in a Tabu list, evaluate the fitness of the neighbourhood of the current solution, and delete the neighbours that are already in the Tabu list. Determine the best neighbour to be the next current solution.

The Genetic Algorithm (GA) method

The GA algorithm is based on the mechanics of natural selection and natural genetics. This method, which was first proposed by Golberg (1989) and Holland (1992), is based on a random search within a defined search space.

The GA has been broadly utilised for determining signal timings for the reason that this method is able to solve combinatorial optimisation problems and to find a near optimal solution. Therefore, this method has been studied broadly and extensively from the time it was first proposed until now. However, it is debatable whether or not such an algorithm actually computes a global minimum. Hadi and Wallace (1992) proposed the use of GA with TRANSYT-7F to select all signal timing design elements including phase sequences. Applications of the algorithm suggested that it has potential for optimising signal phasing and timing for arterial streets and multi-arterial networks, but this

experimental was not computationally efficient.

Cantarella et al. (2006) applied the HC, SA, TS, and GA methods to solve mutually consistent problem (i.e. when the flow pattern is a function of the signal timings and the signal timings are a function of the flows). They found that GA, SA and TS perform similarly; however, a hybrid GA and TS might be an efficient method. Ngoduy and Maher (2011) compared the GA and CE methods. They found that the CE method performs better than the GA method in terms of computational time and producing near global optimum solution. For instance, the CE method requires 8.33 hours for 1,000 sample size compared to 5.24 hours for 50 sample size applying the GA method to find the optimal solution. However, it is worth mentioning that increasing the sample size to 1000 in GA does not significantly improve the final near optimum solution, but considerably increases the computational time (i.e. 8.38 hours). In addition, Maher (2008) reported that the CE method has a more formal mathematical and statistical basis than the GA algorithm, making it worthy of more investigation.

To this end, the CE method appears to be a good method to be used to optimise the signal settings. Therefore, the CE method is used to optimise traffic signals in disrupted road networks in this thesis and described in detail in the next paragraphs.

The Cross-Entropy method and formulation

The Cross-Entropy (CE) method was proposed by Rubinstein (1997). Chepuri and Homem-de Mello (2005) used this method to solve the vehicle routing problem; then Maher (2008) used the CE algorithm to optimise the signal settings on a six-arm signalised roundabout. Ngoduy and Maher (2011) and Maher et al. (2013) further explored the CE method to optimise traffic signals in an urban network with 19 links and 6 nodes. The results of applying the CE method showed encouraging advantages for computational efficiency and convergence, with its more formal mathematical and statistical basis making it simple to apply (Maher, 2008), as was also found by Ngoduy and Maher (2011), Ngoduy and Maher (2012), and Zhong et al. (2016), who used the same method to calibrate microscopic traffic models.

The CE method is used to solve combinatorial optimisation problems when the objective function is very complicated (to find a near optimal solution among a finite collection of possibilities), and when it is necessary to do a lot of sampling. The CE method is used in this research to optimise traffic signals in disrupted road networks. A general description of the CE method, based on Homem-de Mello and Rubinstein (2002), Rubinstein and Kroese (2004), and de Boer et al. (2005), is given below.

The idea behind the CE method is to produce a random sample from a pre-specified probability distribution function, and then evaluate this sample in order to generate a better one in the next iteration.

The general problem is to minimise the objective function $PI(\mathbf{X})$ over all $\mathbf{X}$ in Ω, which denotes the feasible space, where the optimal solution is $\mathbf{X}^*$. Then:

$$PI(\mathbf{X}^*) = \gamma^* = arg\,min\,PI(\mathbf{X}), \qquad \forall \mathbf{X} \in \Omega \tag{2.7}$$

where γ^* is the minimum value over the given set of $\mathbf{X}$ (i.e the optimal performance index value).

To find the discrete solution $\mathbf{X} = \mathbf{X}^*$, the CE method requires that an estimation problem be associated with the optimisation problem of Equation 2.7. To do so, it is assumed that random solutions can be generated from a density function $p(\mathbf{X})$ (e.g. Gaussian, uniform, etc.) that are parameterised by a real-valued vector v (e.g. the mean and standard deviation of the Gaussian distribution). Then, the optimisation problem can be transformed into estimating the probability $l(\gamma)$ that a randomly chosen solution $\mathbf{X}$ in Ω from a density distribution function $p(\mathbf{X})$ has a value of the objective function $PI(\mathbf{X}) \leq \gamma$, where γ is close but greater than γ^*. Then:

$$l(\gamma) = P(PI(\mathbf{X}) \leq \gamma) \tag{2.8}$$

where P denotes the probability.

Estimating this probability by generating solutions from $p(\mathbf{X})$ will generally be very inefficient, because $PI(\mathbf{X}) \leq \gamma$ is a rare event (i.e. a very small probability) and one would perform an exhaustive search on the solution space to estimate $l(\gamma)$. The practical way is to use importance sampling (i.e. particular values of the input random variables have more impact on the parameter being estimated, based on the objective function, than on others) to generate a density function $g(\mathbf{X})$. Specifically, generate N samples drawn from $p(\mathbf{X}; v)$ and estimate $l(\gamma)$ as:

$$\hat{l}(\gamma) = \frac{1}{N} \sum_{n=1}^{N} I(PI(\mathbf{X}_n) \leq \gamma) \frac{p(\mathbf{X}_n)}{g(\mathbf{X}_n)}, \tag{2.9}$$

where $\hat{l}(\gamma)$ is an estimator of $l(\gamma)$. The indicator variable $I(PI(\mathbf{X}_n) \leq \gamma)$ takes the value of 1 if $PI(X_n) \leq \gamma$ or zero otherwise.

The optimal way to estimate $l(\gamma)$ is to use the change of measure with the ideal density function $g^*(\mathbf{X})$, as given by Equation 2.10:

$$g^*(\mathbf{X}) = \frac{I(PI(\mathbf{X}) \leq \gamma)\, p(\mathbf{X};v)}{l(\gamma)}, \tag{2.10}$$

What the CE method does is to tell how to construct the density function $g(\mathbf{X}_n)$ from amongst a family of distributions $p(\mathbf{X};v)$ which is as close as possible to $g^*(\mathbf{X})$ by minimising the Kullback-Leibler distance (D) between $g(\mathbf{X})$ and $p(\mathbf{X};v)$. However, this distance is not a distance in the formal sense, but to show that this value will be zero only when $p(\mathbf{X};v)$ is equal to $g(\mathbf{X}_n)$. It is then a matter of choosing the values of the parameter v, to minimise D (i.e. expected value should be maximal) to make the sampling as efficient as possible. It is shown in de Boer et al. (2005) that this problem of minimising D is equivalent to:

$$Max_v\, D(v) = Max_v\, E\left[I(p(\mathbf{X}) \leq \gamma)\, ln\, p(\mathbf{X};v)\right] \tag{2.11}$$

where $E[\bullet]$ is the expected value.
This leads to the following general form of the CE algorithm:

- initialise by setting the iteration counter t to 0, the parameter value v to v^0 that is used for termination check, and the sample size N.
- generate a set of candidate solutions $\mathbf{X}_n^t, n = 1,2,...N$ from a density distribution $p(\mathbf{X};v^t)$, and calculate the PI values $PI(\mathbf{X}_n^t)$.
- sort the PI values into ascending order, and select a subset of best performing samples (i.e. the lowest 100 ρ, ρ is the ratio of the best samples, typically ρ = 0.05) so that the estimate of the 100 ρ is γ^t. Let T_{best} denote the set of indices t for which $PI(\mathbf{X}_n^t) \leq \gamma^t$;
- use only the best solutions $\mathbf{X}_n^t$, $t \in \mathrm{T}_{best}$ to find the values of the parameter v that minimises $p(\mathbf{X};v^t)$, denoted as v_{new}^t. Then update the parameter vector according to the following rule:

$$v^{(t+1)} = \alpha v_{new}^{(t)} + (1-\alpha)v^{(t)} \tag{2.12}$$

where α is a smoothing parameter, varies between $\alpha \in [0,1]$.

- update the v^t based on the best sample which should be less than or equal v^0.
- increase t by 1, and return to step 2, unless a stopping criterion is reached, that is $v^{t+1} \approx v^t$

To improve the algorithm's performance the following steps can be taken:

- the population size N can be increased to maximise the possibility of having a good random sample. Tan and Gaona (2017) used a real network to assess the performance of the CE method using different combinations of the sample size and number of iterations. They found that the computation time increases as the sample size increases, and the improvement in the value of the objective function (as the sample size increases) decreases. A sample size ranges from 1,000 to 2,000 is recommended in the literature (Zhong et al., 2016);
- the smoothing factor α ranges from 0 to 1. The main reason why this parameter is important is to reduce the probability of zero or one at the first few iterations. Otherwise, the algorithm converge to a wrong solution. It was found empirically that a value of $\alpha \in [0.4, 0.9]$ gives the best results (de Boer et al., 2005). However, it should be noted that increasing the smoothing parameter, will reduce the running time;
- the parameter value v^0, which is the threshold to terminate the CE algorithm, should be small to ensure a good near optimum value.
- the percentage used for the best sample ρ ranges from 0 to 1. In each iteration, the best sample size (i.e. the elite sample) is ρ x N. This helps to update the parameters for the next generated solutions to improve the quality of the solution and speed the model towards finding an optimum solution. Typically, a value of $\rho \in [0.01, 0.1]$ is recommended (de Boer et al., 2005);

The CE settings which are used in this thesis are addressed in Chapter 3.

2.3.2 The bi-level formulation

Based on the discussion above, the Cross-Entropy method is used in this thesis. More details about this method is given in the below section.

Ngoduy and Maher (2011) used a bi-level optimisation framework to optimise traffic signals in urban road networks to optimise performance measures (they used the travel time as their performance measure). The upper level optimisation problem represents planners trying to minimise the average travel time when equilibrium has not yet been reached among the road users (Fig. 2.4).

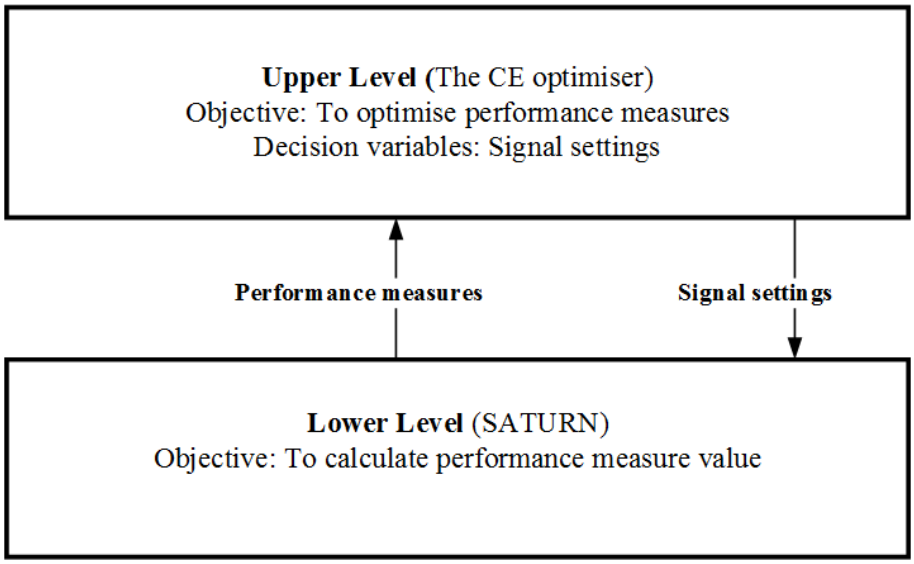

Figure 2.4: The bi-level approach

The upper level of the problem is formulated as follows:

$$Min\, PI(\mathbf{X}, \mathbf{q_{UE}}(\mathbf{X})) = \sum_{a=1}^{L} q_a t_a(\mathbf{X}, \mathbf{q_{UE}}(\mathbf{X})); \tag{2.13}$$

$$subject\ to: \mathbf{X}(\boldsymbol{\beta}, \boldsymbol{\theta}, \mathbf{C}) \in \Omega \tag{2.14}$$

where $PI(\mathbf{X}, q_{UE}(\mathbf{X}))$ is the performance index function (i.e. the travel time in the network) which depends on the vector of equilibrium link flows $\mathbf{q_{UE}}$ and the vector of signal timings $\mathbf{X}$, consisting of the vector of offsets β, the vector of green times θ, and the cycle length $\mathbf{C}$; L is the number of links; q_a is the flow on link a; t_a is the average travel time for the link flow a (consistent units are assumed throughout the research).

Since changing the signal timings in a network will generally cause re-routing of traffic $\mathbf{q}_{UE} = \mathbf{q}_{UE}(X)$, Ω denotes the feasible space of $\mathbf{X}$ defined as follows:

$$C_{min} \leq C \leq C_{max}; \tag{2.15}$$

$$0 \leq \boldsymbol{\beta}_n \leq \mathbf{C} - 1; \tag{2.16}$$

$$\theta_{n,s}^{min} \leq \theta_{n,s} \leq \theta_{n,s}^{max}; \tag{2.17}$$

$$\mathbf{C} = \sum_{s=1}^{S_n} \theta_{n,s} + \sum_{s=1}^{S_n} I_{n,s} \tag{2.18}$$

where C_{min} and C_{max} are the lower and upper bounds of the cycle length, respectively; $\boldsymbol{\beta}_n$ is the offset at node n; $\theta_{n,s}$ is the green time at node n for phase s; $\theta_{n,s}^{min}$ and $\theta_{n,s}^{max}$ are the lower and upper bounds of the green time at node n for phase s; S_n is the number of phases at node n; and $I_{n,s}$ is the inter-green time at node n for phase s. The signal settings are considered to be discrete integer values.

The lower level represents users following the user equilibrium principle under the given network condition. This can be formulated as follows:

$$\mathbf{t}(X, q_{UE}).(\mathbf{q} - \mathbf{q}_{UE}) = 0 \qquad \forall q \in \Theta \tag{2.19}$$

where $\mathbf{q}$ is the vector of link flows, and $\mathbf{q}_{UE}$ is the vector of equilibrium link flows. In Equation 2.19, $\mathbf{t}(\mathbf{X}, \mathbf{q}_{UE})$ denotes the vector of link travel times, which is dependent on the vector of signal timings and the equilibrium link flows. Θ denotes the feasible space of the link flow vector and is defined as in Equations 2.2-2.5.

This approach, as described above, was adopted and extended (as detailed in Chapter 3) to account for urban network degradation to optimise traffic signals to minimise the travel time and/or carbon dioxide emissions in degraded road networks.

2.4 Modelling carbon dioxide emissions in disrupted road networks

This section discusses the literature related to the environmental impact of road transport, along with modelling emissions generated from road transport.

2.4.1 Background

In New Zealand, the transport sector produces over 45% of all energy sector of carbon dioxide emissions (manufacturing, electricity, and fugitive emissions: emissions of gases or vapours mostly from industrial activities due to leaks) as reported by the MBIE (2017), with road transport accounting for half of this percentage. The situation is not much different in Europe: for instance, a UK study (DBEIS, 2018) reported that the transport sector accounted for 34% of all emission sectors (energy supply, business, and residential sectors). In the USA, half of the greenhouse emissions (GHG) of the transport sector are from road transport (EPA, 2018). This makes road transport a significant source of GHG emissions. These aforementioned percentages are expected to increase due to the growth in travel demand.

Road transport generates a number of emissions. The general list includes carbon dioxide (CO_2), carbon monoxide (CO), nitrogen oxides (NO_X), lead compounds (Pb), and hydrocarbons (HC). The effect of a number of emissions generated from the road transport sector is summarised in Table 2.1. Among all the different kinds of emissions generated from road transport, carbon dioxide (CO_2) emissions are considered to be the largest contributors to global warming. For instance, CO_2 emissions contribute 81% of the UK total of GHG (DBEIS, 2018) and around 80% of the EU total of GHG emissions (Eurostat, 2018). In addition, CO_2 emissions create the greatest concern as they have direct consequences on human health (Bektaş and Laporte, 2011). As a consequence, a number of initiatives to control CO_2 emissions have been proposed: see, for example, the United Nations Framework Convention on Climate Change (UNFCCC) (Sands, 1992) and the Kyoto Protocol (Grubb et al., 1997).

Table 2.1: The effect of transport related emissions (Hickman et al., 1999)

Effect	**Emissions**				
	CO_2	**CO**	**NO_X**	**Pb**	**HC**
Health impact	✓	✓	✓	✓	✓
Global warming potential	✓	✓	✓	✓	✓
GHG effect (directly)	✓		✓		
GHG effect (indirectly)		✓		✓	✓
Ozone layer			✓		

Therefore, there are two options to alleviate emissions generated from road transport: 1. to reduce the amount of travel by means of traffic demand management (e.g. car-pooling); 2. to reduce emissions associated with travel that continues to occur, by optimising traffic management (e.g. better signal control). The most common approach is to minimise the travel times in a road network, which might result in reducing the environmental impact. For example, see Sugawara and Niemeier (2002). However, it is felt that this is not enough (Sharma and Mathew, 2011) since this approach was modelled in the traffic assignment stage using a generalised cost function (i.e. the criterion that determines the minimum paths in the assignment stage, based on the travel time and distance, but not on the emissions). Therefore, the second option is investigated in this study: optimising the signal settings to reduce CO_2 emissions and to improve the environmental sustainability.

Sharma and Mathew (2011) implemented a multi-objective optimisation to minimise the travel time and emissions in road networks using a Genetic Algorithm, taking into account three pollutants (CO, NO_X, and HC), as well as various transport modes. In their model, they used the average link speed to estimate the link emissions. However, models using average speed as the only independent variable, do not allow for variations in fuel consumption rates while cruising (i.e. travelling a distance using the average speed for a given flow level and under the prevailing roadway conditions), idling (i.e. when a vehicle is stopped by a control element of the traffic system such as a traffic sign) and stop-start manoeuvres.

To this end, this study investigates minimising CO_2 emissions, as a goal of optimisation of the upper level, as previously investigated by Sharma and Mathew (2011), but using Cross-Entropy optimisation along with the semi-dynamic approach embedded in SATURN software package (as discussed in Chapter 6), to optimise signal settings (i.e. green times and offsets) to minimise CO_2 emissions.

2.4.2 Emissions modelling

A number of models have been proposed to estimate the amount of CO_2 emissions generated from road transport, including a wide range of simulation-based models. Among others, SIDRA, AIMSUN, and SATURN are discussed below.

- **SIDRA emissions model**

  Akçelik (1983) developed a fuel consumption and emission model for urban traffic management, which is based on three elements namely cruising, idling, and stop-start manoeuvres, which can all be added together to find the total fuel consumption (Equation 2.20).

$$F = f_1 x_s + f_2 d_s + f_3 h \tag{2.20}$$

  where F is the average fuel consumption per vehicle (mL); f_1 is the fuel consumption rate while cruising (mL/km); x_s is the total section distance (km); f_2 is the fuel consumption per unit time while idling (mL/s); d_s is the average stopped delay (s) per vehicle (i.e. idling time); f_3 is the extra fuel consumption involved in stopping and starting (mL); and h is the average number of effective stops per vehicle (stop rate).

  This model is embedded in the SIDRA package developed by Akcelik (1991). Results showed that the minimum fuel consumption occurs at a steady cruising speed in the range of 40-60 km/h. This is consistent with Everall (1968) and Evans et al. (1976), who concluded that fuel consumption is high in low speed traffic and also high in high speed traffic, and the minimum of the curve of fuel consumption against speed occurs in the range of 48-64 km/hr (Fig 2.5).

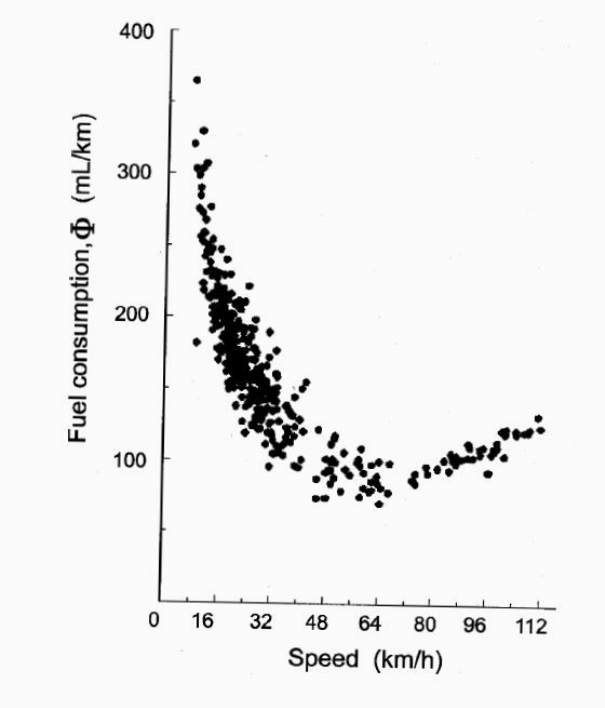

Figure 2.5: Fuel consumption and speed (Evans et al., 1976)

- **AIMSUN emissions model**

  The AIMSUN fuel consumption model calculates fuel consumption for each of the four operating modes (i.e. idling, deceleration, acceleration, and cruising). Nanduri (2013) reported that the fuel consumed during the idling, deceleration, and acceleration modes are derived from Ferreira (1982), while the fuel consumed during the cruising mode is derived from Akçelik (1983). The sum of the following equations is used to calculate the fuel consumption of all of the fuel consumption modes during a given simulation time (Swidan et al., 2011), as follows:

  Idle fuel consumption

$$F_u = F_i \, \delta \, t \tag{2.21}$$

  Acceleration fuel consumption

$$F_u = (C_1 + C_2\, a\, v)\, \delta\, t \tag{2.22}$$

Cruise fuel consumption

$$F_u = (K_1 (1 + \left(\frac{v}{2V_m}\right)^3) + K_2\, V_m)\, \delta\, t \tag{2.23}$$

Deceleration fuel consumption

$$F_u = F_d\, \delta\, t \tag{2.24}$$

where F_u is the fuel consumption for each vehicle mode (ml); F_i is the fuel consumption rate for idling vehicles (ml/s); δt is the simulation time step; C_1 and C_2 are constants for the fuel consumption rate for accelerating vehicles; a is the vehicle acceleration ($m/s/s$) and v is the speed (m/sec); K_1 is a constant for vehicles travelling at a constant speed of 90 km/h; K_2 is a constant for vehicles travelling at a constant speed of 120 Km/h; V_m is the speed at which the fuel consumption rate (ml/s) is at minimum for a vehicle cruising at constant speed; F_d is the fuel consumption rate for decelerating vehicles in ml/sec. This model can provide total emissions (kg) of CO_2, CO, NO_X and HC. Nanduri (2013) provides a full description of how to determine the constants.

Recently, AIMSUN emissions model has been developed in collaboration with Transport for London.

- **SATURN emissions model**

  The SATURN emissions model can predict five standard emissions: CO, CO_2, HC, NOx and Pb. This model is based on a model developed by Matzoros and van Vliet (1992). The basic equation for emissions of pollutant (i) from a link is given by:

$$E^i = (a_1^i\, d + a_2^i\, t_c + a_3^i\, t_q + a_4^i\, s_1 + a_5^i\, s_2)\, q \tag{2.25}$$

  where d is link distance; t_c is average cruise travel time on the link; t_q is the time spent idling in queues at the junctions; s_1 is the number of primary stops per vehicle; s_2 is the number of secondary stops per vehicle (i.e. the primary and secondary stops are used to calculate the delays); q is the vehicle flow; $a_1^i, ...a_5^i$ are (user-set) coefficients. This model predicts air pollution emissions and concentrations from urban road networks with high pollution near junctions, levelling off towards mid-link points. The default values for the coefficients are listed in Table 2.2.

Table 2.2: Default values for the emission model coefficients (van Vliet, 2018)

Grams\PCU	**Kilometres (a_1)**	**Cruise (a_2)**	**Idling (a_3)**	**Primary Stop (a_4)**	**Secondary Stop (a_5)**
CO_2	70	0	1200.00	16.00	5.000
CO	0	304.80	180.00	2.22	0.444
NO	0	102.60	1.80	0.42	0.084
HC	0	57.00	30.00	0.39	0.078
Pb	0	0.36	0.09	0.0024	0.0005

The above discussed emission models all take account of the cruise time, idling time, and number of stops. In this study, the emission model embedded in SATURN is used to calculate CO_2 emissions, for the reason that the semi-dynamic assignment embedded in SATURN package is used in this study. However, it is important to note that 1. the SATURN trip assignment model output is based on a standard trip-assignment model algorithm that does not consider emissions as part of the assignment; 2. the parameters which are used in SATURN emissions model were determined based on a PhD dissertation (Matzoros and van Vliet, 1992); another study could be done to improve these parameters. It is worth noting that changing the parameters of the SATURN emissions model could affect the results of estimating emissions.

2.5 Summary

To sum up, this chapter has reviewed the literature related to resilience of road networks, traffic signal optimisation, along with modelling carbon dioxide emissions in disrupted road networks, to define the gaps and determine the research objectives and methods. The reviewed literature revealed the following:

- in terms of road network resilience, there are a number of terms used to describe the robustness and resilience of road networks. In this study, the term 'resilience' is used and defined as: to improve the ability of a road network to accommodate different levels of capacity reductions for different durations.
- a number of indices and methods have been proposed in the literature to improve road networks resiliency. These methods focused on complete link capacity reductions or partial link capacity reductions. Little literature has focused on varying the level of capacity reductions along with the reduction durations, thus, to have a better understanding of the impact of the level of disruption and the duration of the disruption, this study considers different capacity degradations (i.e. 25%, 50%, 75%, and 100%) with various durations (4 minutes, 20 minutes, 36 minutes, and 60 minutes).
- in terms of the simulation and assignment methods, the semi-dynamic assignment approach is considered a reasonable midpoint between the static and dynamic assignment models, as it combines the computational efficiency of static assignment models and much of the realism of traffic flow in dynamic assignment models. However, little has been done to investigate the semi-dynamic approach in simulating disrupted road networks. It therefore seems reasonable to investigate the semi-dynamic approach to simulate disrupted networks (as proposed in this thesis) since this approach approximates the dynamic assignment with less computational effort. The semi-dynamic model developed by van Vliet (1982) and embedded in the SATURN mesoscopic simulation package is used in this study.
- in terms of optimising traffic signal control, a wide range of signal optimisation algorithms have been implemented to optimise traffic signals. The CE optimisation method has proved more efficient in finding near optimum solutions compared to other optimisation methods (e.g. the GA method). Therefore, this study implements the CE method, along with the semi-dynamic approach, to optimise traffic signal control in disrupted road networks to minimise the travel time.

- in terms of emissions modelling, road traffic is a significant source of emissions and CO_2 emissions are one of the largest contributor to global warming. Computer-based emissions models are all based on the cruise, idling, and stops parameters; however, these models differ with respect to the assignment method and might result in differences in cruise time, idling time, and the number of stops calculations. In this study, the mesoscopic model and the semi-dynamic assignment embedded in SATURN package are implemented. Thus, the emission model in SATURN is used to calculate CO_2 emissions. However, it is important to note that the SATURN trip assignment model output is based on a standard trip-assignment model algorithm that does not consider emissions as part of the assignment.
- in terms of the OD matrix, this study uses a dense network as a case study, and a fixed OD matrix is modelled. This assumption is realistic when modelling a dense network where there are a large number of alternative routes and the trip durations are short. However, in sparse networks this assumption is not realistic, and elastic demand can be implemented to give a realistic estimate of the number of trips.

2.6 Conclusions

The ultimate objective of this study is to evaluate optimising the signal settings to minimise the travel time or CO_2 emissions. Based on the above discussion, the simulation method of the semi-dynamic approach embedded in the SATURN software package, along with the Cross-Entropy method to optimise traffic signal control, assuming a fixed trip matrix, will be used to simulate disrupted road networks (Fig. 2.6). The next chapter presents the method formulation.

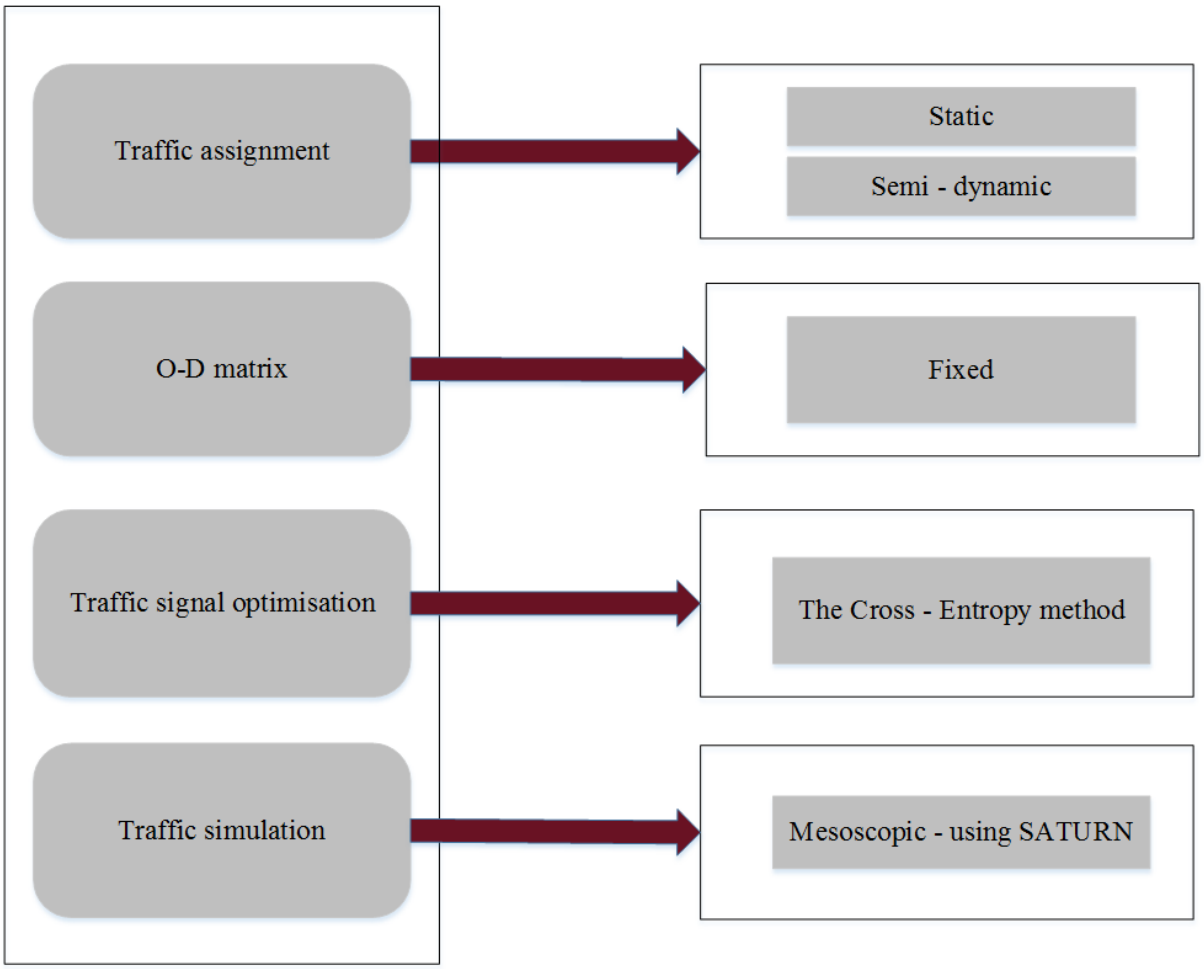

Figure 2.6: The research method

Part II

Method and Results

CHAPTER 3

FORMULATION OF THE DEGRADED NETWORK OPTIMISATION PROBLEM

3.1 The bi-level framework in disrupted networks

To understand the impact of disruptions on road network performance under optimum signal control, a bi-level optimisation problem was formulated. The approach, which was chosen by Ngoduy and Maher (2011), was adopted and extended to account for urban network degradations.

The process of optimising the signal settings (Phase A green times and offsets) involves iterating between the CE algorithm and SATURN V11.3 (van Vliet, 2004). The CE algorithm searches for the combinations of signal settings that minimise the travel time and/or CO_2 emissions, while calling SATURN to estimate the link flows, the link travel times, the delays, and CO_2 emissions for the specified combinations of signal settings, considering the re-routing effects. SATURN passes this information back to the CE algorithm for re-computation of the objective function (i.e. the travel time or CO_2 emissions in the disrupted road network). The iterative process between the CE algorithm and SATURN continues until satisfactory convergence is achieved (Fig. 3.1).

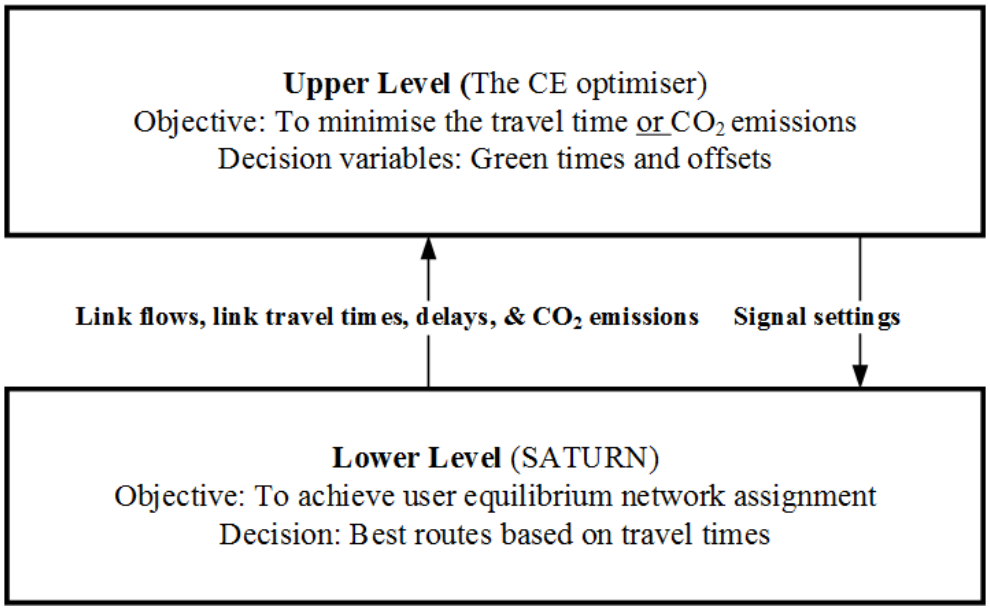

Figure 3.1: Bi-level optimisation framework

The upper level optimisation problem represents planners trying to minimise the average travel time when equilibrium has not yet been reached among the road users. The lower level represents users following the UE principle under the given network condition as described in Chapter 2, Section 2.3.2.

The travel time is calculated within the CE algorithm as the sum of the products of the link flows and link travel times, plus the sum of the products of the turning flows and the average turn delay, thus:

$$travel\ time = \sum(f_a.t_a) + \sum(f_a.d_a) \tag{3.1}$$

where f_a is the flow on link a; t_a is the travel time on link a; and d_a is the average turn delay per vehicle on link a.

The link travel time t_a on link a is estimated in SATURN as follows:

$$t_a = t_0 + Af_a^n \qquad f_a < q_a^0; \tag{3.2}$$

$$t_a = t_0 + A(q_a^0)^n + \frac{B(f_a - q_a^0)}{q_a^0} \qquad f_a \geq q_a^0; \tag{3.3}$$

where t_0 is the free flow travel time; f_a is the flow on link a; A, B, and n are parameters calculated in SATURN (van Vliet, 2004); and q_a^0 is the link capacity.

The total CO_2 emissions in the network is calculated within the CE code as the summation of the CO_2 emissions on link a (as discussed in Chapter 2), thus:

$$CO_2 = \sum CO_{2,a} \tag{3.4}$$

In this thesis two objective functions are separately investigated:

- minimising the travel time: to optimise the sets of Phase A green times and offsets;
- minimising CO_2 emissions: to optimise the sets of Phase A green times and offsets.

Based on the results of the above two objective functions, the interaction between minimising the travel time and minimising CO_2 emissions will be investigated.

3.2 The simulation

To assess the performance of the CE algorithm, two different combinations of the sample size (N) and iterations (t) were evaluated (Table 3.1), and the smoothing factor (α) was fixed to 0.9 as discussed below. Those terms were defined in Chapter 2, Section 2.3.1. The results (as shown in Table 3.1) indicate that simulation A (N=1,000 and t=30) gives better results, in terms of minimising the travel time and better convergence to a stable value, than simulation B (N=5,000 and t=10)[1]. The reason behind the two different simulations is that some combinations give better convergence of the objective function with a reasonable computational demand than others; however, one should keep in mind that better convergence does not necessarily mean that the signal settings for all nodes would converge to one stable value.

Table 3.1: Simulation combinations

Simulation	N	t	α	**Minimising the travel time (hours)**
A	1,000	30	0.9	17,893.55
B	5,000	10	0.9	17,902.52

[1]The convergence results and the signal settings are included in Appendix A.

The CE settings and assumptions used in this thesis are (see Chapter 2, Section 2.3.1, for definitions of the terms used below):

- the sample size N is 1,000 and the number of iteration t is 30 as in the results shown above and as also recommended by Tan and Gaona (2017);
- the smoothing factor α is 0.9: This value is within the limit of α that was suggested by de Boer et al. (2005) as discussed in Section 2.3.1. This means more weight is given to the new updated sample and less weight is given to the previous sample. The reason for choosing this value is that having a large smoothing parameter will reduce the time needed to calculate the objective function. However, this does not necessarily generate the optimal solution. One might need to alter the smoothing parameter to check which value gives better results;
- the ratio ρ is 5% and the elite sample (i.e. N x ρ) then is 500 as used by Maher et al. (2013);
- the parameter value ν was set as 0.1.

It is recommended to run small trials to determine the CE parameters, to improve the performance of the CE algorithm. However, this is beyond the scope of this thesis.

The bi-level framework was repeated ten times with random seed values for the random number generator to identify how sensitive the results are to different seed values. The results for ten different seed values, along with the mean (μ) and the standard deviation (STD) are shown in Table 3.2. The results indicate that while the optimal value of the objective function (the travel time) does not appear to be sensitive to the seed value, the optimal values of the green times and offsets are. For instance, the differences between the results of the travel time are very small. The % of error between the smallest travel time value (simulation No. 1) and the largest travel time value (simulation No. 5), highlighted in grey in Table 3.2, is less than 0.04%. However, the signal settings are quite different, especially the offsets as shown in Appendix A, Tables A.3 and A.4. This is due to the fact that this problem is not strictly convex (i.e. there is no unique solution), which reflects the stochastic nature of the CE method (using probabilities to find solutions). This indicates that the signal settings are dependent on the seed value, as also found by Laguna et al. (2009).

Table 3.2: Simulation results using different seed values

Simulation No.	**Minimising the travel time (hours)**
1	17,888.93
2	17,889.58
3	17,894.28
4	17,895.57
5	17,896.22
6	17,892.68
7	17,890.25
8	17,892.36
9	17,890.87
10	17,893.76
μ	17,892.45
STD	2.52

Based on the results obtained from the above simulations, a number of simulations were carried out to achieve the objectives of this study (to minimise the travel time or CO_2 emissions). These simulations can be categorised as follows:

- no optimisation (**the base case**): this means not using the CE algorithm to optimise the signal settings. However, a simple signal optimisation tool within SATURN is used (as described in Chapter 2). This particular simulation will be used as a benchmark to evaluate the performance of the CE method.

- optimising the signal settings (i.e. Phase A green times and offsets) applying the CE method, along with the static assignment approach (**CEM-static**) for various disruption scenarios, to minimise the travel time (Table 3.3, a);

- optimising the signal settings (i.e. Phase A green times and offsets) applying the CE method, along with the semi-dynamic assignment approach (**CEM-semi**) for various disruption scenarios, to minimise the travel time (Table 3.3, b);

- optimising the signal settings (i.e. Phase A green times and offsets) applying the CE and the semi-dynamic assignment approach (**CEM-semi**) for various disruption scenarios, to minimise CO_2 emissions (Table 3.4).

Table 3.3: Capacity reductions and durations, when minimising travel time, applying CEM-Static and CEM-semi

Capacity reduction	**0%**	**25%**	**50%**	**75%**	**100%**
a. static	60 min.	60 min.	60 min.	60 min.	60 min.
b. semi-dynamic	60 min.	4 min.	4 min.	4 min.	4 min.
		20 min.	20 min.	20 min.	20 min.
		36 min.	36 min.	36 min.	36 min.
		60 min.	60 min.	60 min.	60 min.

Table 3.4: Capacity reductions and durations, when minimising CO_2 emissions, applying CEM-semi

Capacity reduction	**0%**	**50%**	**75%**	**100%**
semi-dynamic	60 min.	20 min.	20 min.	20 min.
		36 min.	36 min.	36 min.
		60 min.	60 min.	60 min.

The results obtained from the simulations of these scenarios were compared as below:

- applying the **CEM-static** for optimising Phase A green times and offsets, when minimising the travel time is compared with applying the **CEM-semi** for optimising Phase A green times and offsets, when minimising the travel time (cells highlighted in grey in Table 3.3).
- applying the **CEM-semi** for optimising Phase A green times and offsets, when minimising the travel time (cells highlighted in grey in Table 3.3, b) is compared to applying the **CEM-semi** for optimising Phase A green times and offsets, when minimising CO_2 emissions (cells highlighted in grey in Table 3.4).
- applying the CE method for optimising Phase A green times and offsets is compared to not applying the CE method for optimising Phase A green times and offsets, when minimising the travel time.

3.3 Testbed description

The performance of the proposed approach was assessed by applying it to the Cambridge (UK) network (Fig. 3.3). The reason behind choosing the Cambridge network is that this network seems to be convenient to apply the proposed bi-level framework for a number of reasons:

- the Cambridge network comprises 141 zones (the zones within the central area are shown in Fig. 3.6), 1,091 links and 608 nodes, including 24 signalised junctions within the central area (Fig. 3.5). The network size is large enough to accommodate virtually all the re-routing when a disruption happens. It is worth noting that the running time is expected to increase with an increase in the network size;
- all signalised intersections have 2-phase arrangements, with a common cycle length fixed at 60 seconds. Having a fixed cycle time and two phases at every intersection reduces the number of decision variables and simplifies the optimisation task. This makes applying the CE method is convenient;
- this network is dense in the middle and relatively sparse in the North-West part, which makes it convenient to test different locations of the degradation.
- the total demand in this network reflects one peak hour, with a total number of 42,023 commenced vehicle trips. This demand is enough to cause re-routing of traffic in the case of disruptions.

The objective was to find the set of values for the 47 decision variables (i.e. 24 Phase A green times and 23 offsets) that minimises the travel time or CO_2 emissions in the network in the case of disruption. These variables were constrained to be integers (i.e. they were rounded to whole seconds), with a standard minimum green time being set to 7 seconds (i.e. the lower bound), and all inter-greens (i.e. between the end of Phase A green times and the start of the next phase green times at a node for safety purposes) were set to 5 seconds, and the maximum green time being 43 seconds (i.e. the 60 seconds cycle time, minus the 7 seconds lower bound green times, and minus two 5 seconds inter-green times). This means there are 37 possible green times ranging from 7seconds to 43 seconds. The offsets ranged from zero to 59 seconds, with the offset at node 2045 being set to zero. This means there are 60 possible solutions for the offsets.

The traffic flow at the most congested signalised intersection (node 2010) was degraded by applying several blockage scenarios, which involved various combinations of two main factors: the severity of the blockage (i.e. 25%, 50%, 75%, and 100% capacity reductions) and the duration of the blockage (i.e. 4, 20, 36, and 60 minutes), as described previously in Tables 3.3 and 3.4. The optimum Phase A green times and offsets in the case of degradation were determined for each scenario (Phase B green times are deduced from the cycle length and the inter-green times).

However, other nodes in the network could be more critical for the network performance (i.e. the nodes in the centre of the network where the network is more dense). Therefore, some other simulations were carried out on another node in the centre of the network (i.e. node 3810) to check the impact of disruptions at this node, in terms of travel time, and compare it to the impact of disruptions at node 2010. The results of simulating a 50% disruption at node 3810 for 4 minutes revealed that the impact of a blockage at node 2010 is greater than the impact of a blockage at node 3810. For instance, the travel time when there is a 50% disruption for 4 minutes at node 3810 is 17,780.52 hours compared to 17,786 hours when there is a 50% disruption at node 2010. This means more delays are expected when there is a blockage at node 2010. This could be due to the availability of alternative routes to get around node 3810, while this is not the case for node 2010.

Based on this, node 2010 is used to apply the degradation scenarios at. Node 2010 connects three nodes: 2055, 2015, and 2020. This means there are six possible movements through node 2010. To simulate a disruption, the saturation flows for all six movements through node 2010 were reduced. For instance, in the case of a complete capacity reduction at node 2010, movements 2015-2010-2055, 2015-2010-2020, 2055-2010-2020, 2055-2010-2015, 2020-2010-2055, and 2020-2010-2015 are closed as highlighted in red as shown in Fig. 3.2.

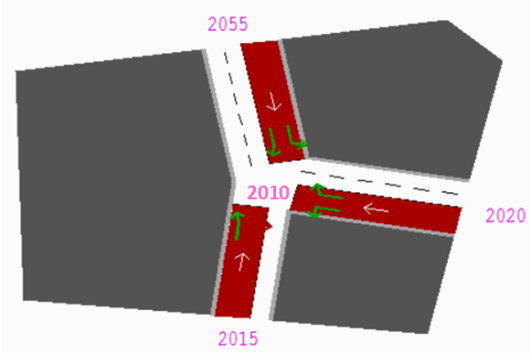

Figure 3.2: Node 2010 with a complete closure

The phasing arrangements for node 2010 and the adjacent nodes 3089, 2040 and 2045, are shown in Figs. 3.7, 3.8, 3.9 and 3.10, respectively [2]. Those nodes are the nodes surrounding node 2010; therefore, they will be analysed in detail in this study. The full set of results are included in the appendices.

In terms of the trip matrix, it is assumed to be fixed (the demand is independent of the cost of travel). This is a reasonable assumption as the duration of the blockage is short (less than one hour), but if the blockage duration is long, then a variable trip matrix is recommended.

It is worth noting that the Cambridge network was coded, calibrated, and validated by Atkins (a British engineering company based in London, the UK); however, the process of calibration and validation could not be documented in this thesis as these reports are confidential documents and unavailable to public. Calibration involves ensuring that the model results match observed data (flows, delays, etc.). Such data are available only for the non-disrupted situation. Validation of the model involves ensuring that the model accurately predicts the flows, delays, etc. one should keep in mind that changing the capacity in the network, including the signal green times, could have the potential to invalidate the model. Flows, delays, etc. have not been observed for the disruption scenarios, and creating a disruption to observe flows, delays, etc. during the disruption, so the model can be validated, is very unlikely to be permitted. Hence, validation of the model (as a predictor of what will happen to flows, delays, etc. during a disruption) is not practical. Therefore, the Cambridge network which is used in this thesis is a generic test of an algorithm rather than reflecting absolute reality on the ground.

[2]The phasing arrangements for the 24 signalised intersections are included in Appendix B.

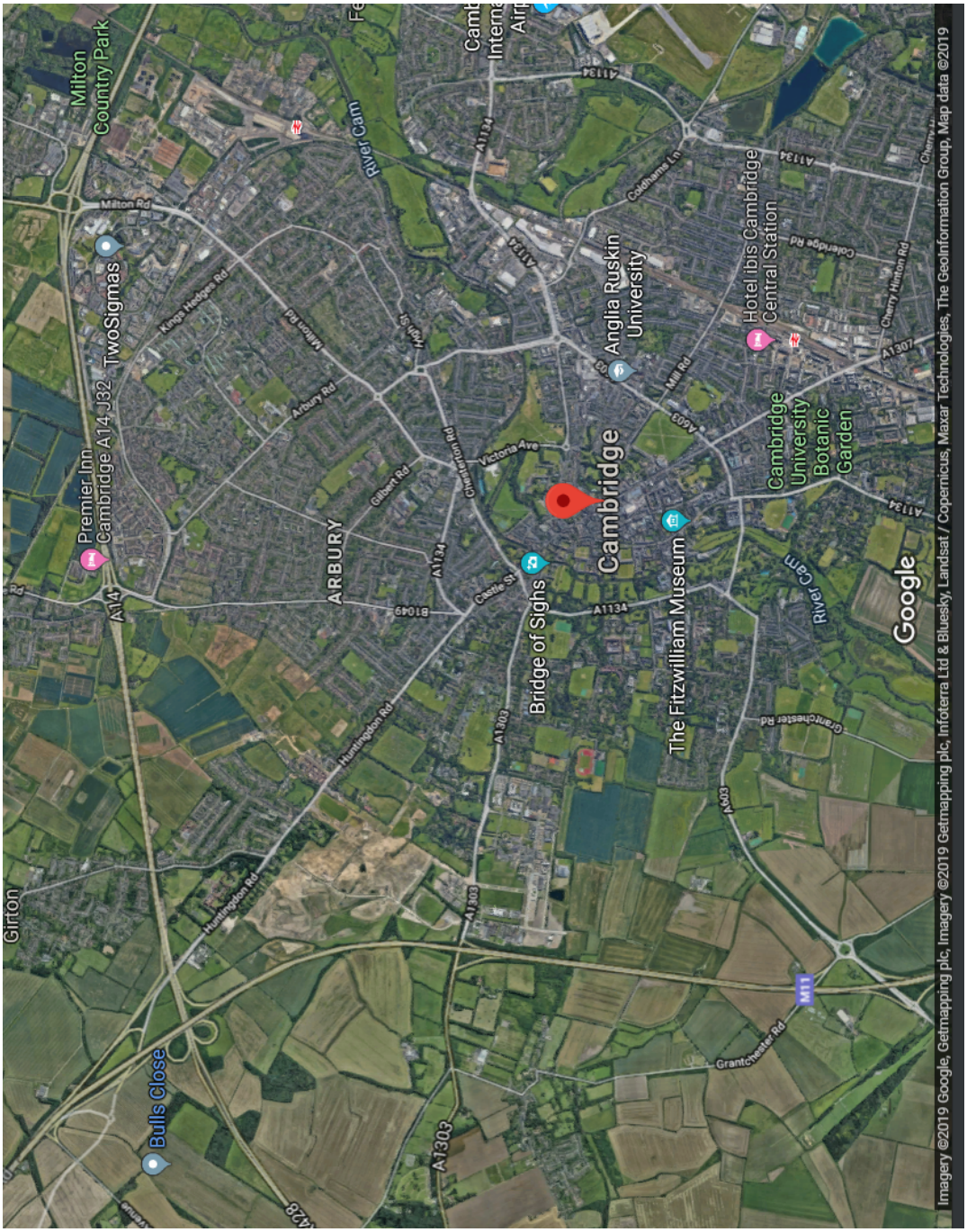

Figure 3.3: A Google map for the Cambridge network (Google, 2019)

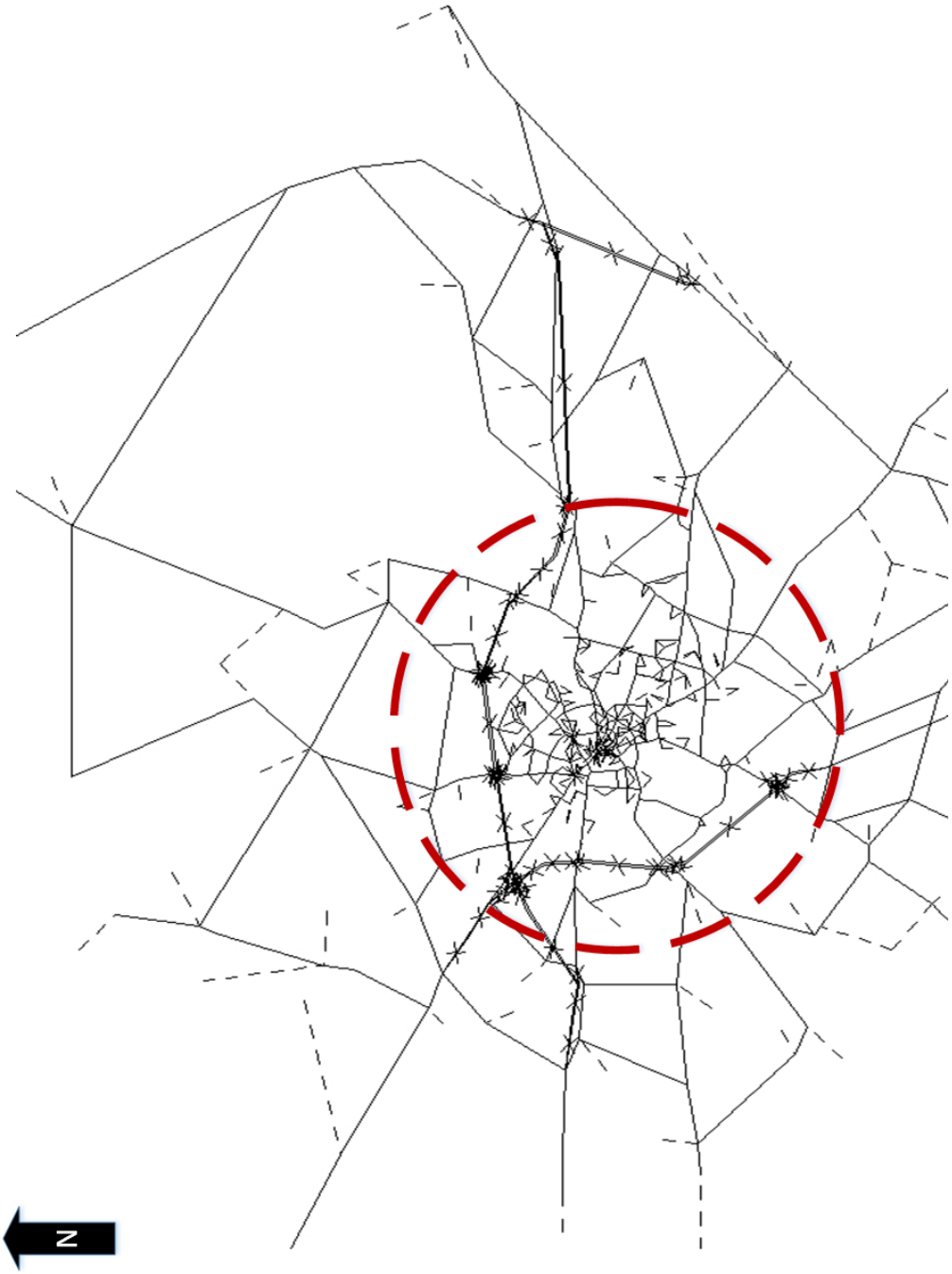

Figure 3.4: Cambridge network modelled in SATURN, the dotted circle representing the central area (Ngoduy and Maher, 2011)

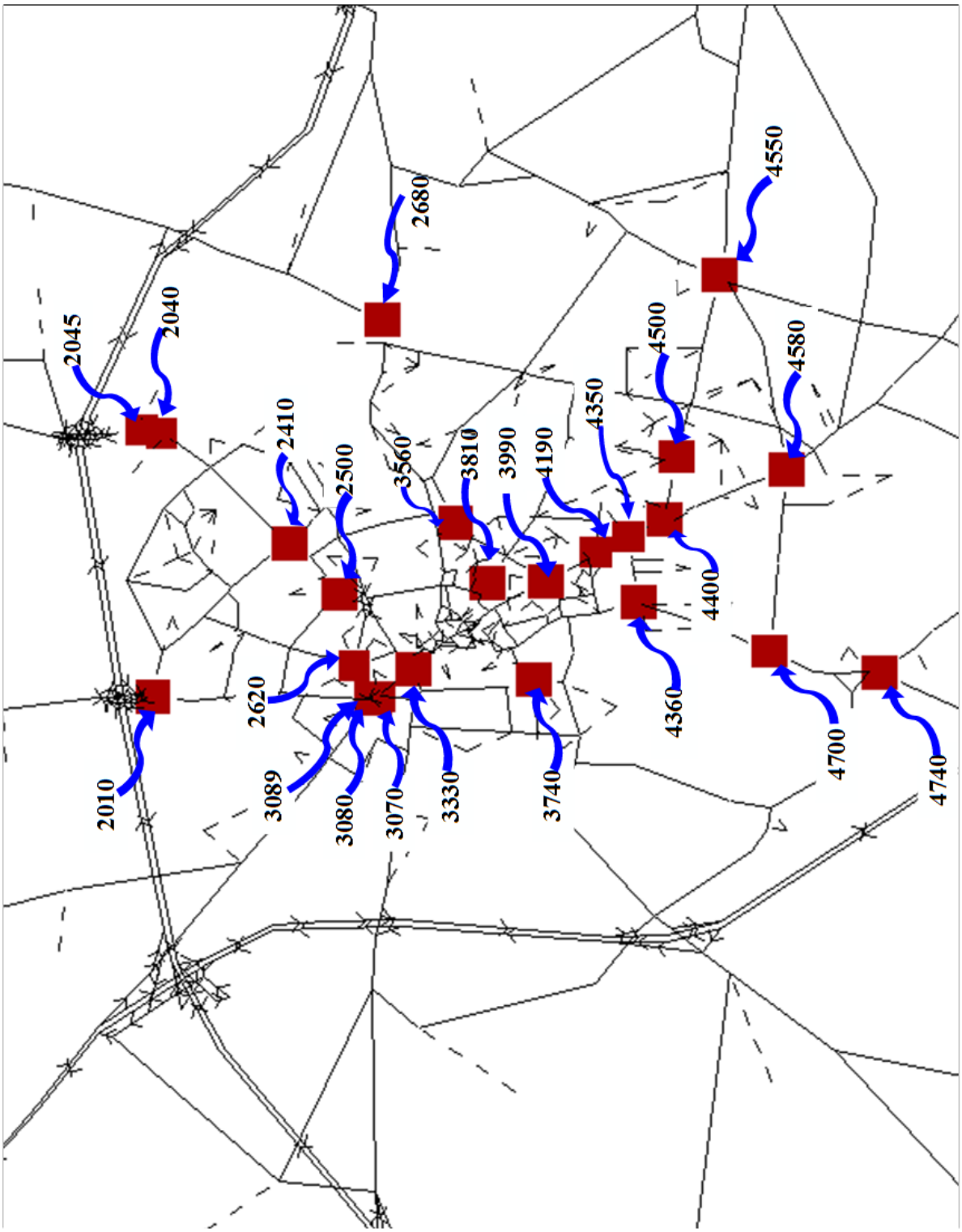

Figure 3.5: The location of the 24 signalised intersections in the central area, Cambridge network

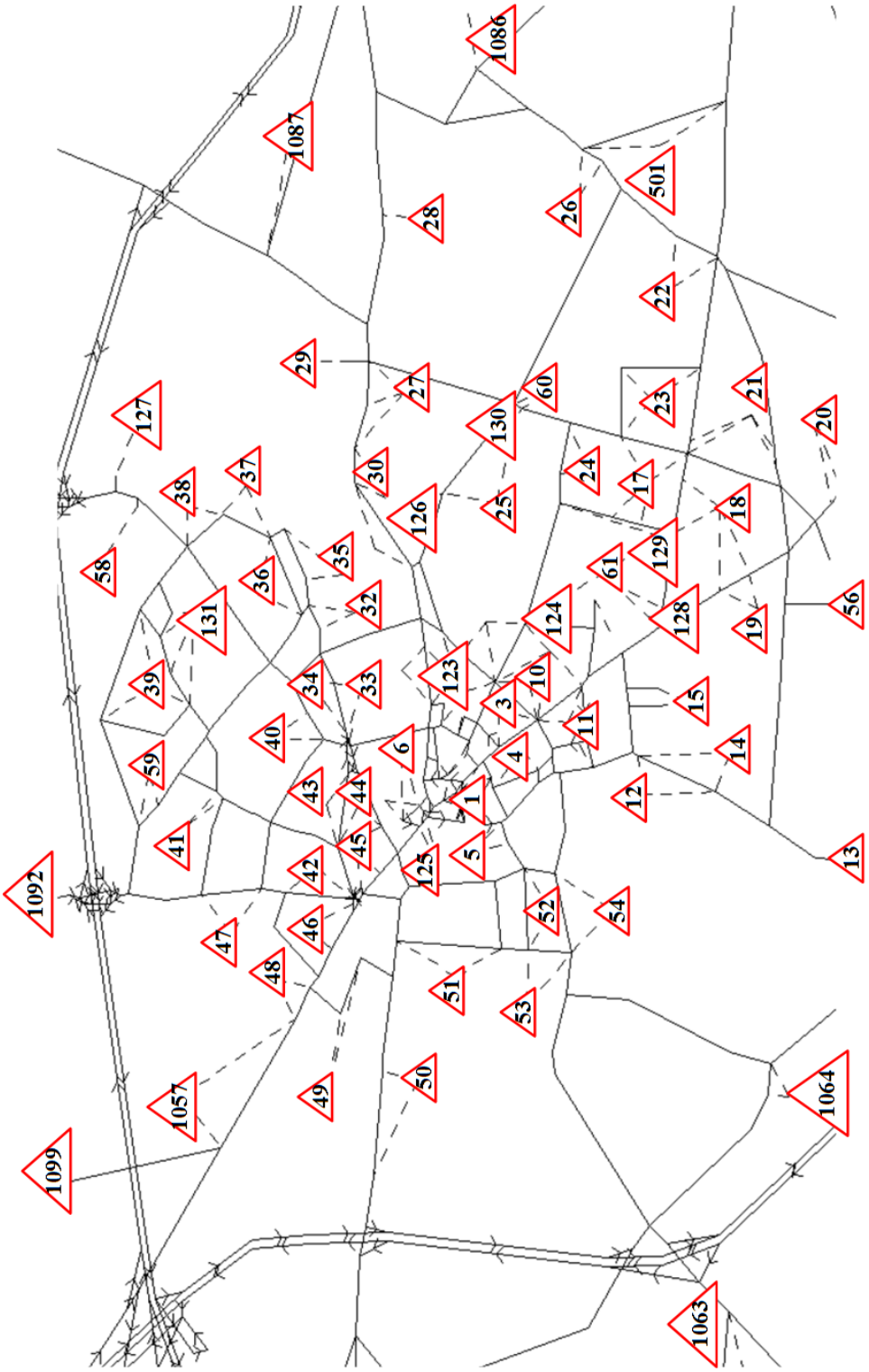

Figure 3.6: The location of the zones and centroid connectors within the central area, Cambridge network

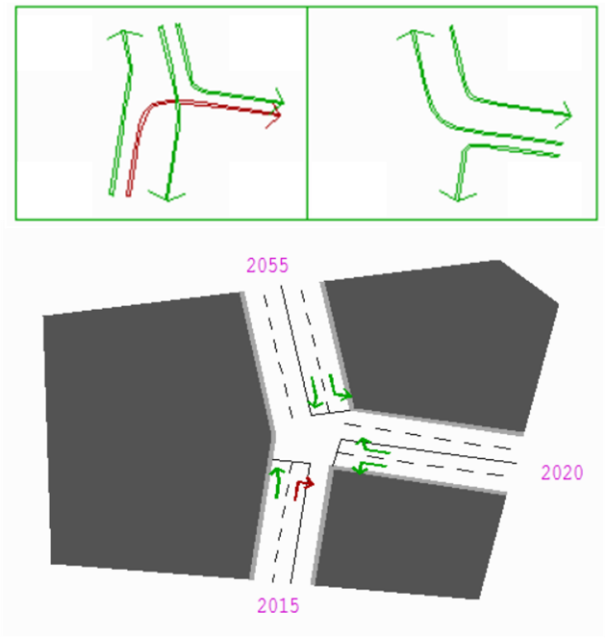

Figure 3.7: The phasing arrangements for node 2010: the red arrows represent a filter right turning movement

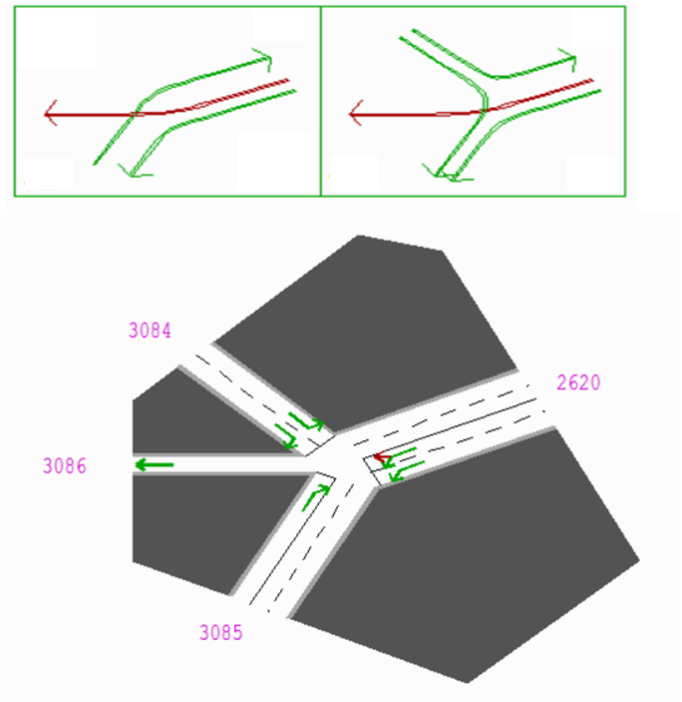

Figure 3.8: The phasing arrangements for node 3089

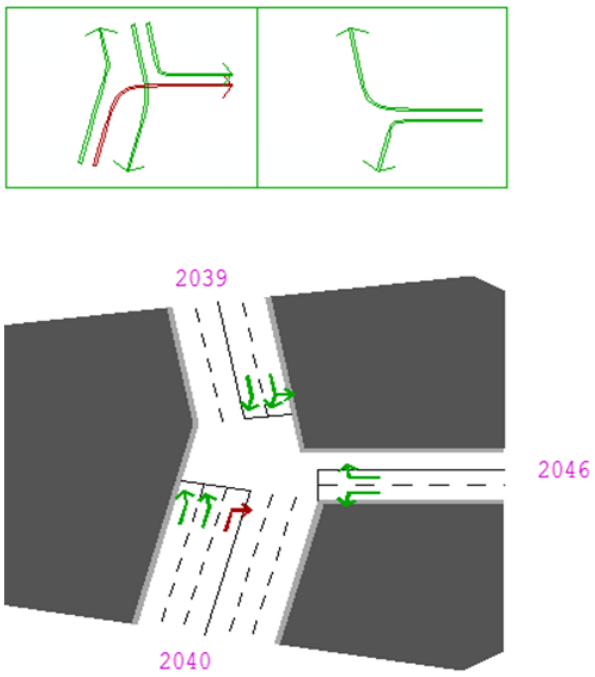

Figure 3.9: The phasing arrangements for node 2045

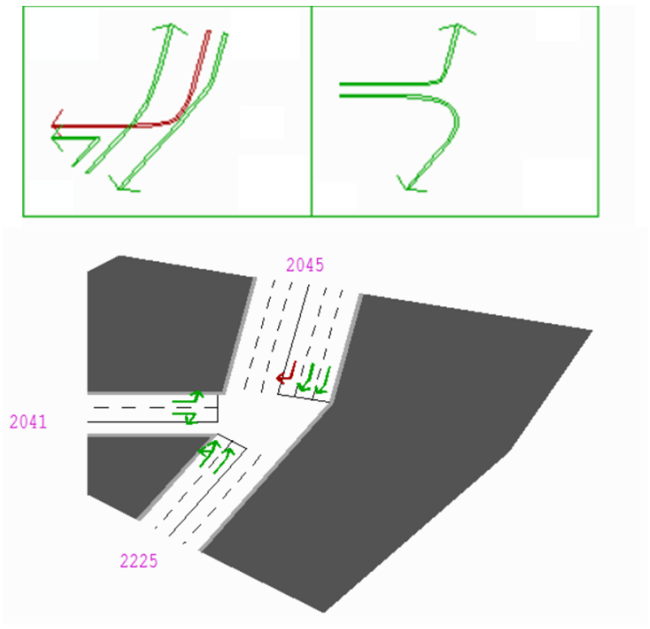

Figure 3.10: The phasing arrangements for node 2040

3.4 Conclusions

This chapter presented the formulation of the bi-level framework which consists of the Cross-Entropy optimisation method in the upper level and the user equilibrium assignment in the lower level.

The Cross-Entropy parameters used in this study are: 1,000 sample size with 30 iterations. The smoothing parameter is 0.9, the elite sample ratio is 0.1, and the smoothing factor is 0.5.

Moreover, this chapter presented the results of altering the seed values which revealed that while the optimal value of the objective function (the travel time) does not appear to be sensitive to the seed value, the optimal values of the green times and offsets are. This is due to the fact that this problem is not strictly convex (i.e. there is no unique solution).

A number of simulation scenarios are defined in this study, these scenarios are applied on Cambridge test network to evaluate the proposed approach. This network consists of 24 signalised intersections with two-phase arrangement. The green times range from 7 seconds up to 43 seconds, and the offsets range from 0 seconds to 59 seconds. The objective is to find the set of values for 47 decision variables (i.e. 24 Phase A green times and 23 offsets) that minimises the travel time or CO_2 emissions.

In the next chapter, the Cross-Entropy method along with the static bi-level framework results are presented. This includes testing four capacity reductions at one intersection: 25%, 50%, 75%, and 100% and comparing them to the case of no reduction. The degradation will last for one hour time period.

CHAPTER 4

STATIC ASSIGNMENT APPROACH

4.1 Static assignment results

This chapter describes the results obtained from applying the CE method, along with the static assignment embedded in SATURN (CEM-static). The traffic flow rate at the most congested signalised node (2010) was degraded for one hour by applying several partial and complete blockage scenarios, as described in Chapter 3, Table 3.3 a, which involved four combinations of the duration and the capacity reduction. The location of the most congested node 2010 and the adjacent nodes 3089, 2045, and 2040 are shown in Fig. 3.5.

The convergence of the Phase A green times and offsets for three nodes (2010, 3089, and 2040) are presented in Fig. 4.1 and Fig. 4.2, respectively. This convergence is for a 50% reduction in capacity at node 2010.

Initially, the probability of occurrence for each solution is uniformly distributed, with a probability of 0.0270 for each combination of the 37 possible green times (from the minimum Phase A green time 7 seconds to the maximum Phase A green time 43 seconds), and 0.0167 for each of the 60 possible offsets (from zero up to 59 seconds) as described in Chapter 3, section 3.3. The probability of each solution is then updated after each iteration based on the elite sample generated initially from a discrete uniform distribution with the mean and the standard deviation of the values in this sample to create a new distribution. This distribution becomes less uniform and more concentrated as the number of iterations increases, until the solution stabilises and has a probability close to one (the maximum possible value) for the value of the variable. For instance, the probability of the solution being 43 seconds for the Phase A green time at node 2010 is one (Fig. 4.1 c), after 15 iterations. If the solution in the upper level did not converge, then the value with the highest probability was chosen as a solution. However, the solution with the highest probability might not be the optimum one. Fig. 4.4 b and c show that the offset with the highest probability after 15 iterations was not the offset with the highest probability after 30 iterations. If the search for the optimum offset had been stopped after 15 iterations and the offset with the highest probability had been chosen, then the chosen offset would not be the optimum offset.

Convergence of offsets is difficult to obtain, particularly for the disrupted node 2010 (Fig. 4.2 c). The offset values in Table 4.3 are those with the highest probability after 30 iterations. For example, for a 50% reduction in capacity at node 2010, the offset at node 2010 with the highest probability is 55 seconds, which has a probability of 0.8. These values have been used for estimating the total travel times. One should note that the offsets at some nodes do not necessarily converge after 30 iterations, especially at nodes with reductions in capacity (Fig.4.2). This indicates that an increase in the number of iterations might be needed to find a better solution.

To evaluate how the percentage of capacity reduction affects the convergence characteristics, the results obtained from a 50% capacity reduction are compared to those obtained from a 75% capacity reduction, as shown in Fig. 4.3 and Fig. 4.4[1]. The results show that as the capacity reduction increases, convergence is harder to achieve as the travel time is increased and it takes longer time to achieve equilibrium compared to the case of no capacity reduction in the network. This is clear in the case of a 100% reduction in capacity, as shown in appendix C, Figs. C.1, C.2, C.3, C.4, and C.5.

[1]The convergence results for all capacity reductions are included in Appendix C.

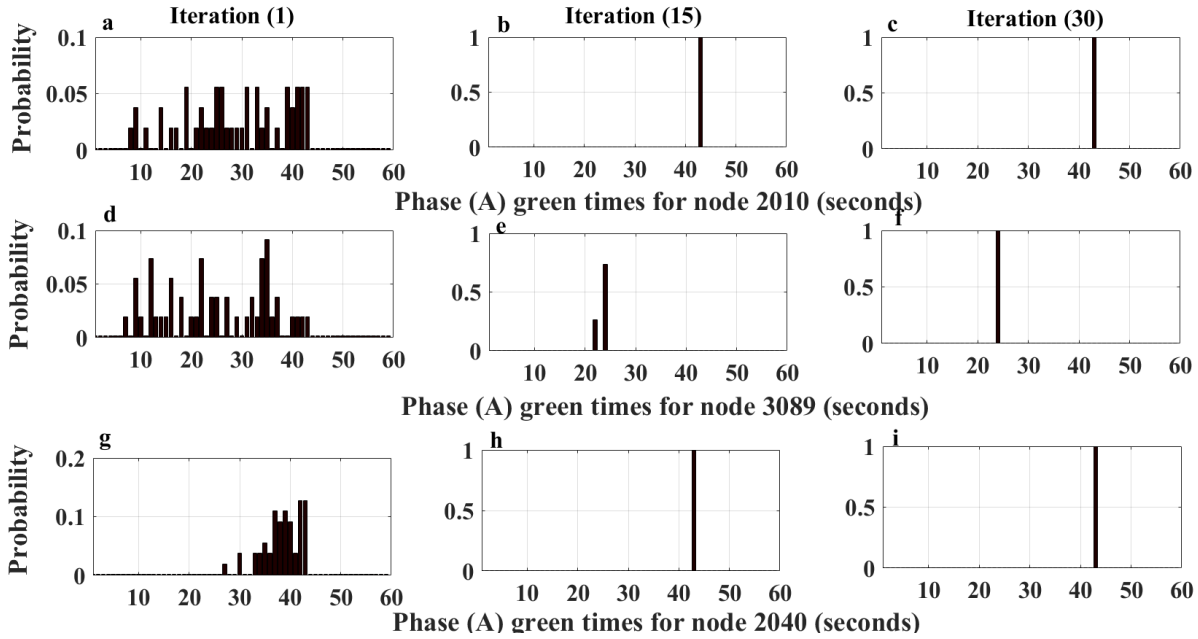

Figure 4.1: Convergence of Phase A green times for a 50% capacity reduction at node 2010, using the CEM-static framework, for nodes 2010 (a-c), 3089 (d-f), and 2040 (g-i)

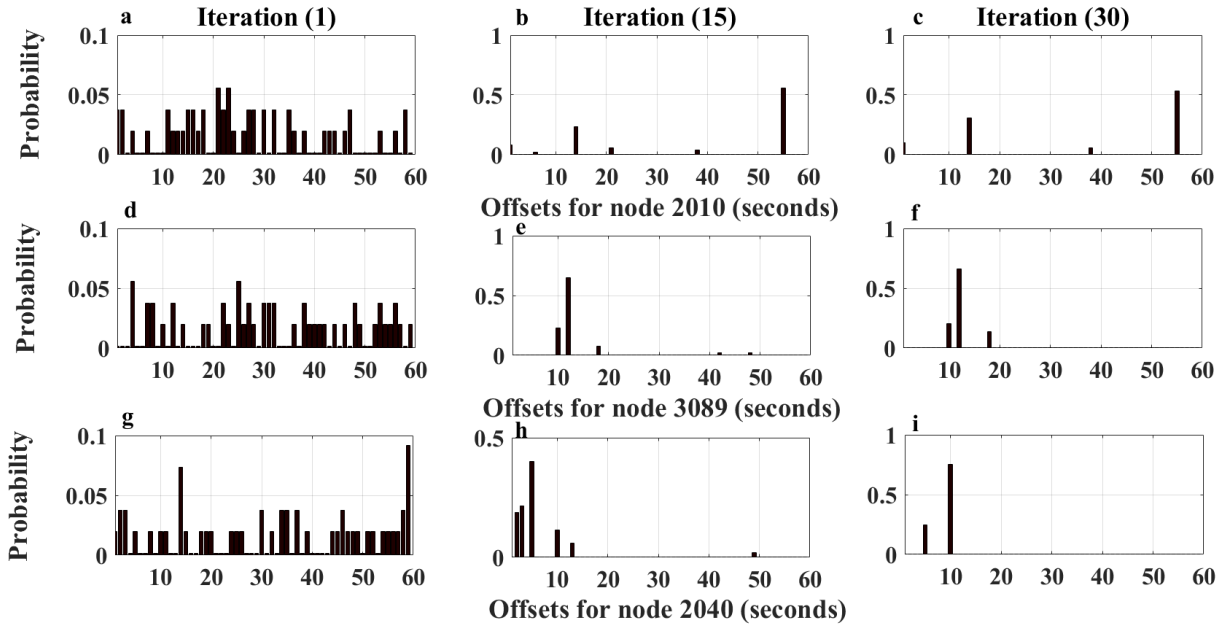

Figure 4.2: Convergence of the offsets for a 50% capacity reduction at node 2010, using the CEM-static framework, for nodes 2010 (a-c), 3089 (d-f), and 2040 (g-i)

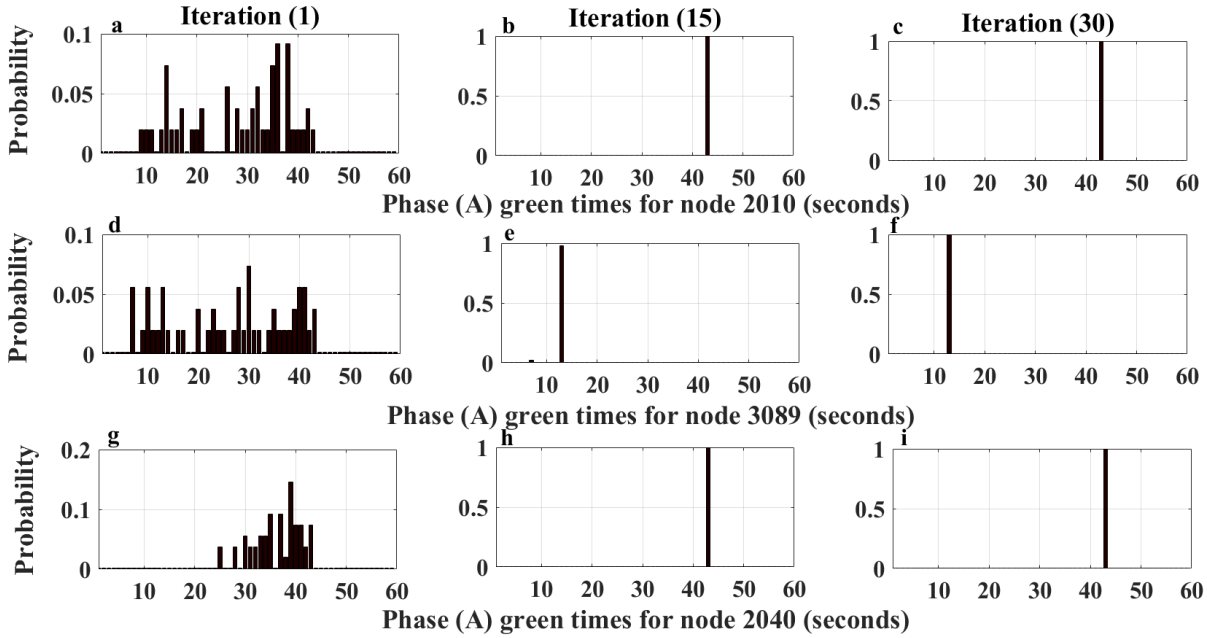

Figure 4.3: Convergence of Phase A green times for a 75% capacity reduction at node 2010, using the CEM-static framework, for nodes 2010 (a-c), 3089 (d-f), and 2040 (g-i)

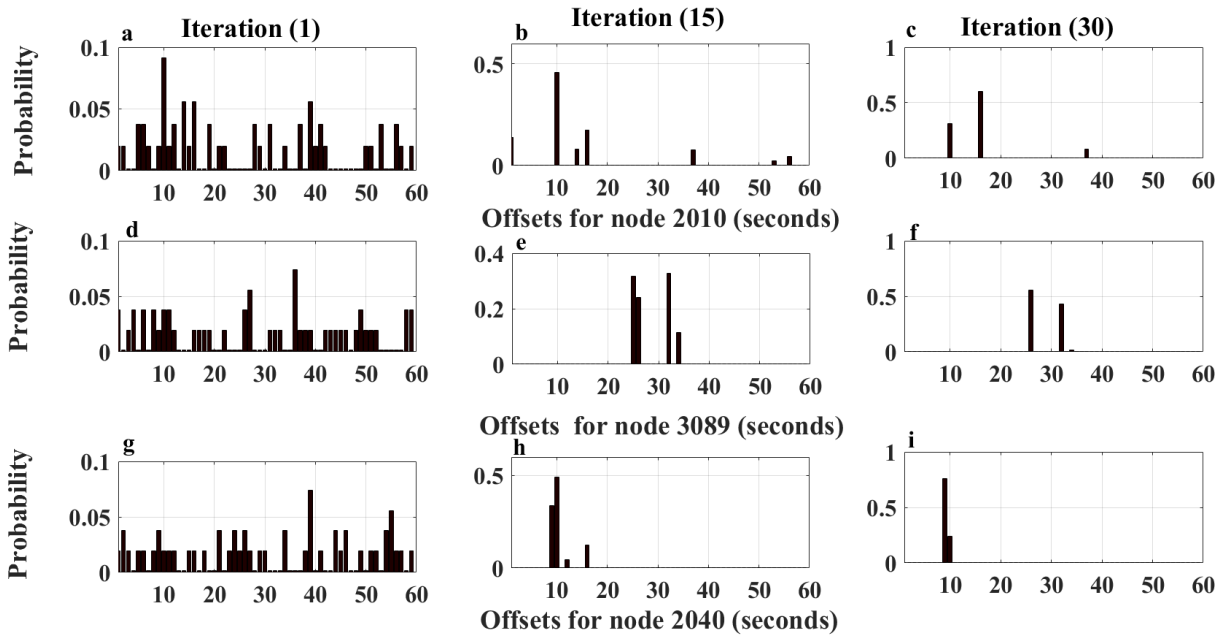

Figure 4.4: Convergence of the offsets for a 75% capacity reduction at node 2010, using the CEM-static, for nodes 2010 (a-c), 3089 (d-f), and 2040 (g-i)

Fig. 4.5 shows the convergence of the objective function (i.e. the travel time) for a 50% reduction in capacity. It can be seen that the mean of all solutions converged to a stable value of 17,976 hr after 12 iterations.

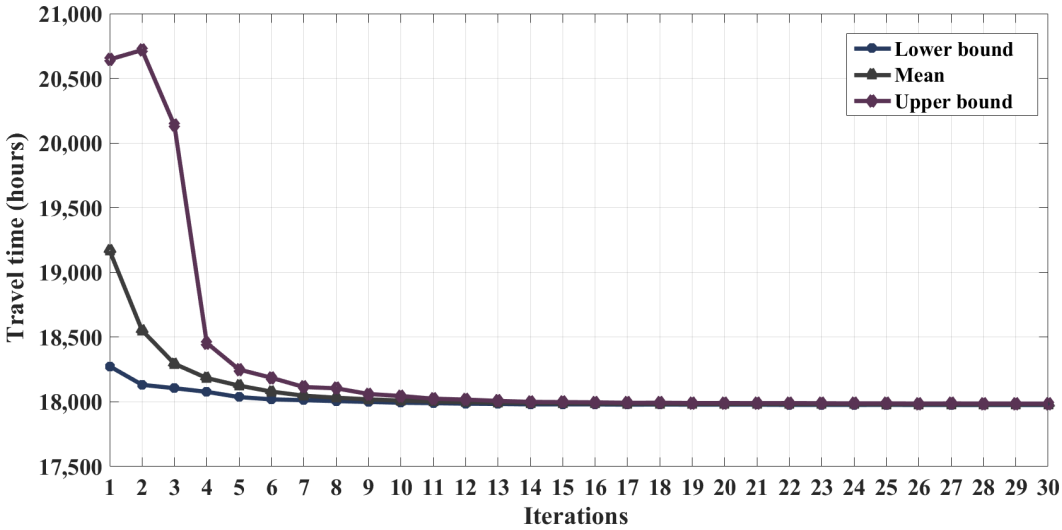

Figure 4.5: Convergence of the travel time for a 50% capacity reduction

Table 4.1 shows the travel time for all capacity reductions. The results indicate that the network performance is resilient to small capacity reductions. In contrast, large capacity reductions resulted in a pronounced increase in the travel time from 17,894 hr in the case of no capacity reduction to 18,777 hr for a complete reduction in capacity at node 2010. Fig. 4.6 depicts the travel time for different capacity reductions. As can be seen in Fig. 4.6, the travel time values increased as the percentage of capacity reduction increases. This increase is non-linear (a 5 hr increase in the case of a 25% reduction, a 77 hr increase in the case of a 50% reduction, a 274 hr increase in the case of a 75% reduction, and a 527 hr increase in the case of a 100% capacity reduction).

Table 4.1: Travel time (hours) for different capacity reductions at node 2010, using the CEM-static framework

% of capacity reduction	**0%**	**25%**	**50%**	**75%**	**100%**
Travel time (hours)	17,894	17,899	17,976	18,250	18,777

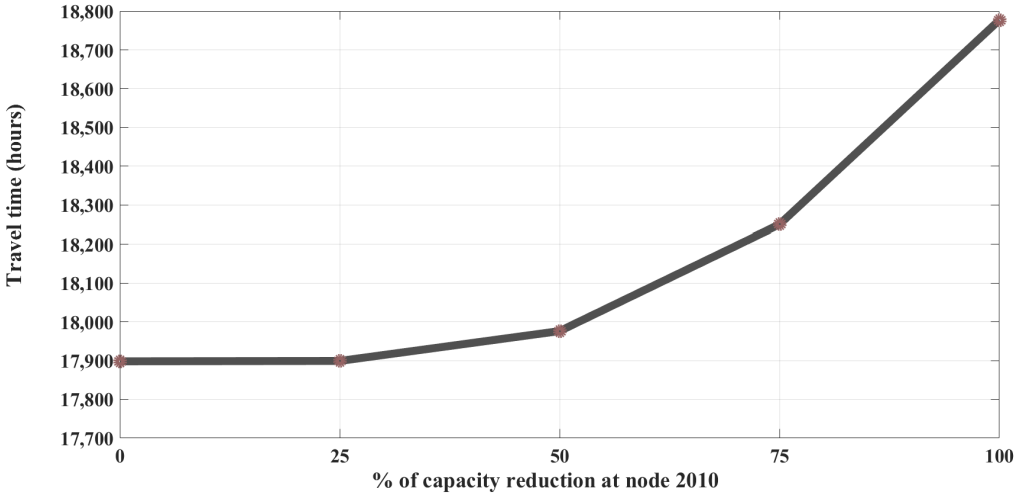

Figure 4.6: Travel time (hours) for different capacity reductions at node 2010, applying the CEM-static framework

In terms of signal settings, the results of Phase A green times and offsets simulating different blockage scenarios are summarised in Table 4.2 and Table 4.3, respectively, for node 2010, where the blockage occurs, and the adjacent nodes 3089, 2040, and 2045, along with the nearby nodes 2410, 2500, 2620, and 3080 [2]. These results are for 0%, 25%, 50%, 75%, and 100% capacity reductions at node 2010 for a period of one hour.

Table 4.2: Phase A green times for different nodes, applying the CEM-static framework

Capacity reduction	**0 %**	**25%**	**50%**	**75%**	**100%**	**Mean**	**STD**
Node 2010	40	40	43	43	40	41.2	1.64
Node 3089	18	18	24	26	34	24	6.6
Node 2040	43	43	43	43	43	43	0
Node 2045	43	43	43	43	43	43	0
Node 2410	15	17	22	29	32	23	7.4
Node 2500	24	22	27	27	22	24.4	2.5
Node 2620	23	14	23	12	21	18.6	5.2
Node 3080	29	26	31	37	31	30.8	4

[2]The Phase A green times and offsets results for the 24 signalised nodes are included in Appendix C.

Table 4.3: Offsets for different nodes, applying the CEM-static framework

Capacity reduction	**0 %**	**25%**	**50%**	**75%**	**100%**	**Mean**	**STD**
Node 2010	11	16	55	26	33	28.2	17.3
Node 3089	8	11	12	28	7	13.2	8.5
Node 2040	15	6	10	2	5	7.6	5.1
Node 2045	0	0	0	0	0	0	0
Node 2410	18	26	1	19	24	17.6	9.9
Node 2500	30	39	59	20	18	33.2	16.7
Node 2620	1	3	4	11	25	8.8	9.8
Node 3080	13	17	22	32	6	18	9.8

The results in Table 4.2 indicate that the Phase A green times for node 2010 and the surrounding nodes appear to be sensitive to capacity reduction (but not as sensitive as other nodes: 3089, 2410, and 2620). For example, if the case of no capacity reduction is taken as a base for comparison, it is clear that the Phase A green times at node 2010 do not change for small capacity reductions (i.e. 25%), but they rise for high capacity reductions (i.e. 50% and 75%) to reach the maximum Phase A green time allocation (i.e the upper bound). However, the Phase A green time decreases for a complete closure at node 2010 (i.e. 100% reduction). This suggests that the demand for reductions up to 75% is within the capacity of this intersection; however, for a complete closure, the intersection does not have sufficient capacity to meet the increased flows. Also, changes at other modes could mean a reduction in optimal Phase A green times at node 2010. The standard deviation for nodes 3089 and 2410 in Table 4.2 are the highest due to the fluctuation in the Phase A green times at these nodes.

The results of the adjacent and nearby nodes show how the degradation at one node affects the optimal signal settings at the nearby nodes (Table 4.2 and Fig.4.7). Those results show three trends: 1. an increase in the Phase A green times as at nodes 3089 and 2410, indicating that those nodes have enough capacity to accommodate increased flows at those nodes; 2. constant Phase A green times equal to the maximum green time allocation (i.e. 43 seconds) as at nodes 2040 and 2045 to meet the total demand, implying that there is no decrease in the traffic using Phase A at these intersections; 3. a fluctuation in Phase A green times at nodes 2500, 2620, and 3080. This could be due to the fact that drivers have a number of alternative routes to divert to; thus drivers can switch between alternative routes if there are several alternative routes. Overall, the three trends reflect that traffic arranges itself to achieve a state equilibrium, such that all users experience the lowest travel time, as SATURN assumes that drivers adjust

their route choice according to the signal settings.

SATURN captures the re-routing of drivers at node 2010, where the capacity reductions occur, and in the surrounding nodes. Fig. 4.7 shows how traffic is diverted away from node 2010 using nodes 2045 and 2040 in the case of a complete capacity reduction at node 2010. This indicates that the optimal signal settings at the node where the disruption occurs and at other signalised node in the vicinity of the node where the disruption occurs, can result in re-routing of drivers around the blockage.

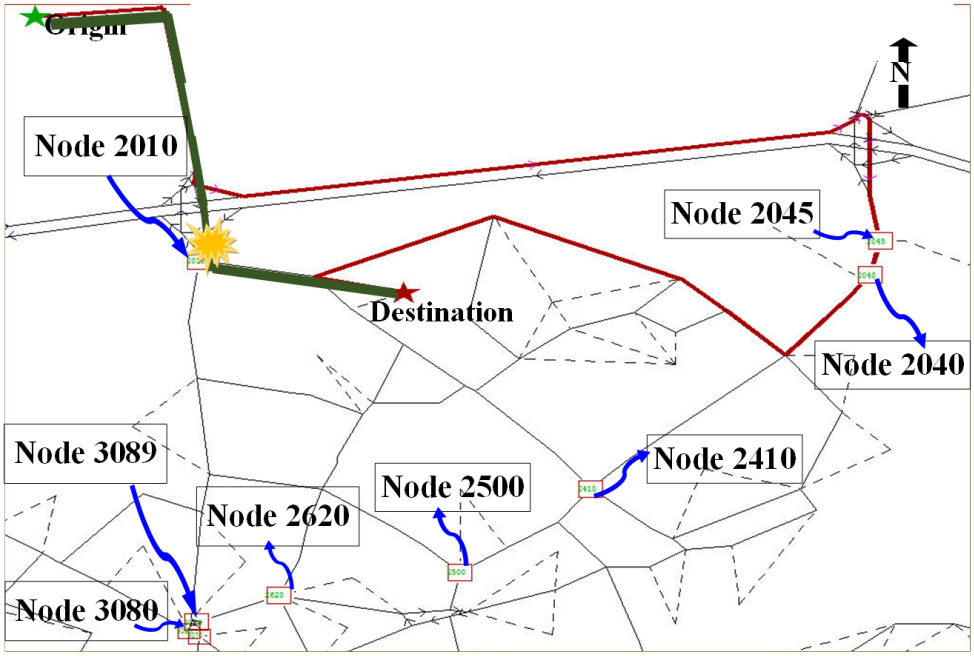

Figure 4.7: The optimum path obtained from SATURN with no reduction in capacity (green) and with a 100% reduction in capacity at node 2010 (red)

Moreover, the changes in the offsets, as the capacity reduction increases from 0% up to 100% , are non-linear (they tend to fluctuate), as can be seen in Table 4.3. For example, the offsets at node 2010 are: 11s, 16s, 55s, 26s, and 33s, respectively. This indicates that the offsets are sensitive to the changes in flow, which is in line with expectations as the green times between the 24 signalised nodes are related through offsets. This suggests increasing the number of iterations for offsets to achieve convergence, as discussed later in this chapter.

The network is analysed in terms of the node arrival flows (veh/hr) to show the effect of the disruption on the disrupted node 2010 and at the surrounding nodes.

This is presented using two 'heat maps', a graphical representation in which numeric values are presented as shades of grey, with no reduction in Fig. 4.8, and with a 50% reduction in capacity at node 2010 in Fig. 4.9. A 'heat map' shows contour lines, which are based on interpolating between values of the arrival flow rates at the nodes. The changes in the position of the contour lines show how far the effect of a disruption can spread. The arrival flow rate at node 2010 dropped from 2,916 veh/hr (with no capacity reduction) to 1,830 veh/hr (with a 50% reduction in capacity), while the arrival flows at the surrounding nodes 2040 and 3089 increased from 2,294 veh/hr and 1,376 veh/hr (with no capacity reduction) up to 3,050 veh/hr and 1,746 veh/hr (with a 50% reduction in capacity), respectively. This demonstrates how traffic was diverted around the disrupted node 2010 to nodes 2040 and 3089. This also indicates nodes in which the likelihood of congestion is higher than other nodes.

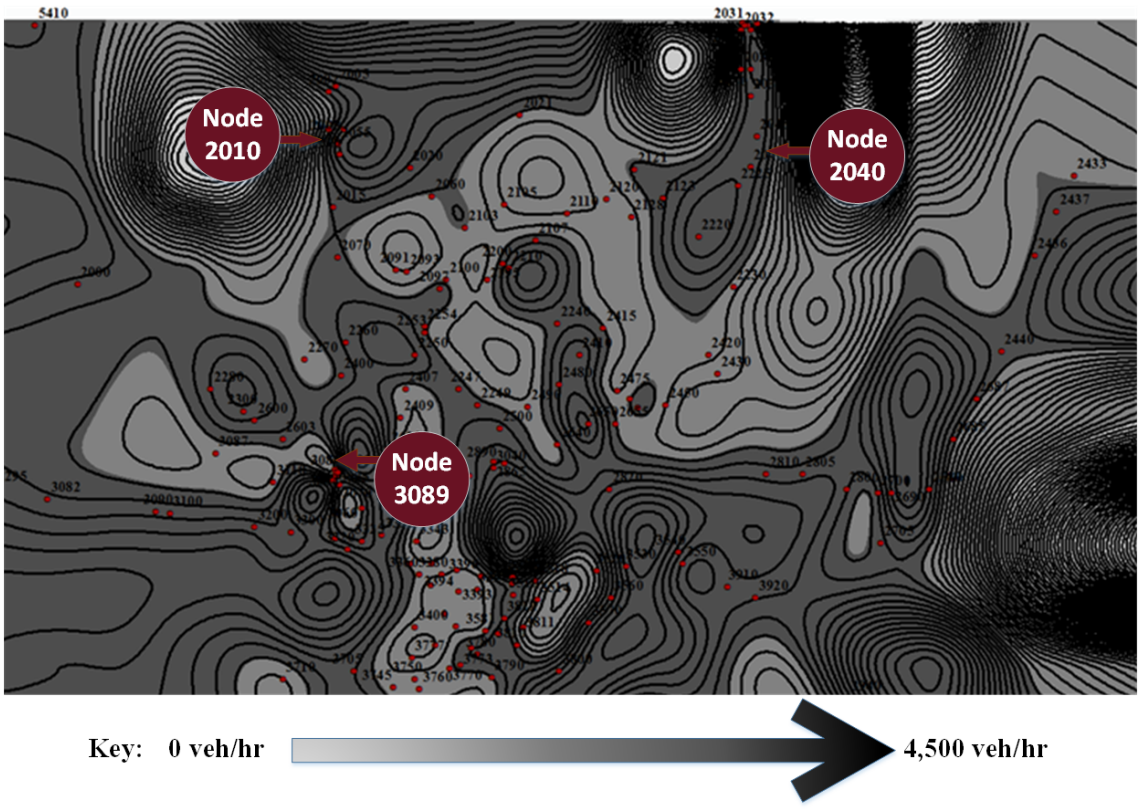

Figure 4.8: Dispersion of the traffic flow for no capacity reduction

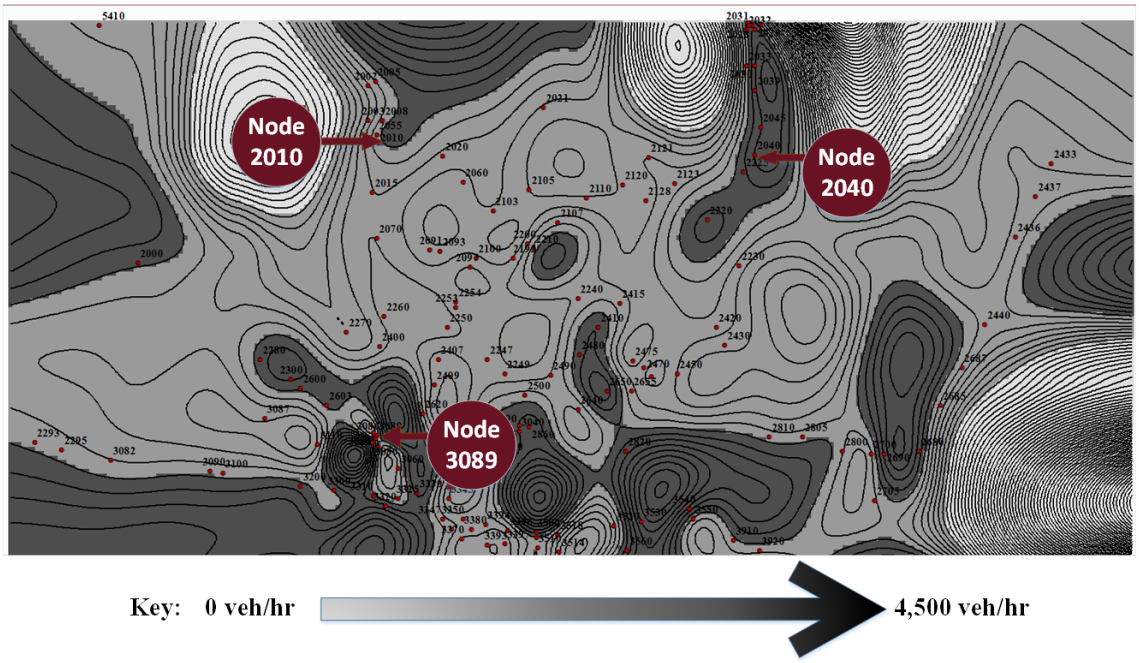

Figure 4.9: Dispersion of the traffic flow for a 50% capacity reduction at node 2010

4.2 Discussion of results

This chapter presented results for different blockage scenarios applying the static approach to simulate a one-hour time horizon to model a user's route choice behaviour in the period immediately following a disruptive event (during the recovery period). The results of applying the CEM-static framework to optimise the signal settings indicate that optimising traffic signal control to minimise the travel time can assist traffic to divert around blockages.

Several points can be observed from the results. Firstly, changes to the optimal signal settings at the node where the disruption occurs and at other signalised intersections in the vicinity of the node where the disruption occurs, can result in re-routing traffic around the disruption. Secondly, heat maps can be used to demonstrate how a disruption at one node affects the overall network. This representation can be used to get a better understanding of the impacts of network disruptions on network reliability in the case of disruption at one or more nodes. Thirdly, it was noticed that the level of reduction in capacity (i.e. 25% up to a complete closure) has an impact on convergence. For instance, the Phase A green time convergence was quicker for a 25% reduction in capacity (i.e. it takes less iterations) than a complete reduction in capacity. Fourthly, the offset results

show that the offset timings take longer to converge. In addition, the offsets show a higher tendency to fluctuate than the green times, as the offsets depend on the convergence of the 24 signalised intersections at the same time.

One should keep in mind that the impact of a one node closure depends on the characteristics of the road network and how sparse the network is (the number of alternative routes), as will be discussed in Chapter 7.

4.3 Conclusions

This chapter presented and discussed the results of applying the CEM-static framework. As discussed in this chapter, it was noticed that the level of reduction in capacity (i.e. 25% up to a complete closure) has an impact on convergence. For instance, the Phase A green time convergence was quicker for a 25% reduction in capacity (i.e. it takes less iterations) than a complete reduction in capacity. The offset results show that the offset timings take longer to converge.

The following chapter will present the results and discussion of applying the CEM-semi approach, then will compare the results to the CEM-static approach, to evaluate which approach gives better results in terms of minimising the travel times and the convergence of the signal settings (i.e. green times and offsets).

CHAPTER 5

SEMI-DYNAMIC ASSIGNMENT APPROACH

5.1 Semi-dynamic assignment results

This chapter describes the results obtained from applying the CE method, along with the semi-dynamic assignment model embedded in SATURN (CEM-semi), to the Cambridge (UK) network. The semi-dynamic approach allows for simulating small disruption durations (i.e. 4 minutes) unlike the static approach. Using this approach, the simulated hour was divided into 4-minute (i.e. 15 time slices) to test various degradation durations (4, 20, 36, and 60 minutes) and capacity reductions (25%, 50%, 75%, and 100%), as described in Chapter 3, Table 3.3a. It should be noted that all capacity reductions are centered on the mid-point of the hour (Fig. 5.1).

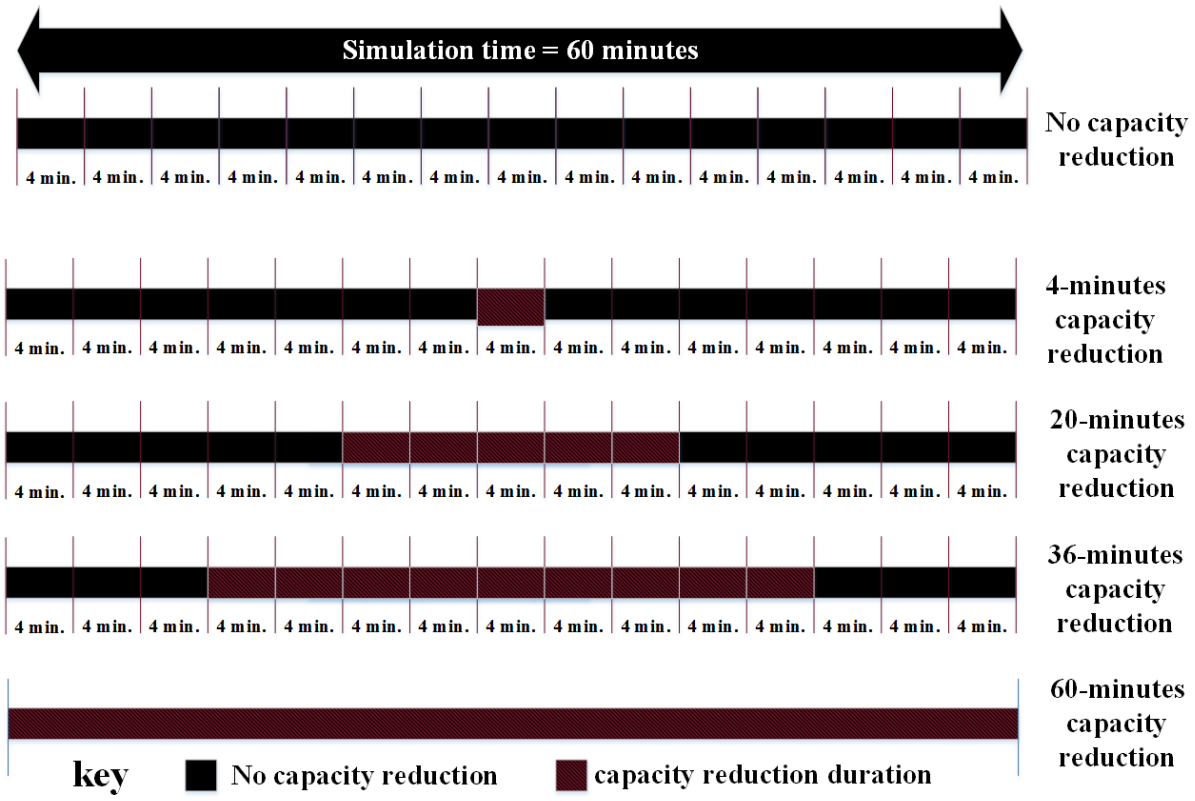

Figure 5.1: Capacity reduction durations

The Phase A green times and offsets convergence results for a 50% capacity reductions for 60 minutes[1] are shown in Figs. 5.2 and 5.3, respectively. The results are for node 2010, where the blockage occurs, and the nearby signalised nodes, 3089 and 2040. The results show that Phase A green times and offsets converged after 30 iterations to one stable value. Fig. 5.4 and Fig. 5.5 show the convergence results of Phase A green times for a 75% reduction in capacity for 60 minutes. The Phase A green times converged after 30 iterations, but the offsets did not converge for node 2010 where the blockage occurred. The convergence of offsets for node 3089 could converge to a value of 21s as the probability of this value is 0.8. The offsets for node 2040 converged to a value of 43s. Overall, the offsets convergence results indicate that the offsets convergence is harder to achieve as the percentage of capacity reductions increases. This is consistent with the results of CEM-static bi-level framework.

[1]Those results are highlighted in grey in Tables 5.1 and 5.2 for Phase A green times and offsets, respectively. The results of other time intervals are also included in those tables.

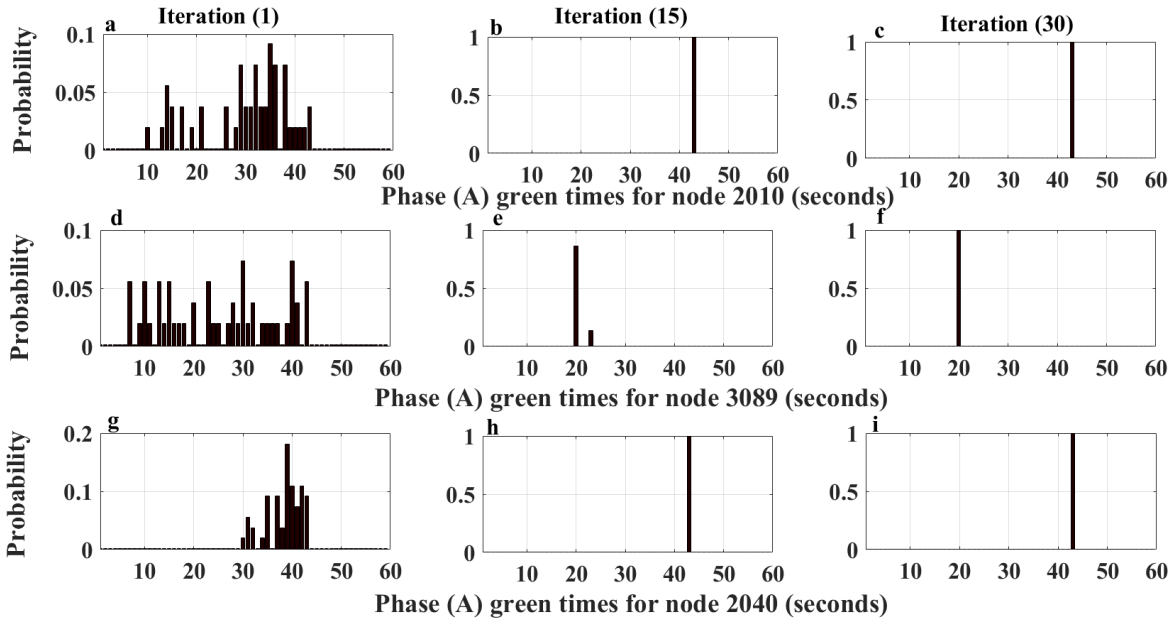

Figure 5.2: The convergence of Phase A green times for a 50% capacity reduction at node 2010 for 60 minutes, applying the CEM-semi framework, for nodes 2010 (a-c), 3089 (d-f), and 2040 (g-i)

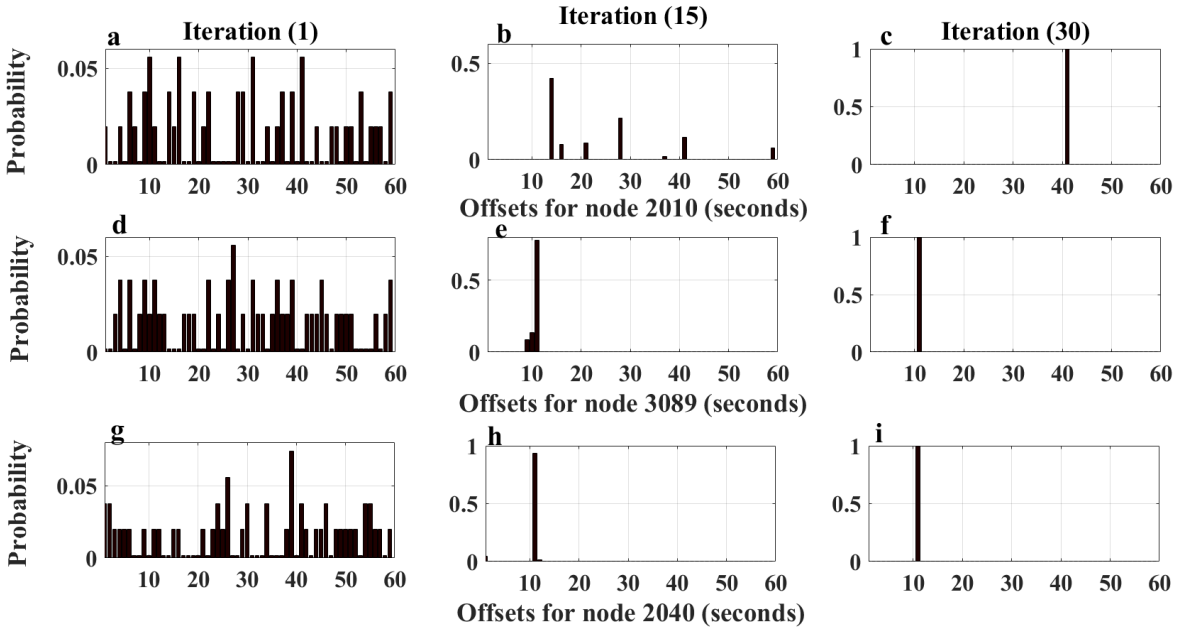

Figure 5.3: The convergence of offsets for a 50% capacity reduction at node 2010 for 60 minutes, applying the CEM-semi framework, for nodes 2010 (a-c), 3089 (d-f), and 2040 (g-i)

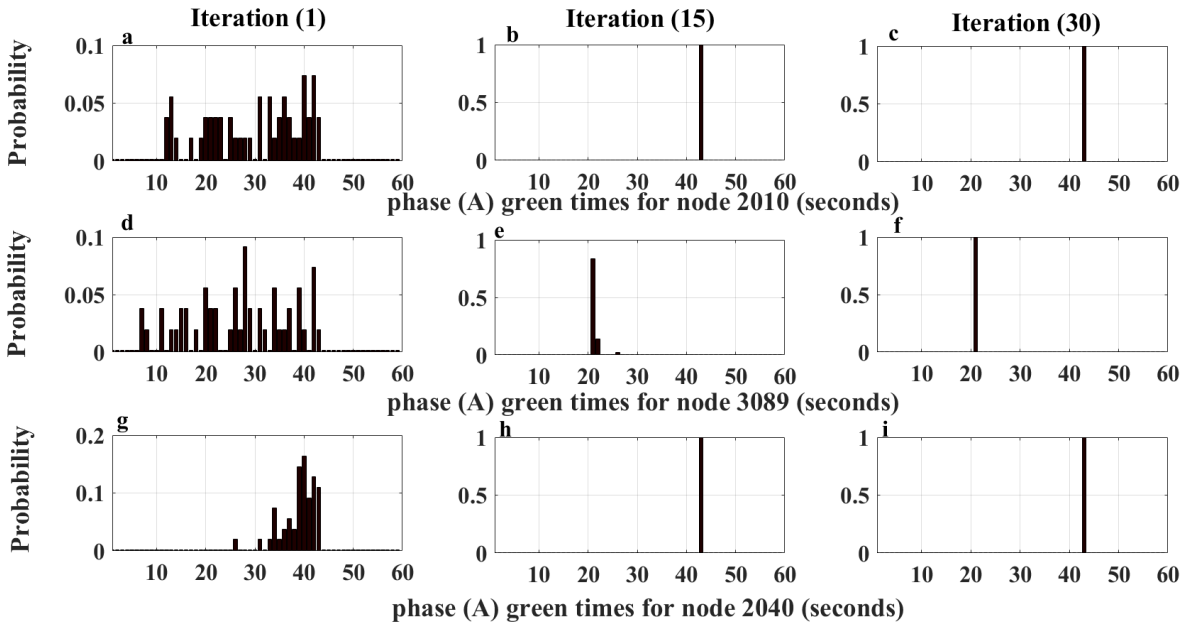

Figure 5.4: The convergence of Phase A green times for a 75% capacity reduction at node 2010 for 60 minutes, applying the CEM-semi framework, for nodes 2010 (a-c), 3089 (d-f), and 2040 (g-i)

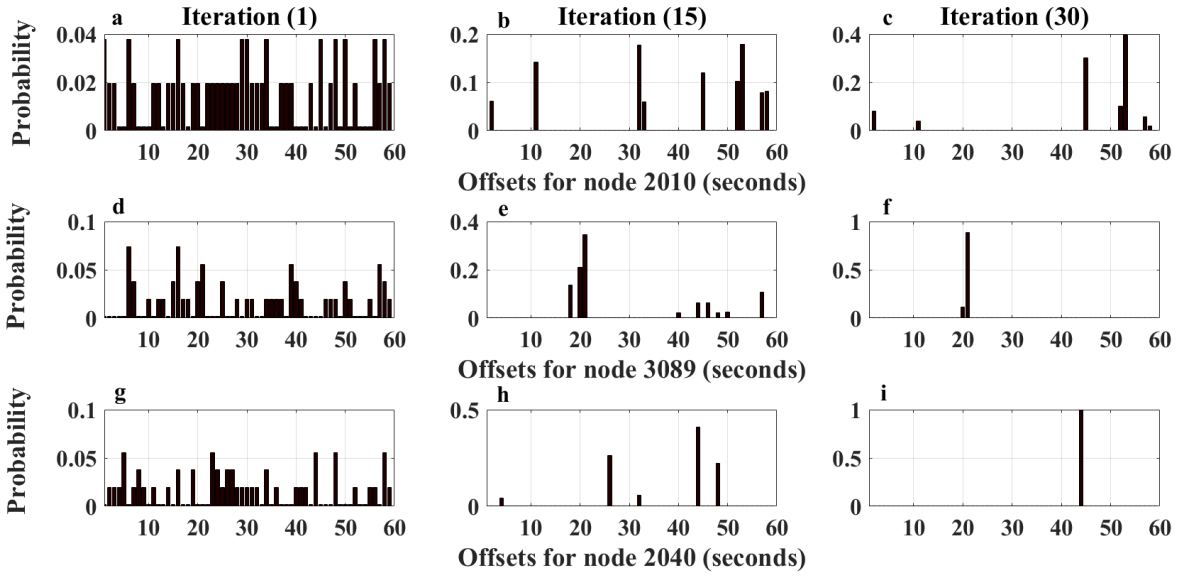

Figure 5.5: The convergence of offsets for a 75% capacity reduction at node 2010 for 60 minutes, applying the CEM-semi framework, for nodes 2010 (a-c), 3089 (d-f), and 2040 (g-i)

The results indicate that the travel time increases as the duration of the degradation and/or the capacity reduction increase. Fig. 5.6 depicts the relation between the travel time, capacity reductions, and reduction durations. Across all capacity reductions, a 25% reduction in capacity for 60 minutes results in a small increase in the travel time (about 4 hrs), compared to no reduction in capacity, while a 100% reduction in capacity for 60 minutes results in an increase of about 774 hrs in the travel time (Fig. 5.7). This confirms that the network performance is more robust to small reductions in capacities than large reductions in capacities. This is due to the spare capacity available in the network to accommodate some disruption. However, one should keep in mind that this also depends on how sparse the road network is (i.e. the availability of alternative routes). For instance, travel demand in dense networks is less elastic than sparse networks due to the availability of alternative routes and trips generally being short.

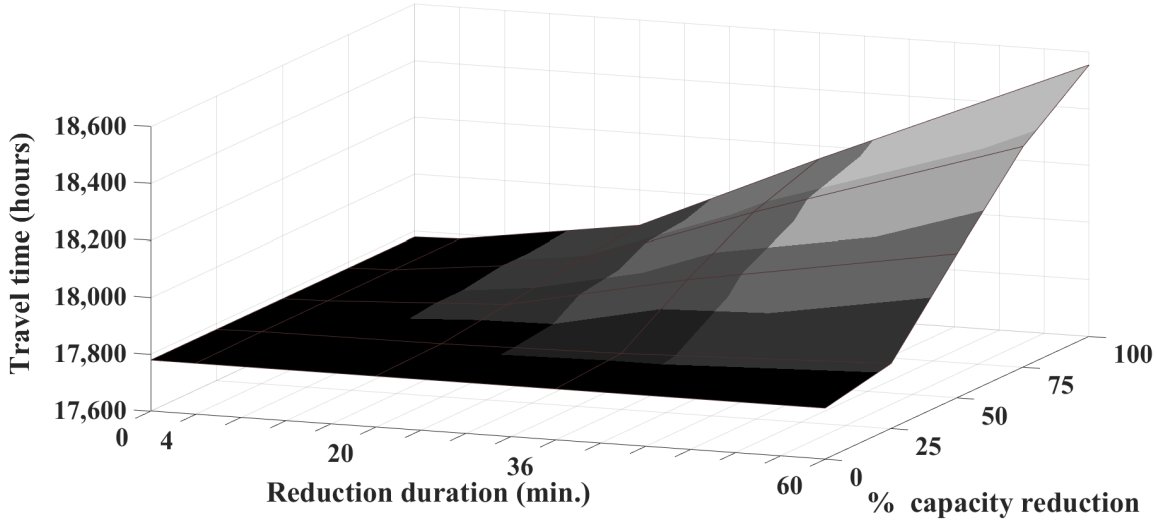

Figure 5.6: Travel times for different capacity reductions and durations

To have a better understanding of the traffic behaviour for each duration, Figs. 5.8 depicts the travel time for different reduction durations (4, 20, 36, and 60 minutes) and different capacity reductions (0%, 25%, 50%, 75%, and 100%). If no capacity reduction is taken as a base to compare, it is clear that the differences in the travel time for all capacity reductions for small durations are very small. One might expect $\Delta 4$ to be larger than $\Delta 3$ but it seems not to be the case.

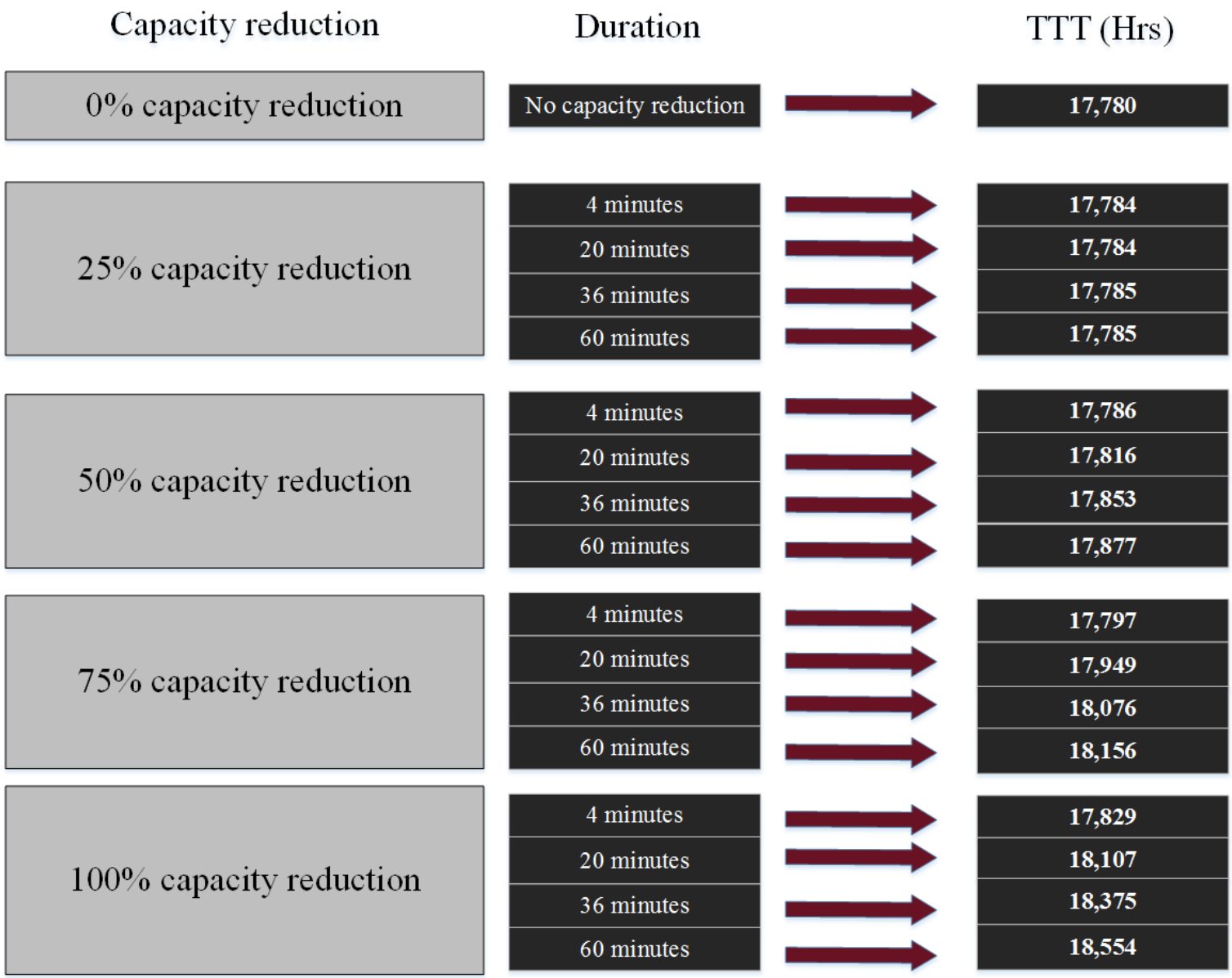

Figure 5.7: The corresponding travel time for each degradation scenario

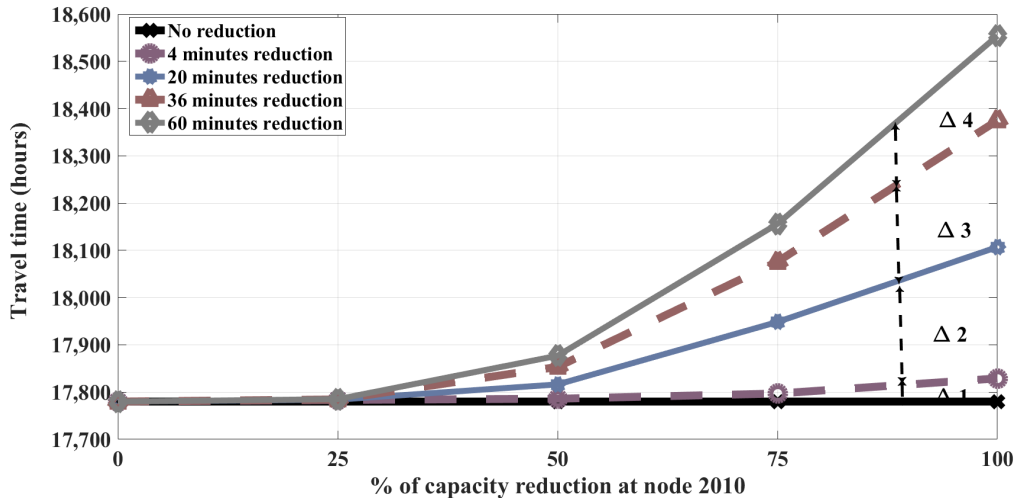

Figure 5.8: The travel time (hours) for different combinations of duration and reduction

Fig. 5.9 shows the convergence of the objective function (i.e. the travel time) for a 50% reduction in capacity for 60 minutes. It can be seen that the mean of all solutions converged to a stable value of 17,877 hr after 15 iterations.

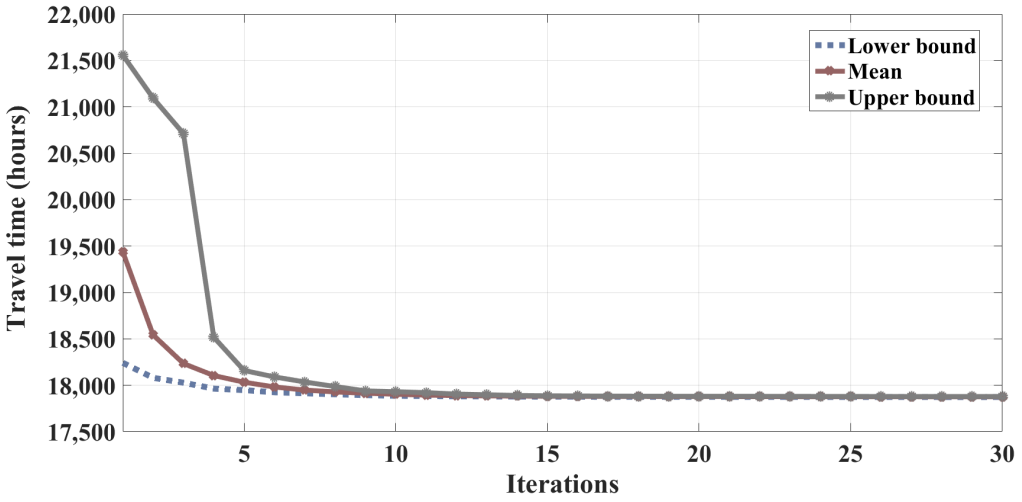

Figure 5.9: The travel time convergence for a 50% capacity reduction for 60 minutes

In terms of signal settings, the results of Phase A green times are summarised in Table 5.1[2]. As it can be seen in Table 5.1, the results of the Phase A green times show that when the capacity at node 2010 is reduced by 50% for various reduction durations (i.e. 4, 20, 36, and 60 minutes), the Phase A green times at the disrupted node 2010, and nodes 2040, 2045, and 2500, are almost constant. This suggests that there is no decrease in traffic at those nodes. Moreover, the Phase A green times at nodes 2410, 2620, and 3080 increase slightly as the duration of the blockage increases. This implies that there is an increase in traffic at those nodes. Additionally, the Phase A green times results show very small changes at all nodes (up to 2 seconds) in the case of a 50% capacity reduction for a short duration (i.e. 4 minutes) compared to a no reduction scenario, which indicates that there is plenty of spare capacity to accommodate the flows resulting from this reduction in capacity. The standard deviation of Phase A green times for nodes 2410 and 2620 in Table 5.1 are the highest due to the fluctuation in the Phase A green times at these nodes.

Table 5.1: Phase A green times for a 50% reduction in capacity at node 2010, using the CEM-semi framework

Duration	**0 min.**	**4 min.**	**20 min.**	**36 min.**	**60 min.**	**Mean**	**STD**
Node 2010	42	42	43	43	43	42.6	0.5
Node 3089	20	18	23	23	20	20.8	1.9
Node 2040	42	42	43	43	43	42.6	0.5
Node 2045	43	43	43	43	43	43	0
Node 2410	16	16	19	20	23	18.8	2.6
Node 2500	23	24	23	24	24	23.6	0.5
Node 2620	9	9	14	16	17	13	3.4
Node 3080	26	28	29	29	29	28.2	1.2

The offset results for a 50% capacity reduction for various reduction durations revealed that the offsets tend to fluctuate considerably as the duration of the degradation increases (Table 5.2). For example, the offsets at node 2010 are 39s for 0 minutes, 28s for 4 minutes, 28s for 20 minutes, 7s for 36 minutes, and 41s for 60 minutes. This means that the offsets are sensitive to the duration of the degradation. One should note that node 2045 is set as a reference point (i.e. the time all offsets are referenced to), so the offset at node 2045 is 0. Moreover, the standard deviations for nodes 2620 and 3080 in Table 5.2 are the highest due to the fluctuation in offsets at these nodes.

[2]The signal settings results for all capacity reductions are included in Appendix D.

Table 5.2: Offsets for a 50% reduction in capacity at node 2010, using the CEM-semi framework

Duration	**0 min.**	**4 min.**	**20 min.**	**36 min.**	**60 min.**	**Mean**	**STD**
Node 2010	39	28	28	7	41	28.6	13.5
Node 3089	12	7	6	11	11	9.4	2.4
Node 2040	16	15	29	23	11	18.8	7.15
Node 2045	0	0	0	0	0	0	0
Node 2410	38	32	26	26	24	29.2	5.2
Node 2500	36	30	20	25	17	25.6	6.8
Node 2620	11	2	54	44	18	25.8	19.8
Node 3080	17	10	6	13	55	20.2	17.7

The Phase A green times and offsets results discussed above are for different reduction durations. To have a better understanding of how the degradation at one node affects other nodes in the network across different capacity reductions, the Phase A green times and offsets for the 24 signalised nodes for different capacity reductions for 60 minutes are presented in Figs. 5.10 and 5.11, respectively.

Those signal settings seem to fluctuate, when optimising the travel time, as the percentage of the capacity reduction increases. However, the offsets seem to be more sensitive (Fig. 5.11) than the Phase A green times (Fig. 5.10). Fig. 5.12 depicts how the optimal Phase A green times for the 24 signalised intersections changed for different capacity reductions and durations. As the percentage of the capacity reduction increases (Fig. 5.12), the optimal Phase A green times increase at some nodes and decrease at others across different durations. For example, for a 25% reduction in capacity, the optimal Phase A green times increase at nodes 4550, 3070, 4400. For a 50% reduction in capacity the Phase A green times increase at nodes 4740, 4500, 4550, 2500, and 3070, and decrease at nodes 2620 and 2680. For a 75% reduction in capacity, the optimal Phase A green times increase at 4740, 4580, 4500, 2410, and 2500, but decrease at nodes 3070, 3560, and 2680. For a 100% reduction in capacity, there is an increase at nodes 4740, 4580, 4360, and 2500, and in contrast, a decrease at nodes 3070 and 3330. Interestingly, the Phase A green times increase for nodes 4580, 4550 and 4740, which are located on the edge of the central area (the area which includes the 24-signalised intersections) and far from node 2010 (see Fig. 3.5, Chapter 3). Fig. 5.13, on the other hand, shows how offsets fluctuate for nearly all capacity reductions and durations. The shape of the offsets profile changes between 4, 20, 36, and 60 minutes and between 25%, 50%, 75%, and 100% capacity reductions.

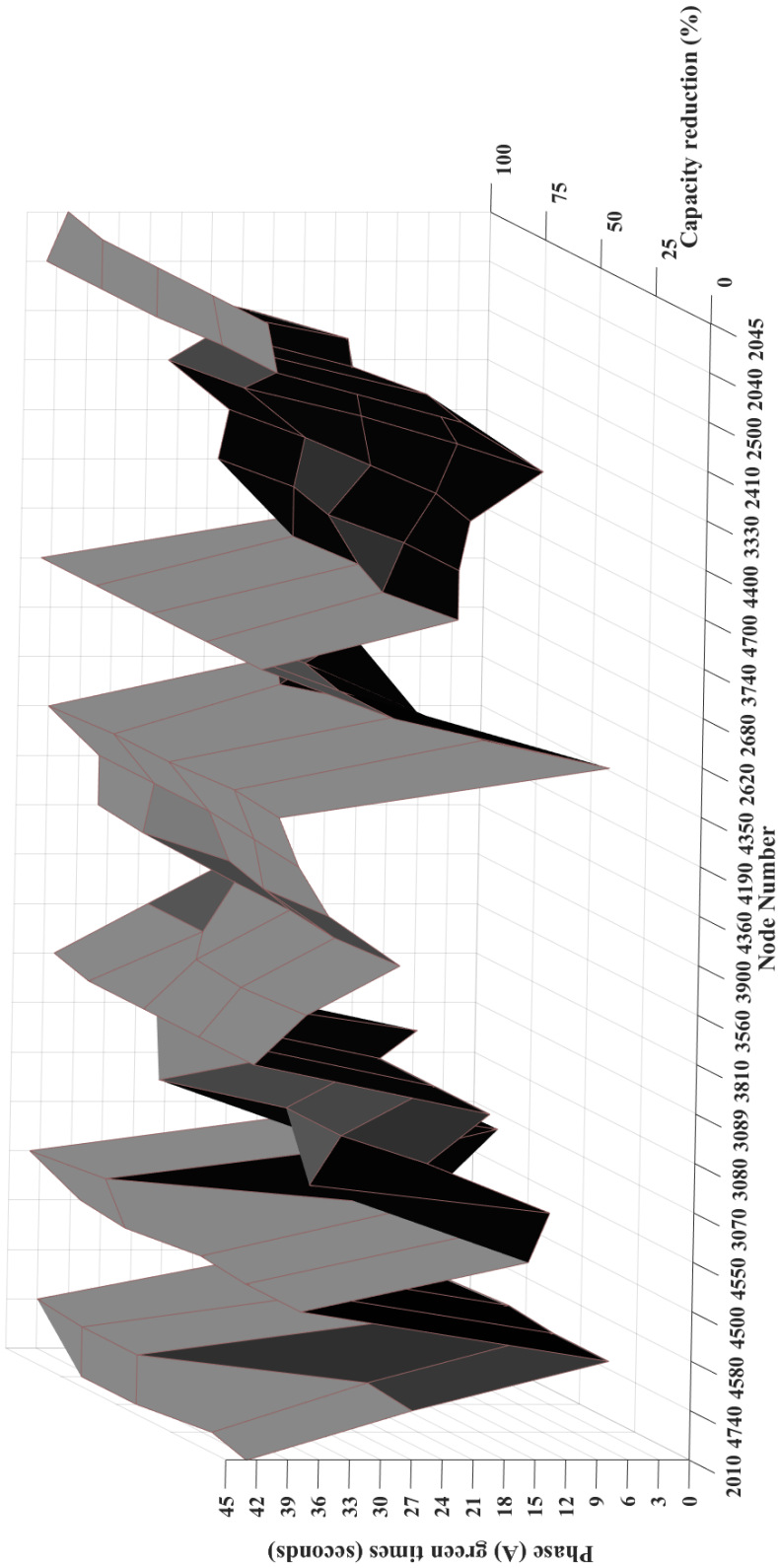

Figure 5.10: Phase A green times for all capacity reductions of 60 minutes duration

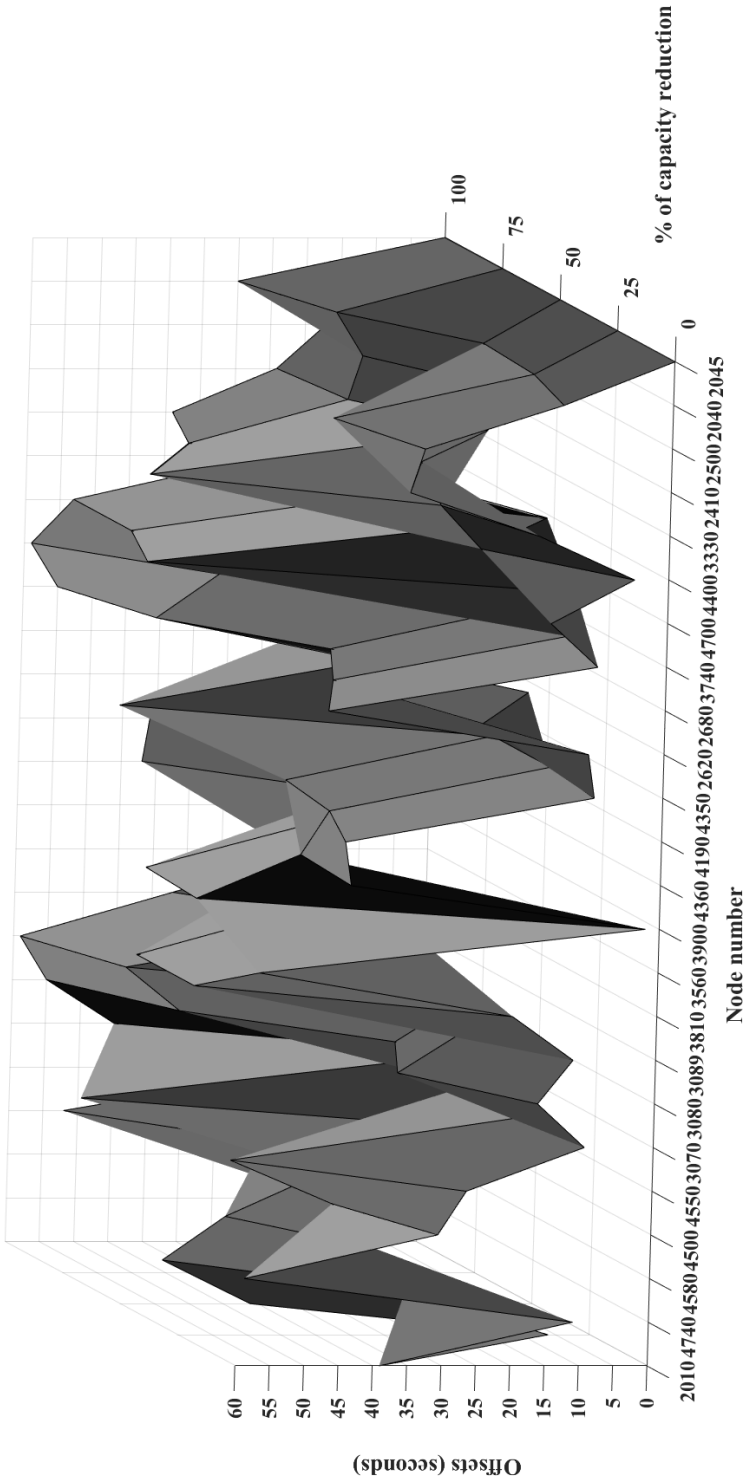

Figure 5.11: Offsets for all capacity reductions of 60 minutes duration

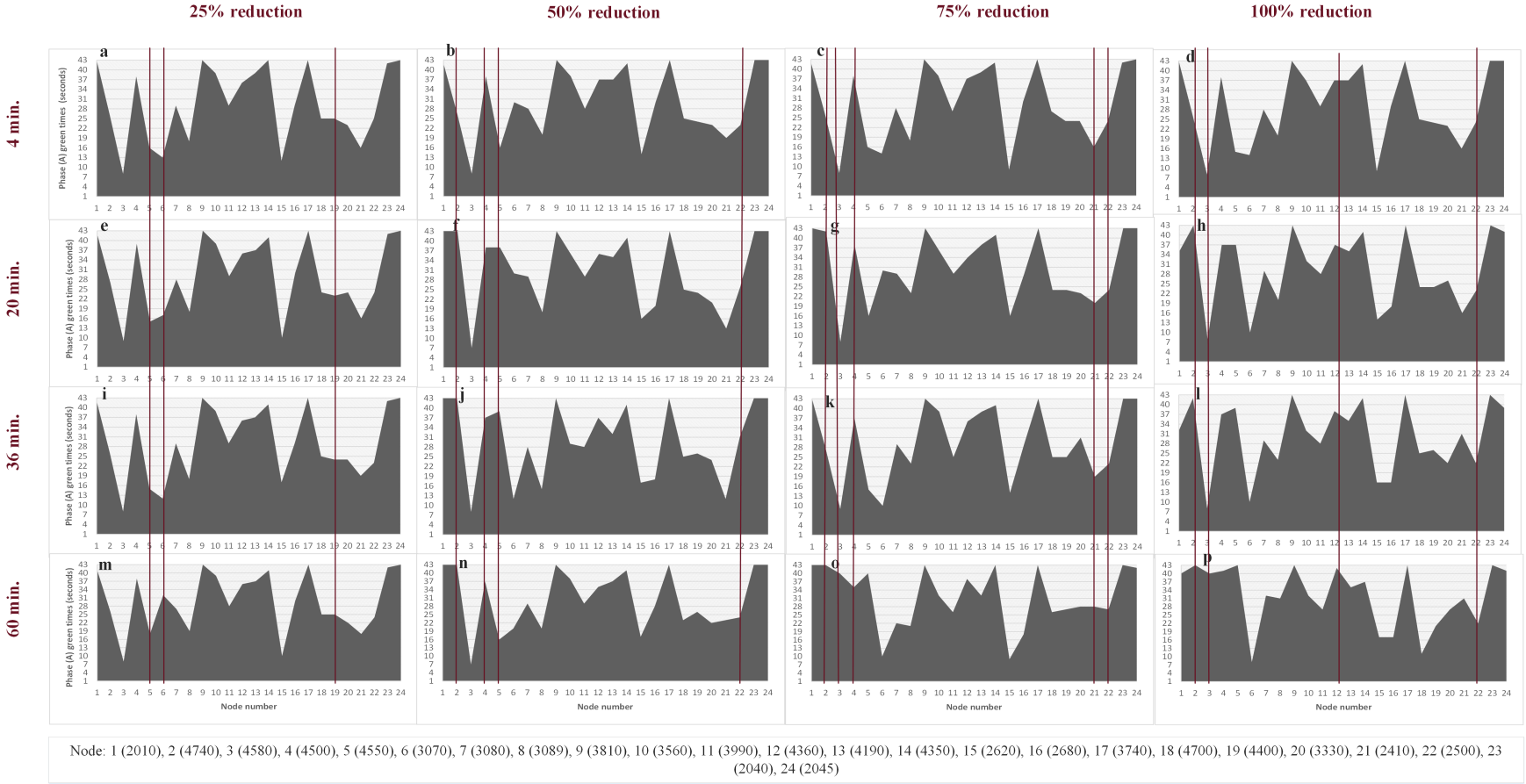

Figure 5.12: Phase A green times for all nodes for all capacity reductions and durations

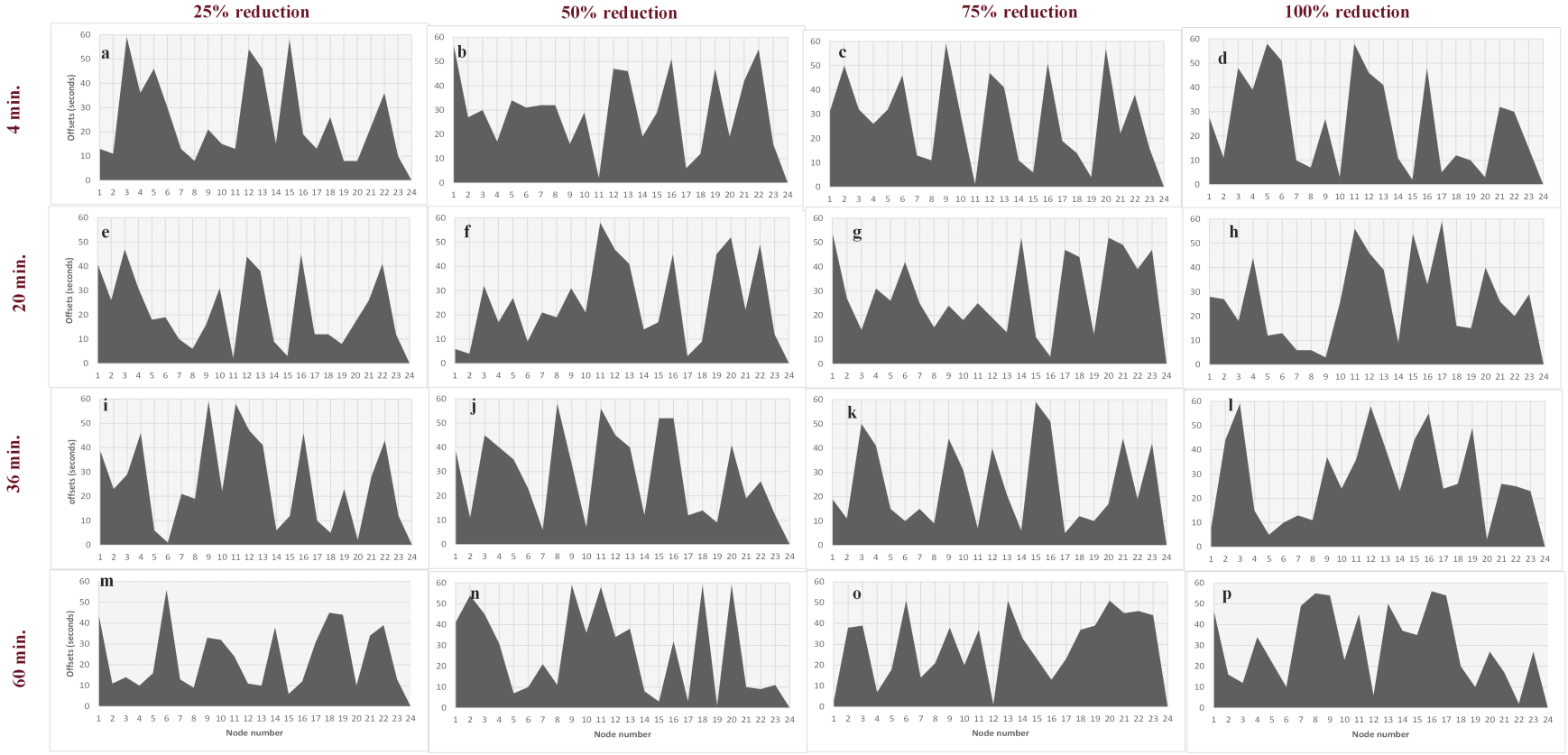

Node: 1 (2010), 2 (4740), 3 (4580), 4 (4500), 5 (4550), 6 (3070), 7 (3080), 8 (3089), 9 (3810), 10 (3560), 11 (3990), 12 (4360), 13 (4190), 14 (4350), 15 (2620), 16 (2680), 17 (3740), 18 (4700), 19 (4400), 20 (3330), 21 (2410), 22 (2500), 23 (2040), 24 (2045)

Figure 5.13: Offsets for all nodes for all capacity reductions and durations

To check the sensitivity of the optimal signal settings (Phase A green times and offsets) to the capacity reductions, Table 5.3 summarises the mean (of all capacity reductions: 0%, 25%, 50%, 75%, and 100% for 60 minutes), the standard deviation, and the coefficient of variation (CV).

Table 5.3: The mean, standard deviation, and coefficient of variation for Phase A green times and offsets

Nodes		**Green times (seconds)**			**Offsets (seconds)**		
No.	**Node**	**Mean**	**STD**	**CV**	**Mean**	**STD**	**CV**
1	2010	41.8	1.17	0.03	31.6	16.81	0.53
2	4740	36.4	8.09	0.22	33.6	17.28	0.51
3	4580	20.6	15.84	0.77	33.2	17.38	0.52
4	4500	37.6	1.96	0.05	17.4	12.47	0.72
5	4550	26.4	12.40	0.47	23.2	15.69	0.68
6	3070	19.8	9.68	0.49	32.4	19.56	0.60
7	3080	27.4	3.26	0.12	30	17.41	0.58
8	3089	22.2	4.45	0.20	28.4	18.71	0.66
9	3810	43	0.00	0.00	43	11.37	0.26
10	3560	36	3.29	0.09	34	13.78	0.41
11	3990	28	1.41	0.05	38.4	12.21	0.32
12	4360	37.2	2.64	0.07	11	11.98	1.09
13	4190	35.4	1.85	0.05	41.2	16.77	0.41
14	4350	40.2	2.04	0.05	28.6	11.00	0.38
15	2620	13.8	3.54	0.26	20.8	14.18	0.68
16	2680	24.4	5.68	0.23	31.2	17.06	0.55
17	3740	43	0.00	0.00	29.8	16.85	0.57
18	4700	22	5.59	0.25	36.6	14.57	0.40
19	4400	24.6	2.06	0.08	27	17.85	0.66
20	3330	24	2.90	0.12	39.2	18.05	0.46
21	2410	23.2	5.71	0.25	29.2	13.47	0.46
22	2500	24	1.67	0.07	28.8	19.38	0.67
23	2040	42.6	0.49	0.01	22.2	12.22	0.55
24	2045	42.4	0.80	0.02	0	0.00	0.00

The CV values for Phase A green times are shown in Fig. 5.14. Four regions of CV values can be defined: 1. low CV values (0 - < 0.1); 2. medium CV values (about 0.1 - < 0.3); 3. high CV values (0.3 - < 0.5); 4. very high CV values (0.5 - < 0.8). As can be seen in Fig. 5.14, the CV values for the green times are high for the nodes that are located on the alternative routes where the traffic is diverting, for example, nodes 2410, 2620, 3089, and 3070. The CV values for those nodes are 0.25, 0.26, 0.20, and 0.49, respectively.

This implies that there is a pronounced change in the Phase A green times for different capacity reductions as traffic is diverted away from node 2010 towards those nodes. Moreover, it is interesting to note high CV values for nodes 4740, 4580, 4550, 4700, and 2680. The CV values for those nodes are 0.22, 0.77, 0.47, 0.25, and 0.23, respectively. Those nodes are located far from node 2010 (Fig. 3.5, Chapter 3) and in the edges of the central area. The CVs for offsets, on the other hand, are shown in Fig. 5.15. Five regions of CV values can be identified: 1. low (0 - < 0.20); 2. medium (0.2 - < 0.42); 3. high (0.42 - < 0.77); 4. very high (0.77 - < 1); 5. extremely high (above 1). Nodes 4360, 4500, 2620, 2500, 4400, 3089, and 3070 are more sensitive to degradations in capacity in the road network, as those nodes have the highest CV values (1.09, 0.72, 0.68, 0.67, 0.66, 0.66, and 0.60).

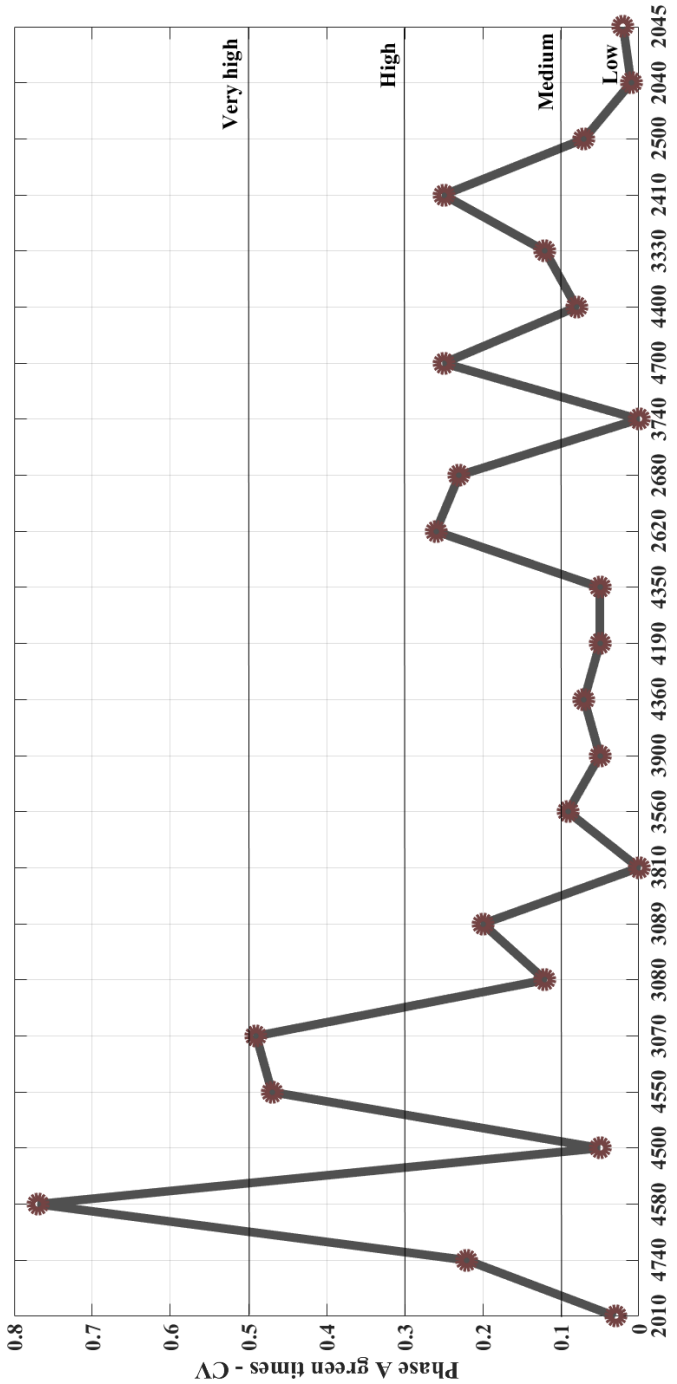

Figure 5.14: Coefficient of variation for Phase A green times

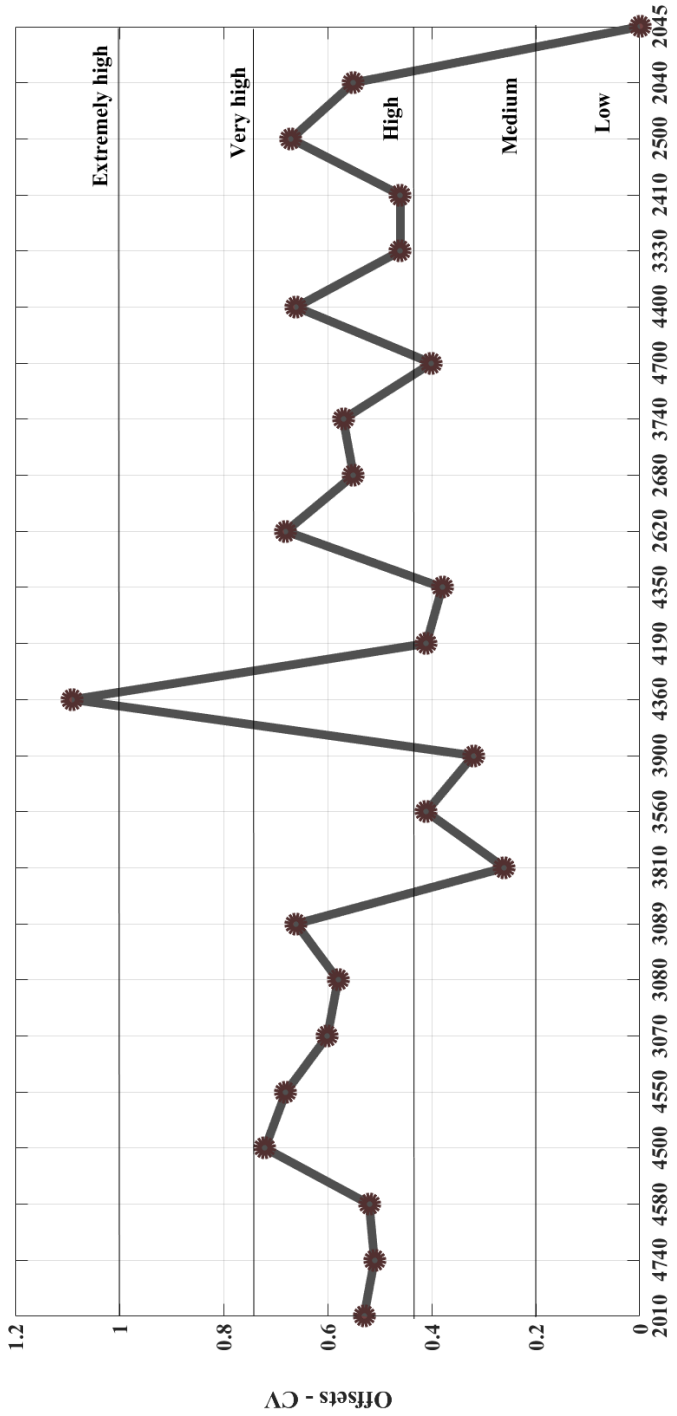

Figure 5.15: Coefficient of variation for offsets

5.2 Comparison of the static and semi-dynamic assignments

This section compares and summarises the results of applying the CEM-static and CEM-semi bi-level framework when minimising the travel time. As only 60 minutes degradation was applied in the CEM-static, the same partial and complete blockages duration (i.e. 60 minutes) are used as a base to compare all capacity reductions (i.e. 25%, 50%, 75%, and 100%).

The convergence characteristics of the CEM-static and CEM-semi methods are shown in Figs. 5.16 and 5.17 for the Phase A green times and offsets, respectively. Those figures describe the standard deviation (STD) of the best solutions over the 30 iterations for three nodes (i.e. 2010, 3089, and 2040), for a 50% reduction for 60 minutes. The convergence of those three nodes is achieved when the STD approaches zero.

The CEM-semi approach convergence for the Phase A green times show better results (less iterations) compared to the static approach. For the CEM-semi approach, it takes 7 iterations for node 2040 to converge, 6 iterations for node 2010, and 16 iterations for node 3089, while for the static approach it takes 7 iterations for node 2040, 9 iterations for node 2010, and 26 iterations for node 3089 (see Fig. 5.16a and 5.17a). Similarly, the CEM-semi approach convergence for offsets was better than with the CEM-static approach, especially for node 2010, where the reduction in capacity occurs (Fig. 5.16b and 5.17b). Moreover, applying the CEM-static approach, the offsets did not converge after 30 iterations, which implies that there is a difficulty in finding an optimal solution.

The travel time values for the CEM-static and CEM-semi methods are shown in Fig. 5.18. Those results come from applying the CEM-static and CEM-semi bi-level framework for different capacity reductions at node 2010 for 60 minutes. The results indicate that the CEM-semi converged faster to a better solution (i.e less iterations and less travel time).

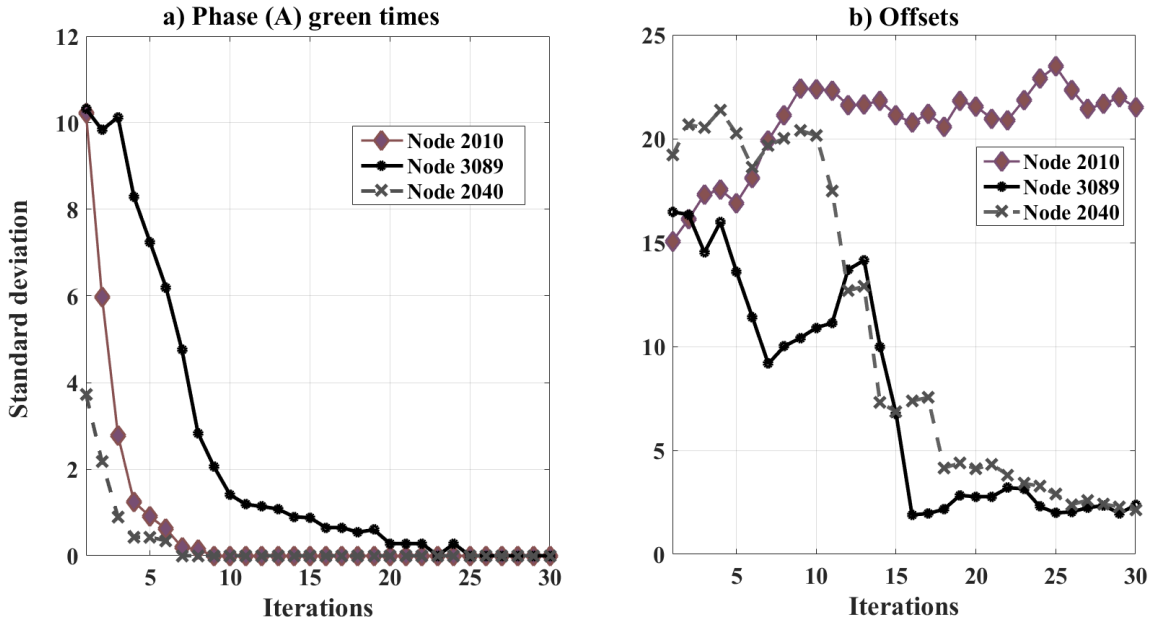

Figure 5.16: The convergence for a 50% capacity reduction of 60 minutes, using the CEM-static framework: (a) Phase A green times, (b) Offsets

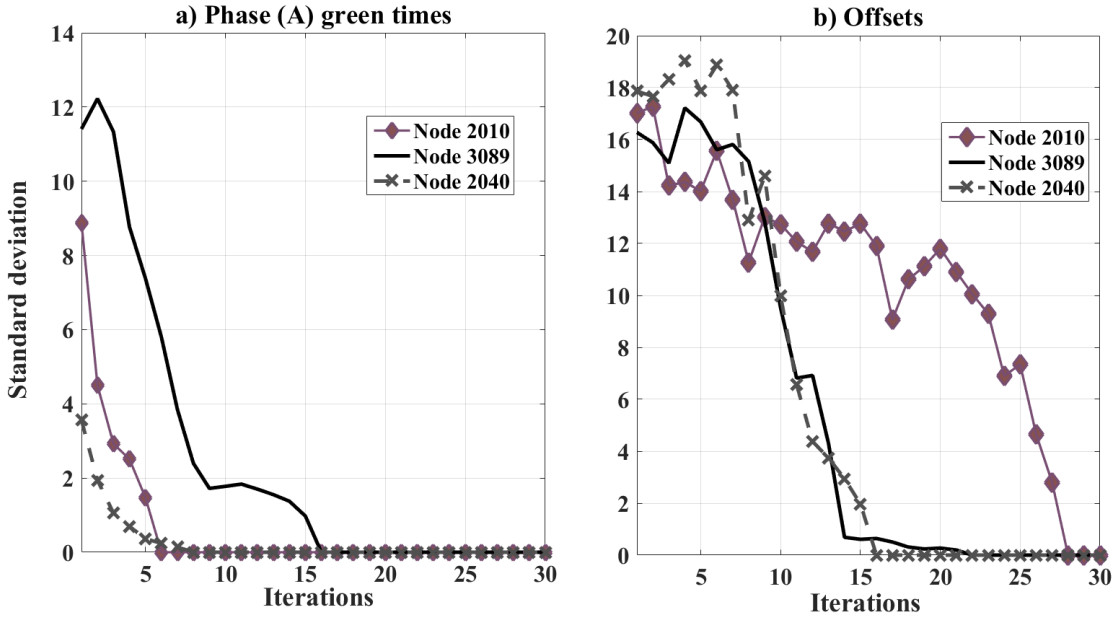

Figure 5.17: The convergence for a 50% capacity reduction for 60 minutes, using the CEM-semi framework: (a) Phase A green times, (b) offsets

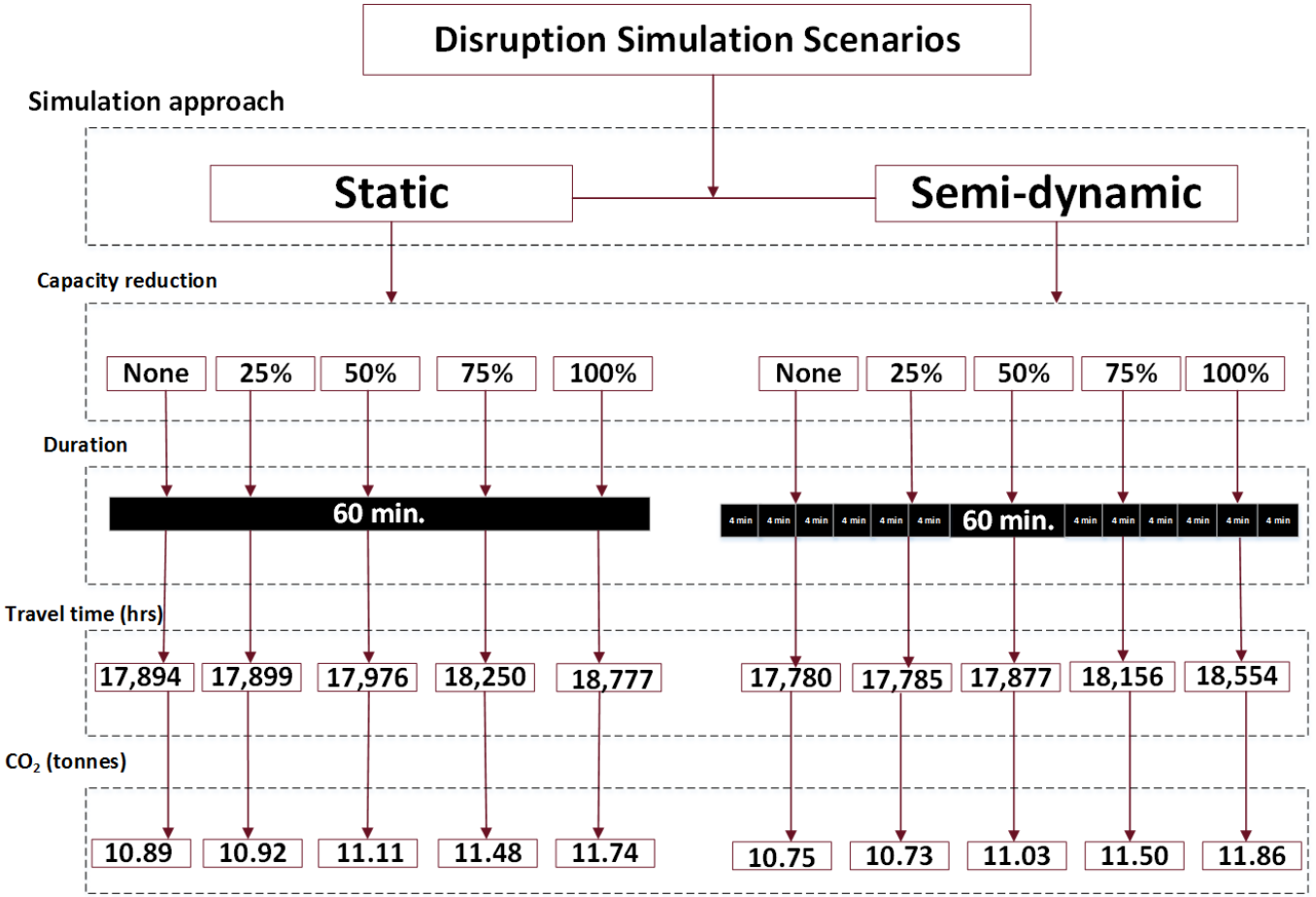

Figure 5.18: Travel time for CEM-static and CEM-semi approaches for each disruption scenario

The travel time values show that the CEM-semi bi-level framework produced a lower travel time compared to the CEM-static approach for all capacity reductions. The most noticeable difference in the travel time values is for a 100% reduction in capacity; the travel time is about 223 hrs less for the CEM-semi approach (i.e. 18,777 hrs when applying the CEM-static method, compared to 18,554 applying the CEM-semi method). Fig. 5.19 shows that the differences in the travel time for the CEM-static and the CEM-semi approaches are largest for the 100% reduction in capacity at node 2010.

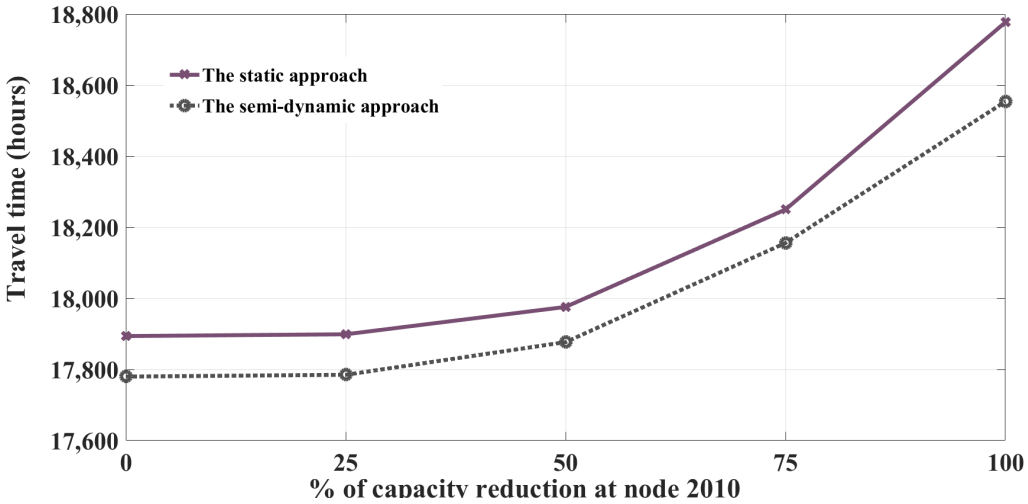

Figure 5.19: The CEM-static versus the CEM-semi framework

One reason for this could be related to the assignment method. In static assignment models, after a partial or complete blockage occurs, traffic generally diverts around the blockage to reduce delays. Static models do not allow for such diversion, thus these models overestimate the impact of the blockage, making it unsuitable for assessing the impact of short-term congestion reductions. This makes semi-dynamic assignment a more realistic model, as in this model, the time period is divided into time slices which allows for re-evaluating the state at the end of each time period and transferring the queue from the previous time period to the next one. This means the assignment of trips commencing in one time slice can differ from the assignment of trips for preceding and subsequent time slices, resulting in a lower travel time and CO_2 emissions.

Another reason why the semi-dynamic approach resulted in a lower travel time is due to the combination of the CE method and the semi-dynamic assignment method (CEM-semi). Optimising the Phase A green times and offsets applying the CEM-semi bi-level framework, results in minimising the objective function (less travel time). Fig. 5.20 shows the travel time results for three scenarios:

- not optimising the signal settings;
- optimising the signal settings, applying the CEM-static framework, to minimise the travel time;
- optimising the signal settings, applying the CEM-semi framework, to minimise the travel time.

It can be seen that optimising the signal settings applying the proposed bi-level framework (either the CEM-static or CEM-semi) results in a significant reduction in the travel time, compared to not applying the bi-level framework (the base-case). For instance, the travel time values in the base case are higher than the CEM-static bi-level approach by 570 hrs, 686 hrs, 897 hrs, 987 hrs, and 929 hrs for 0%, 25%, 50%, 75%, and 100% capacity reductions, respectively. However, there is a slight reduction (about 1%) in the travel time between the CEM-static and CEM-semi methods.

In addition, the results show that CO_2 emissions are generally increasing (Fig. 5.18), as the percentage of the capacity reduction increases. It is interesting to note that applying CEM-semi approach in the case of no disruption results in more reduction in CO_2 emissions compared to applying CEM-static approach. For instance, the amount of CO_2 emissions is 10.89 tonnes compared to 10.75 tonnes of CO_2 applying CEM-semi. This could be related to the differences in the simulation approach. The CEM-semi approach results in less travel time as it converges to a better solution. This decreases the amount of CO_2 emissions. However, this is not the case for a complete reduction in capacity. For instance, the amount of CO_2 emissions when applying the CEM-semi is 11.86 tonnes compared to 11.74 tonnes when applying CEM-static. This could be related due to more to the extensive re-routing when applying the semi-dynamic assignment compared to applying the static assignment. For instance, the distance travelled for a complete blockage for 60 minutes applying CEM-semi is 118,256.6 km compared to 117,027.5 km when applying the CEM-static method.

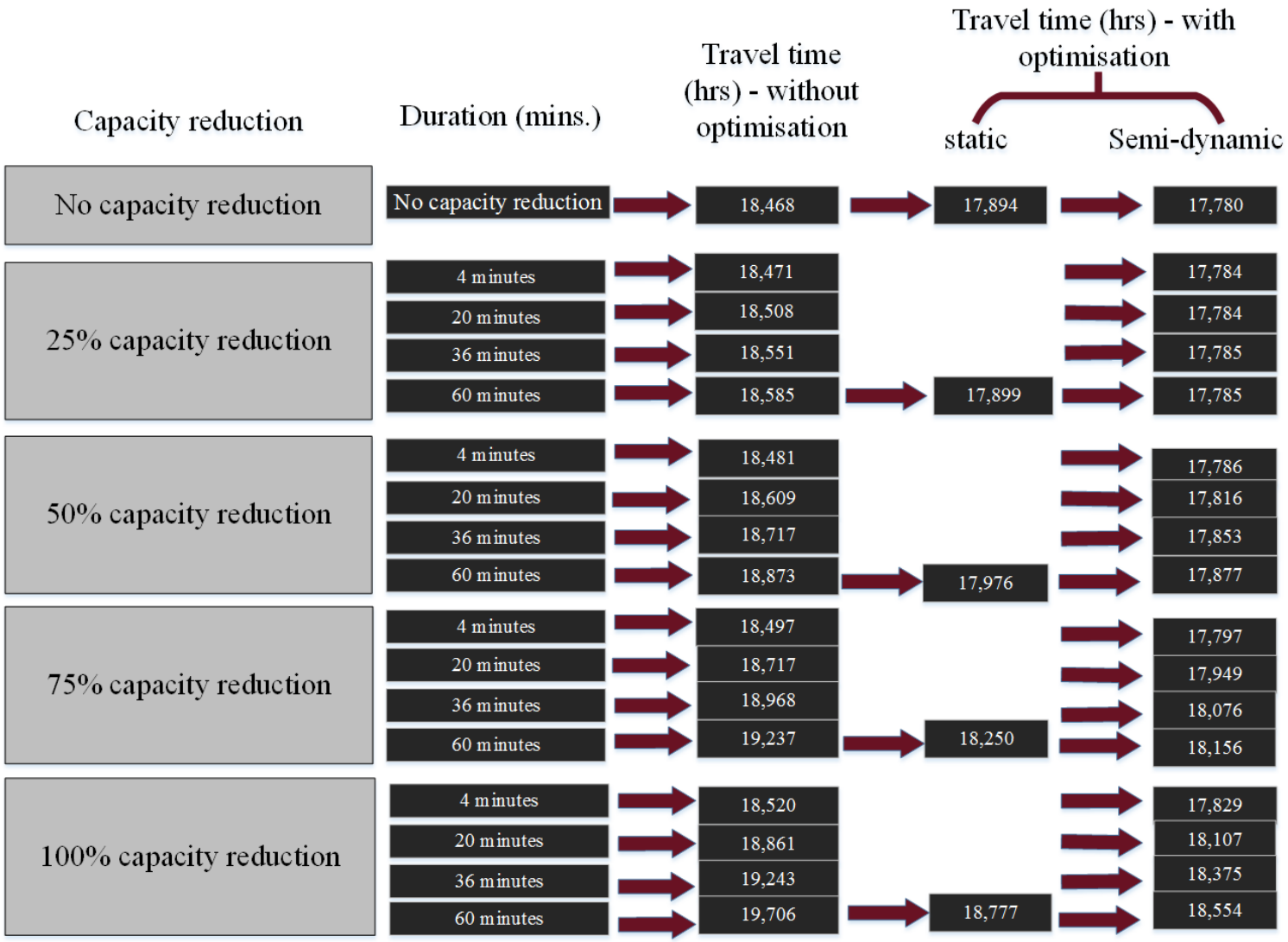

Figure 5.20: Travel times with and without optimisation of traffic signals

Moreover, optimising traffic signals in disrupted road networks could result in reducing the area of the resilience triangle. For instance, Fig. 5.21 shows the arrival flow rate at node 2010 during one hour, where there is a 50% capacity reduction for four minutes in the middle of the hour. As it can be seen in Fig. 5.21, if no optimisation is carried out, the arrival flow rate would drop from 2,742 veh/hr to 1,618 veh/hr, while the traffic flow in the case of optimisation traffic signals would drop from 2,383 veh/hr to 1,851 veh/hr. This likely to be related to the re-routing of traffic that is associated with optimising traffic signals, as drivers tend to adjust their route choice according to how signals are set. In addition, the recovery time to the pre-disruption state is quicker when traffic signals are optimised, as shown in Figs 5.21 and 5.22. Moreover, Fig. 5.21 shows that with optimisation, the flow rate returns to the pre-disruption level within 12 minutes, but without optimisation, the flow rate has not returned to the pre-disruption level even after 32 minutes. In addition, the time it takes the queue to dissipate in the case of no optimisation is longer than in the case of optimisation (Fig. 5.22). For instance, for a 50% reduction for four minutes at node 2010, it takes more than 28 minutes for the queue to dissipate, while it takes only 8 minutes for the queue to completely dissipate when optimising signal control.

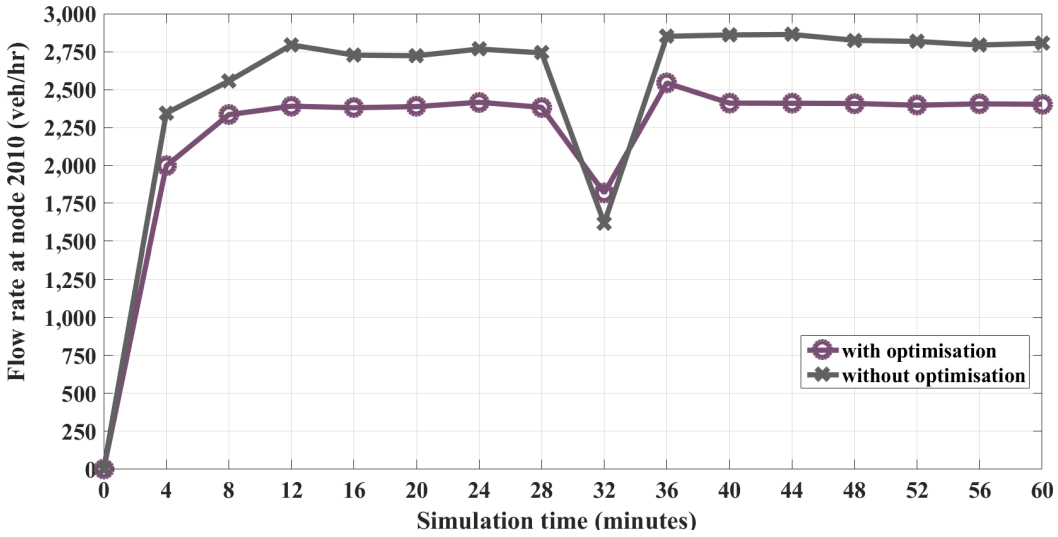

Figure 5.21: Flow rate at node 2010 with and without optimisation of traffic signals

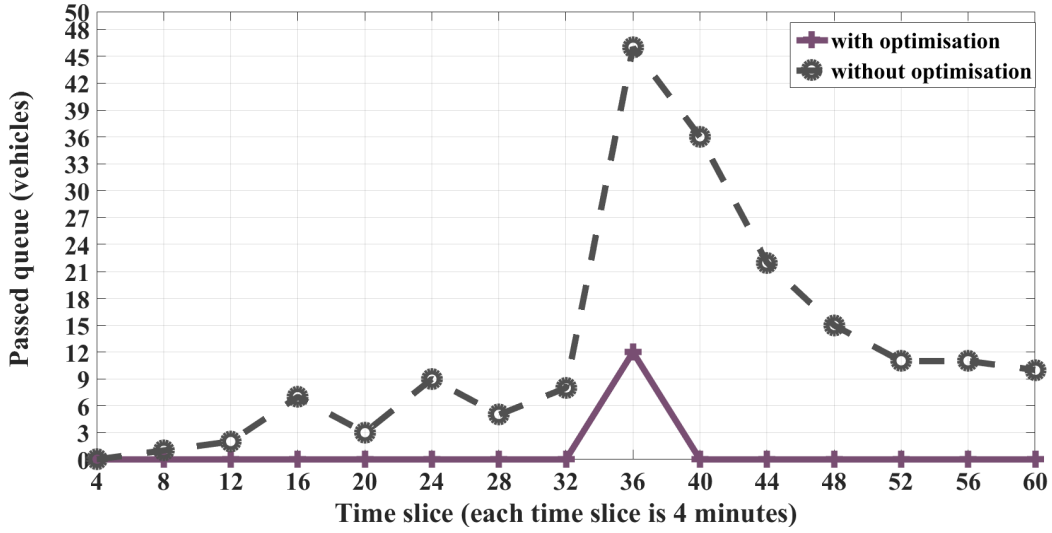

Figure 5.22: Passed queue for each time-slice at node 2010, for a 50% reduction for 4 minutes

In terms of signal settings, the results of a 25% reduction in capacity applying the CEM-static bi-level approach yield lower Phase A green times (i.e. up to 3s) compared to applying the CEM-semi bi-level approach. In contrast, a 50% capacity reduction yields higher Phase A green times (i.e. up to 6s) for the CEM-static approach. Similarly, a 75% and a 100% capacity reduction both resulted in higher Phase A green times for the CEM-static approach (except for node 2010 in case of a 100% reduction). One can also note that the Phase A green times at some nodes (e.g. node 2040) are almost the same applying the CEM-static and CEM-semi bi-level framework.

Table 5.4: Phase A green times for different capacity reductions at node 2010, applying CEM-static and CEM-semi approaches for 60 minutes

Capacity reduction	**25%**		**50%**		**75%**		**100%**	
Assignment	**Static**	**Semi**	**Static**	**Semi**	**Static**	**Semi**	**Static**	**Semi**
Node 2010	40	41	43	43	43	43	40	43
Node 3089	18	20	24	20	26	21	34	31
Node 2040	43	42	43	43	43	43	43	43
Node 2045	43	43	43	43	43	43	43	41
Node 2410	17	19	22	23	29	29	32	31
Node 2500	22	22	27	24	27	19	22	23
Node 2620	14	16	23	17	12	9	21	20
Node 3080	26	29	31	29	37	36	31	14

In terms of offsets, Table 5.5 summarises the results of offsets applying the CEM-static and CEM-semi framework for all capacity reductions (i.e. 25%, 50%, 75%, and 100%). The differences in offset results applying CEM-static and CEM-semi methods vary widely, with higher offsets obtained for the CEM-semi framework for 25% and 75% capacity reductions. One should keep in mind that the offsets are defined as the time that the green phase at an intersection begins after the start of green at the major control intersection or the reference signal. Thus, low offset values at one node (e.g. 1s or 5s) indicate that the offsets have already been started at the previous signalised node.

The results of the Phase A green times and offsets reveal that the CEM-static and CEM-semi approaches can give different Phase A green times and offsets, even though the travel time values are very similar as this problem is not strictly convex (i.e. there is no unique solution).

Table 5.5: Offsets for different capacity reductions at node 2010, applying CEM-static and CEM-semi approaches for 60 minutes

Capacity reduction	**25%**		**50%**		**75%**		**100%**	
Assignment	**Static**	**Semi**	**Static**	**Semi**	**Static**	**Semi**	**Static**	**Semi**
Node 2010	16	6	55	41	26	55	33	14
Node 3089	11	19	12	11	28	21	7	59
Node 2040	6	12	10	11	2	23	5	30
Node 2045	0	0	0	0	0	0	0	0
Node 2410	26	28	1	10	19	22	24	24
Node 2500	39	41	59	9	20	20	18	17
Node 2620	3	18	4	3	11	18	25	18
Node 3080	17	29	22	21	32	44	6	55

5.3 Discussion of results

This chapter has presented results for different disruption scenarios applying the CEM-semi bi-level framework. Several points can be observed from the results. Firstly, it was found that better convergence of the bi-level process results, in terms of iterations, have been achieved for Phase A green times and offsets applying the CEM-semi bi-level approach, especially for node 2010 where the blockage occurs, compared to applying the CEM-static bi-level approach. Secondly, it was noticed that both the level of reduction in capacity (i.e. 25% up to a complete closure) and duration (i.e. 4 minutes closure up to one hour) have an impact on the convergence. For instance, it takes less iterations for a 50% reduction in capacity to converge than for a 75% reduction in capacity.

In addition, using CEM-semi bi-level framework gives significant reductions in travel time compared to not optimising the signal settings (i.e. about 6% reduction in travel time). The benefits of adjusting signal settings applying CEM-semi bi-level framework can result in at least a 1% reduction in the travel time per day (in case of a complete closure) compared to applying the CEM-static bi-level approach.

Moreover, it is important to note that the running time for the semi-dynamic (i.e. time slices) approach is higher than the static approach, since 15 time slices for 4-minute interval are generated to complete one run in the semi-dynamic method versus one time slice in the static method. Thus, it takes around 10 days to finish the simulation applying the CEM-semi framework compared to 4 days applying the CEM-static framework. Those simulations were carried out using SATURN multi-core version on a Xeon (R) machine with 32 GB RAM. This multi-threaded application reduced the overall run times up to half that for not using the multi-threaded version of SATURN. However, there is a possibility to reduce the simulation running time when using the semi-dynamic approach. For instance, the Cambridge network consists of a buffer network and a simulated network [3], and excluding the buffer network will result in reducing the network size, which might reduce the running time. Still, it is important to note that the size of the road network should be large enough to account for the re-routing of drivers.

[3]The difference between the buffer network and simulated network has been discussed in Chapter 2.

5.4 Conclusions

This chapter presented the results obtained from applying the CEM-semi bi-level optimisation, then compared the results to the CEM-static bi-level optimisation. Overall, the results of the CEM-semi bi-level framework indicate that there is value in using this method to optimise traffic signal control, to minimise the travel time and to influence and assist drivers to divert around blockages for short-interval disturbances in road networks, and to reduce the resilience triangle. Therefore, the CEM-semi framework will be used in the next chapter to investigate the benefits of using this method to minimise CO_2 emissions in disrupted networks.

CHAPTER 6

THE EFFECT OF OPTIMISING SIGNAL SETTINGS TO MINIMISE CARBON DIOXIDE EMISSIONS

6.1 Minimising carbon dioxide emissions results

In this chapter signal settings (i.e. Phase A green times and offsets) are optimised using the CEM-semi bi-level approach to minimise CO_2 emissions in the road network. This model was applied to the Cambridge (UK) network (Fig. 3.4, Chapter 3) to identify the effect of optimising the signal settings to minimise the CO_2 emissions. The same approach (CEM-semi) used in Chapter 5 is applied in this chapter but with minimising CO_2 emissions as the objective function. Thus, 0%, 50%, 75%, and 100% capacity reductions for 0 minutes, 20 minutes, 36 minutes, and 60 minutes duration are applied to node 2010.

The convergence of the Phase A green times and offsets for nodes 2010, 3089, and 2040 for a 50% reduction in capacity at node 2010 for 60 minutes are presented in Figs 6.1 and 6.2, respectively [1]. The Phase A green times converged for nodes 2010, 3089, and 2040 (Fig. 6.1). The offsets for node 2010 did not converge after 30 iterations (Fig. 6.2). This shows that there is again difficulty in finding optimal solutions.

[1] The convergence for all capacity reductions are included in Appendix E.

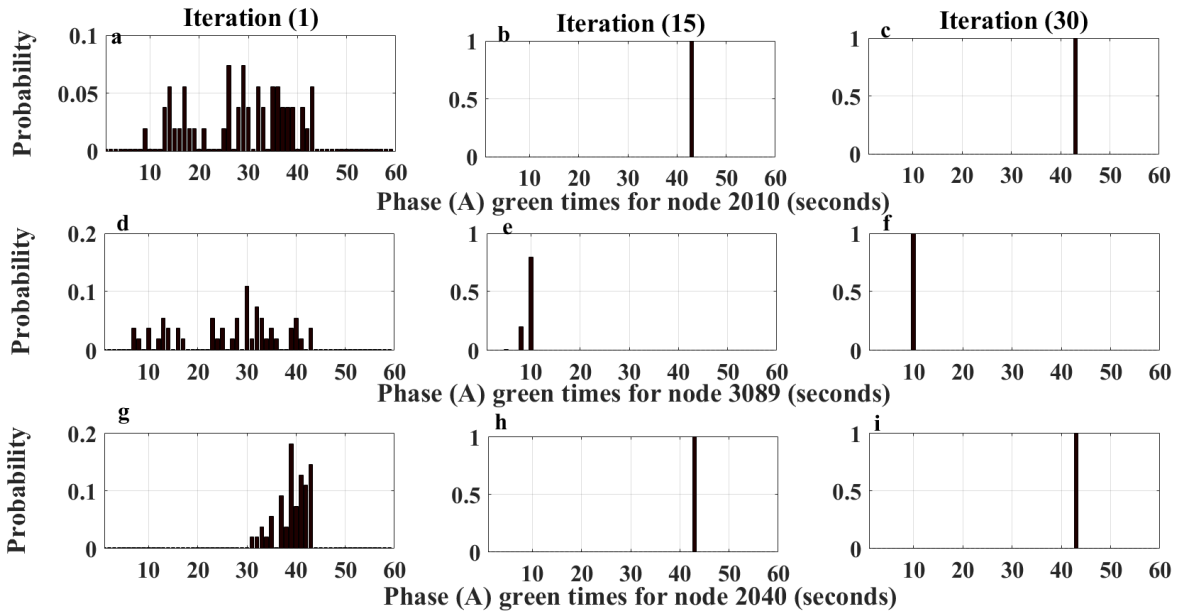

Figure 6.1: The convergence of Phase A green times for a 50% reduction in capacity at node 2010 for 60 minutes, for nodes 2010 (a-c), 3089 (d-f), and 2040 (g-i)

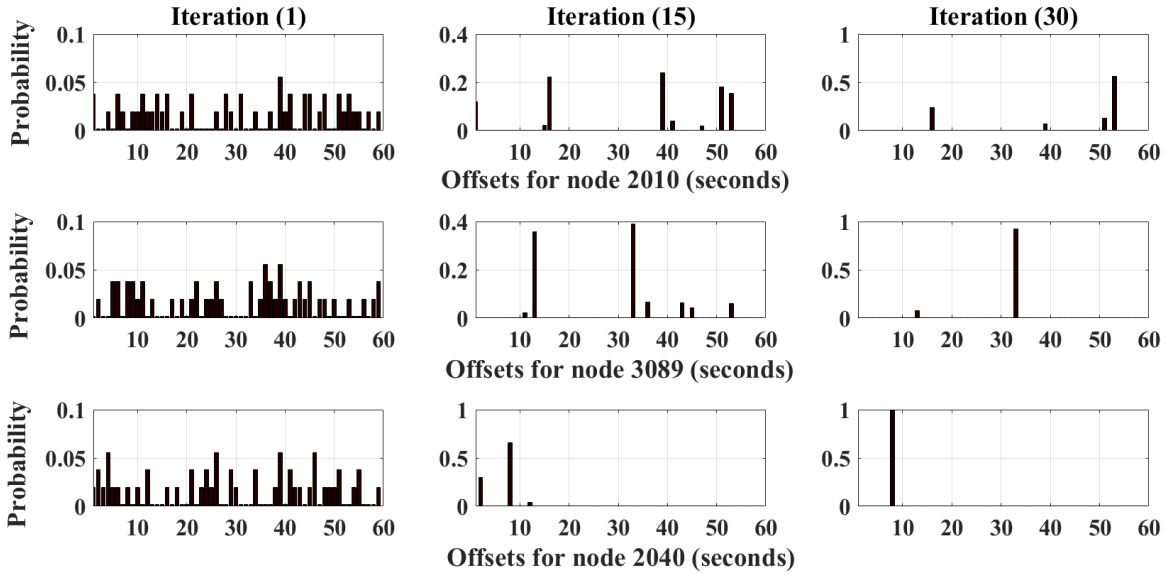

Figure 6.2: The convergence of offsets for a 50% reduction in capacity at node 2010 for 60 minutes, for nodes 2010 (a-c), 3089 (d-f), and 2040 (g-i)

To check the effect of capacity reductions at node 2010 on the convergence, the convergence for a 75% capacity reduction at node 2010 for 60 minutes is investigated for the Phase A green times and offsets for nodes 2010, 3089, and 2040, as in Figs. 6.3 and 6.4, respectively. The results show a convergence for Phase A green times, but not the offsets for node 2010. This means there is a need to increase the number of iterations so that a solution near the optimum can be found. Moreover, the results of the convergence for different capacity reductions indicate that it is hard to achieve convergence for offsets as the percentage of capacity reduction increases, especially for node 2010 where the blockage occurs.

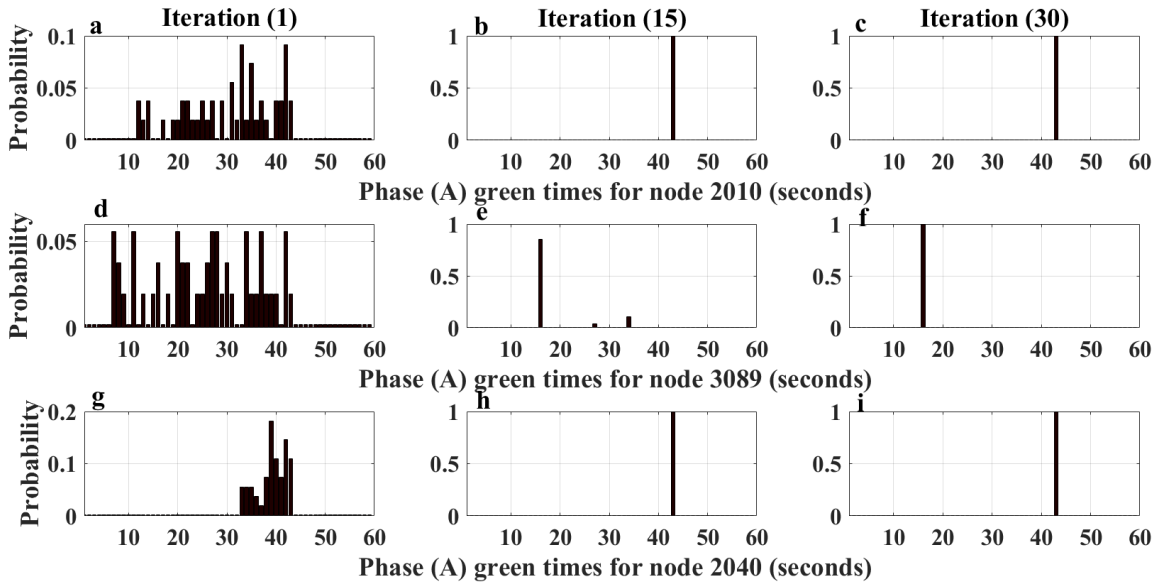

Figure 6.3: The convergence of Phase A green times for a 75% capacity reduction at node 2010, for 60 minutes for nodes 2010 (a-c), 3089 (d-f), and 2040 (g-i)

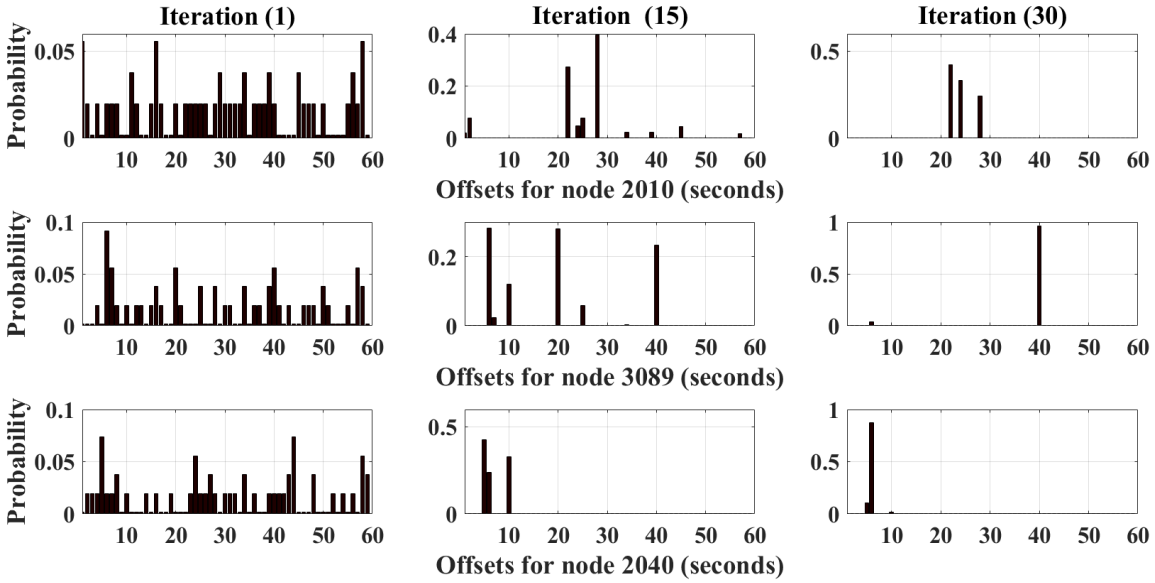

Figure 6.4: The convergence of offsets for a 75% capacity reduction at node 2010 for 60 minutes, for nodes 2010 (a-c), 3089 (d-f), and 2040 (g-i)

The convergence of the CO_2 and the travel time for a 50% capacity reduction at node 2010 for 60 minutes is presented in Figs 6.5 and 6.6, respectively. Those results are for minimising the CO_2 emissions using the CEM-semi bi-level framework. As can be seen in Fig. 6.5 and 6.6, the CO_2 and the travel time converged after 11 iterations to a value of 10.61 tonne and 18,018 hrs for the CO_2 and the travel time, respectively.

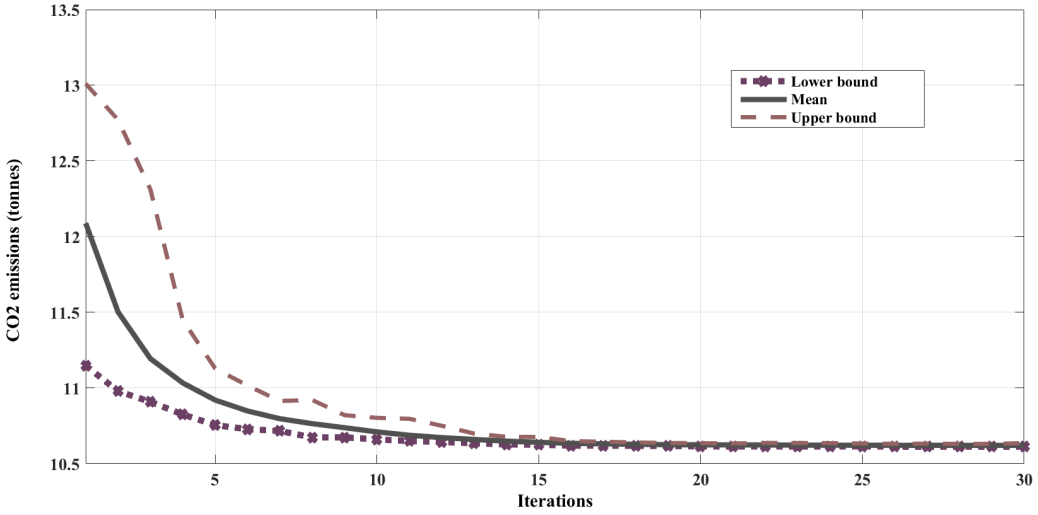

Figure 6.5: Convergence of CO_2 emissions for a 50% reduction in capacity for 60 minutes, when minimising CO_2 emissions

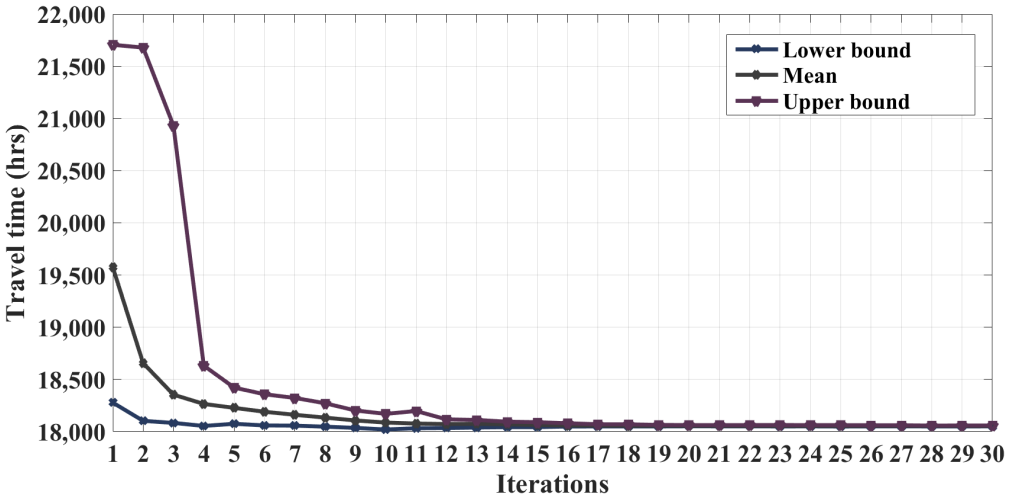

Figure 6.6: Convergence of the travel time for a 50% reduction in capacity for 60 minutes, when minimising the CO_2

In terms of signal settings, the results of Phase A green times when minimising the CO_2 emissions are summarised in Table 6.1 for node 2010, the adjacent nodes 3089, 2040, and 2045, and the nearby nodes 2410, 2500, 2620, and 3080[2]. The location of those nodes are shown in Fig. 3.5, Chapter 3.

As can be seen in Table 6.1, little or no change to the Phase A green times can be

[2]The signal settings results for the 24 signalised nodes are included in Appendix E.

noticed during different reduction durations, when minimising the CO_2 emissions in the case of a 50% reduction in capacity for 60 minutes at node 2010. For instance, the Phase A green times at node 2010 are 42s for no reduction, 43s for 20 minutes reduction, 43s for 36 minutes reduction, and 43s minutes reduction. This small difference (i.e. one second). For the adjacent nodes to node 2010 (i.e. nodes 2040 and 2045), the Phase A green times are constant during all disruption duration (i.e. 43 seconds). This reflects the high traffic flow at these nodes, as 43s is the upper bound of the Phase A green times. A little fluctuation in the Phase A green times can be noticed at the nearby nodes (i.e. nodes 2410, 2500, 2620, 3080, and 3089) during different reduction durations, which could be related to the availability of alternative routes. The standard deviation for nodes 3080 and 2620 in Table 6.1 are the highest due to the fluctuation in the Phase A green times at these nodes.

Table 6.1: Phase A green times for a 50% reduction in capacity at node 2010 for 60 minutes, using the CEM-semi framework

Duration	**0 min.**	**20 min.**	**36 min.**	**60 min.**	**Mean**	**STD**
Node 2010	42	43	43	43	42.8	0.5
Node 3089	11	10	7	10	9.5	1.7
Node 2040	43	43	43	43	43	0
Node 2045	43	43	43	43	43	0
Node 2410	15	15	13	12	13.8	1.5
Node 2500	30	32	28	31	30.3	1.7
Node 2620	35	36	43	40	38.5	3.7
Node 3080	25	28	39	39	32.8	7.3

In terms of offsets, more fluctuation can be noticed in the offset values for some nodes during various reduction durations when minimising the CO_2 emissions (Table 6.2), compared to minimising the travel time (Table 5.2) in the case of a 50% reduction in capacity for 60 minute duration at node 2010. For instance, the offsets for node 2500 are 13s for 0 minute reduction, 7s for 20 minutes reduction, 56s for 36 minutes reduction, and 53s for 60 minutes reduction, compared to 36s for 0 minutes reduction, 30s for 20 minutes reduction, 25s for 36 minutes reduction, and 17s for 60 minutes reduction when minimising the travel time. This implies that the offsets values are more sensitive to the reduction in capacities and durations when minimising the CO_2 emissions as an objective function than minimising the travel time as an objective function. The standard deviation for nodes 3080, 2620, and 2500 in Table 6.2 are the highest due to the substantial fluctuation in the offsets at these nodes.

Table 6.2: Offsets for a 50% reduction in capacity at node 2010 for 60 minutes, using the CEM-semi framework

Duration	**0 min.**	**20 min.**	**36 min.**	**60 min.**	**Mean**	**STD**
Node 2010	42	54	53	53	50.5	5.7
Node 3089	3	22	36	33	23.5	15
Node 2040	7	6	8	8	7.25	1
Node 2045	0	0	0	0	0	0
Node 2410	34	32	28	14	27	9
Node 2500	13	7	56	53	32.3	25.8
Node 2620	30	54	17	9	27.5	19.7
Node 3080	53	19	4	45	30.3	22.7

To understand the impact of the percentage of capacity reductions on the signal settings, when minimising CO_2 emissions, Table 6.3 and Table 6.4 summarise the Phase A green times and offsets for all capacity reductions, respectively. As shown in Table 6.3, across the different reductions in capacity, a pronounced increase (i.e. up to 12s) in Phase A green times can be noticed between a 50% and a 75% reduction in capacity. Moreover, a noticeable fluctuation in offsets can be noticed in Table 6.4 between different reductions in capacity. This implies that the Phase A green times and offsets are sensitive to different capacity reductions when minimising the CO_2 emissions.

Table 6.3: Phase A green times for different capacity reductions at node 2010, applying the CEM-semi framework for 60 minutes

Capacity reduction	**0%**	**50%**	**75%**	**100%**	**Mean**	**STD**
Node 2010	42	43	43	43	42.8	0.5
Node 3089	11	10	16	17	13.5	3.5
Node 2040	43	43	43	43	43	0
Node 2045	43	43	43	43	43	0
Node 2410	15	12	22	34	20.8	9.8
Node 2500	30	31	43	23	31.8	8.3
Node 2620	35	40	43	20	34.5	10.2
Node 3080	25	39	43	43	37.5	8.5

Table 6.4: Offsets for different capacity reductions at node 2010, applying the CEM-semi framework for 60 minutes

Capacity reduction	**0%**	**50%**	**75%**	**100%**	**Mean**	**STD**
Node 2010	42	53	22	57	43.5	15.7
Node 3089	3	33	40	24	25	16
Node 2040	7	8	6	8	7.3	1
Node 2045	0	0	0	0	0	0
Node 2410	34	14	8	12	17	11.6
Node 2500	13	53	33	24	30.8	17
Node 2620	30	9	1	16	14	12.3
Node 3080	53	45	5	48	37.8	22

6.2 The interaction between minimising travel time and CO_2

To check whether the CO_2 emissions and the travel time correlate, the results of applying the CEM-semi bi-level framework to optimise CO_2 emissions are summarised in Fig. 6.7 for a selected number of blockage scenarios (i.e. 50%, 75%, and 100%). The results show that, in the case of a disruption at node 2010, the CO_2 emissions tend to gradually increase as the disruption severity and duration increase: this is clear in Fig. 6.8. For instance, if the no reduction scenario is taken as a base for comparison, a 50% reduction in capacity for 60 minutes results in an increase of 0.61% in CO_2 emissions. This percentage increases to 6.25% for a 100% reduction in capacity for 60 minutes. Those results are compared to the ones obtained in the case of no signal optimisation, as shown in Fig. 6.8, to evaluate the benefits of using the CEM-semi bi-level framework. It is interesting to note that applying the CEM-semi bi-level approach to minimise CO_2 emissions can result in about a one tonne reduction in CO_2 emissions (about 8% reduction in CO_2 emissions) for a complete closure of 60 minutes compared to the base case (no optimisation).

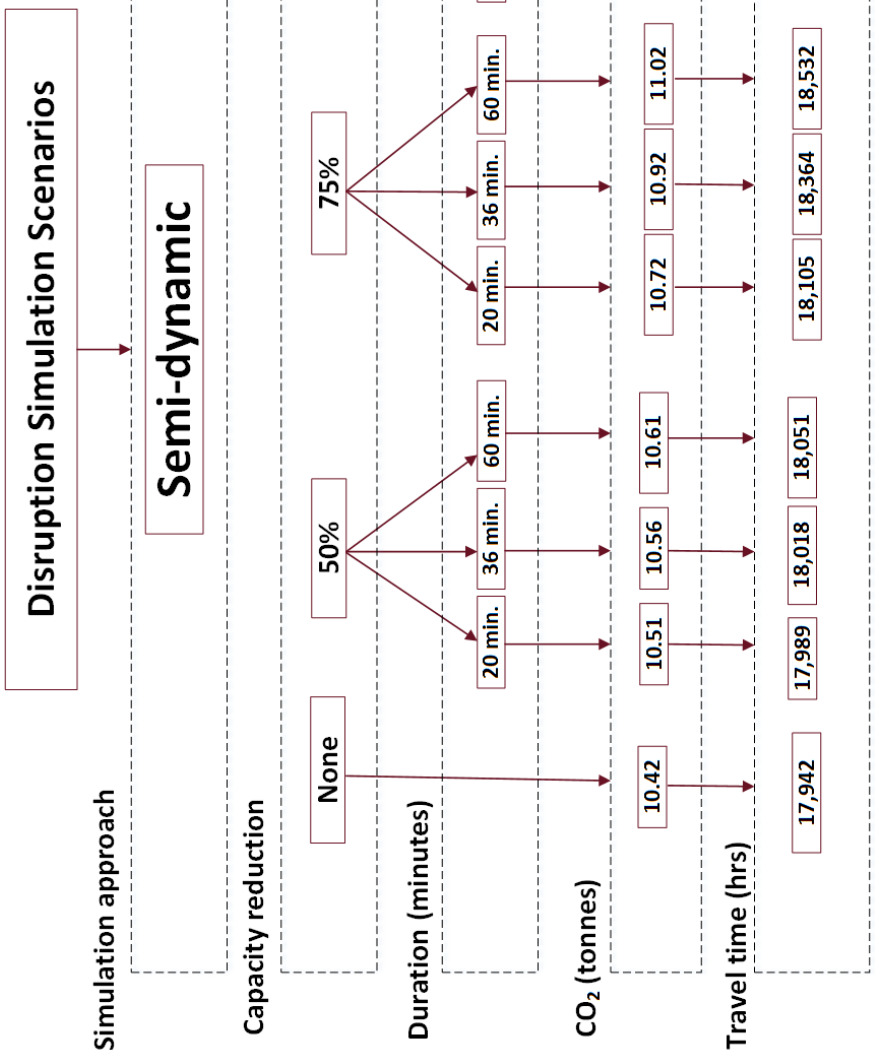

Figure 6.7: Travel time and CO_2 emissions for different disruption scenarios, when minimising CO_2 emissions

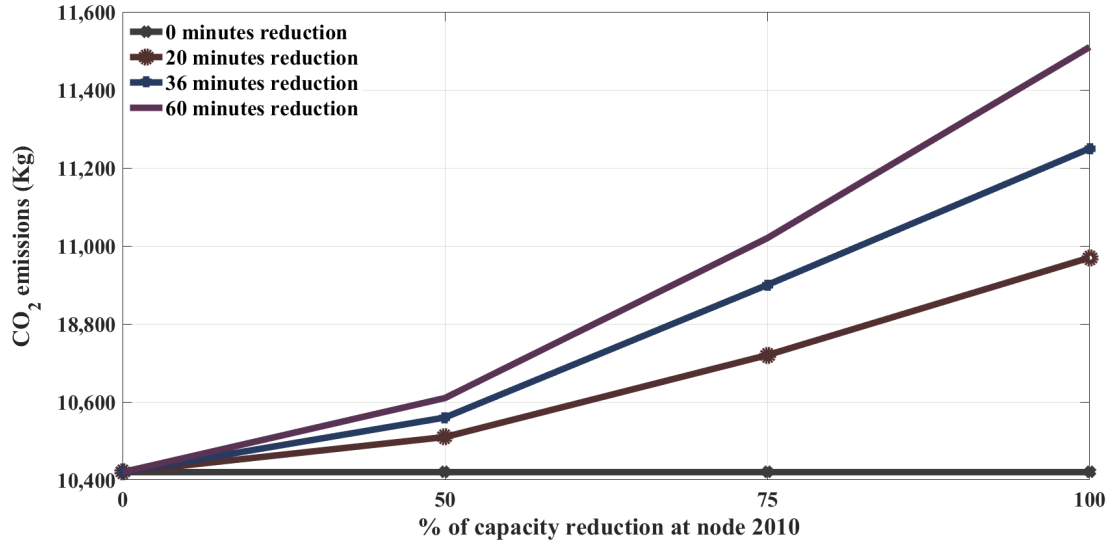

Figure 6.8: CO_2 emissions results for different disruption scenarios, when minimising CO_2 emissions

Apparently, there is a reduction in the travel time as well. Fig. 6.9 illustrates the effect of applying the CEM-semi bi-level framework to minimise CO_2 emissions on reducing the travel time in the network (i.e. the interaction between the travel time and CO_2 emissions, when minimising CO_2 emissions). This figure is for a 50% reduction in capacity for different capacity durations (i.e. 20, 36, and 60 minutes). As can be seen in Fig. 6.9, minimising CO_2 emissions reduces the travel time compared to the base case (i.e. not applying the CEM-semi framework). For instance, the reduction in the travel time when minimising the CO_2 emissions, for a 50% reduction in capacity for 60 minutes, is about 822 hrs (about 4%) compared to the base case.

Fig. 6.10 illustrates the effect of applying the CEM-semi to minimise the travel time on reducing the CO_2 emissions in the network (i.e. the interaction of between the travel time and CO_2 emissions, when minimising the travel time). This is for a 50% reduction in capacity for different capacity durations (i.e. 20, 36, and 60 minutes). As can be seen in Fig. 6.10, minimising the travel time reduces CO_2 emissions compared to not applying the CEM-semi bi-level framework. For instance, the reduction in the CO_2 emissions when minimising the travel time for a 50% reduction in capacity for 60 minutes is about 0.8 tonne (about 7%) compared to not optimising the signal settings.

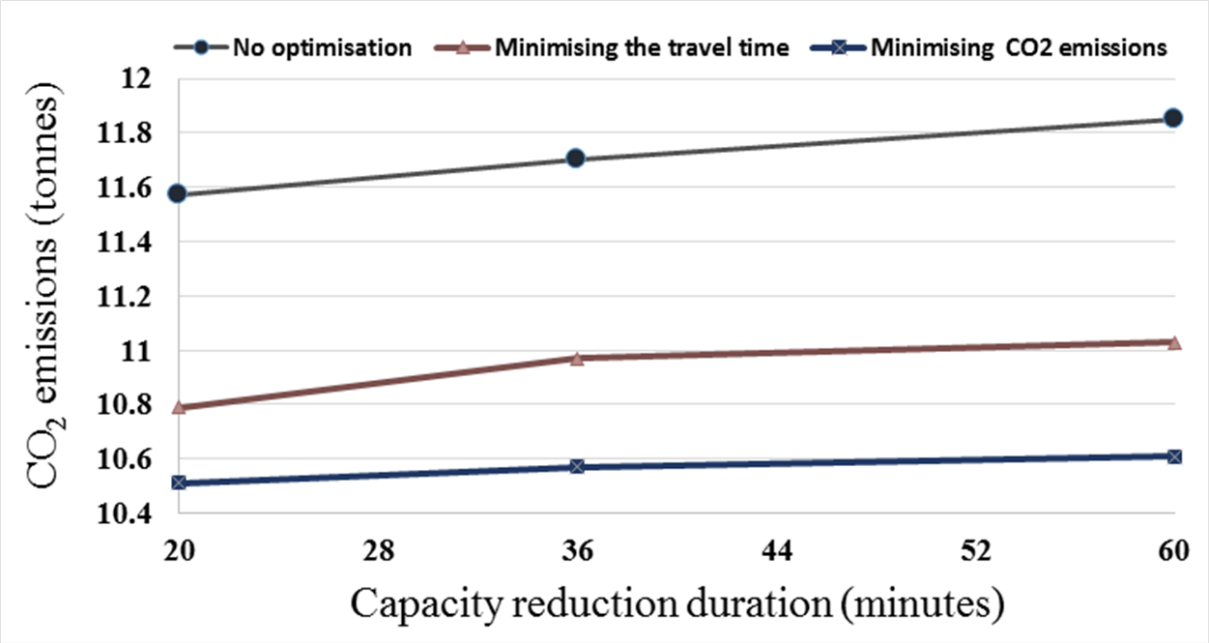

Figure 6.9: CO_2 emissions results for a 50% reduction in capacity for 60 minutes in the case of: 1. no optimisation; 2. minimising travel time; 3. minimising CO_2 emissions

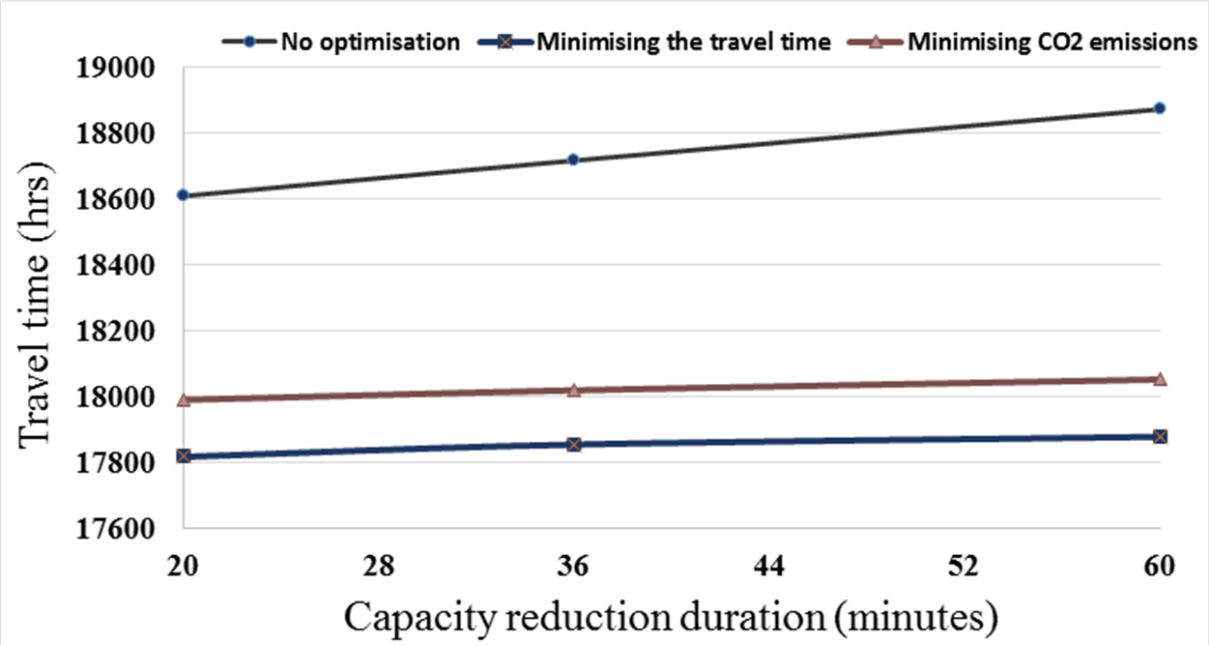

Figure 6.10: Travel time results for a 50% reduction in capacity for 60 minutes in the case of: 1. no optimisation; 2. minimising travel time; 3. minimising CO_2 emissions

Fig. 6.11 summarises the results when minimising travel time as an objective function and minimising CO_2 emissions as an objective function. It is interesting to note that CO_2

emissions percentage decrease is larger than the travel time percentage decrease, when minimising the travel time and when minimising the CO_2 emissions.

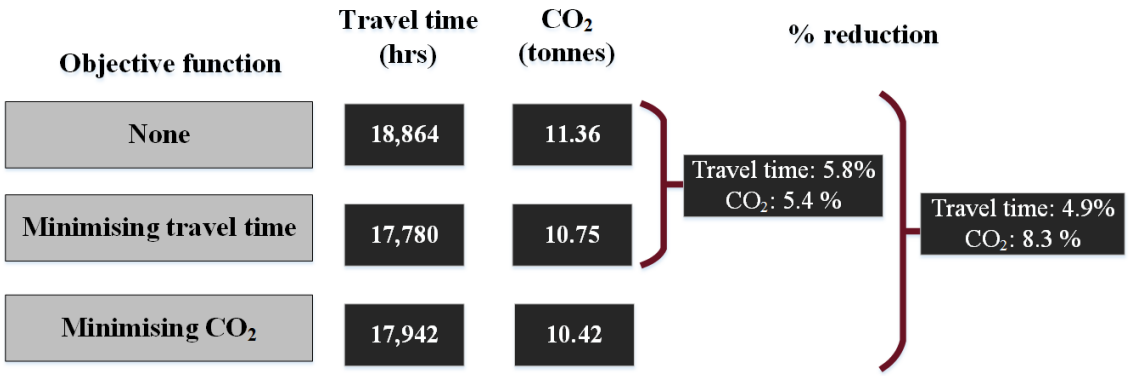

Figure 6.11: The interaction of minimising the travel time and CO_2 emissions

It is worth noting that this thesis considers minimising the total travel time or CO_2 emissions as an objective function, but not both. One could seek to minimise a weighted sum of the travel time and CO_2 emissions, as follows:

$$Z = Z_{travel\,time}.\lambda_1 + Z_{CO_2}.\lambda_2 \tag{6.1}$$

The first part of the objective function ($Z_{travel\,time}$) considers minimising the travel time and λ_1 is the travel time weighting factor. The second part of the objective function (Z_{CO_2}) considers minimising the CO_2 emissions and λ_2 is the emissions weighting factor. To minimise the travel time as a single objective, λ_2 is set to zero and λ_1 is set to 1. To minimise the CO_2 emissions as a single objective function, λ_1 is set to zero and λ_2 is set to 1. To minimise the travel time and CO_2 emissions, the value of travel time and CO_2 emissions would need to be considered.

6.3 Discussion of results

The results show that optimising the signal settings applying the CEM-semi framework can result in a one tonne reduction in CO_2 emissions (about 8% reduction in CO_2 emissions in case of a complete closure for 60 minutes). These results are best estimates and there is some uncertainty regarding them, as it has not been possible to validate the model (i.e. show that it produces accurate estimates of flows, etc. in the case of disruption). The results of the convergence for different capacity reductions, when minimising CO_2

emissions, indicate that it is hard to achieve convergence for offsets as the percentage of capacity reduction increases, especially for node 2010 where the blockage occurs.

The offset values are more sensitive to the reduction in capacities and durations when minimising the CO_2 emissions as an objective function than minimising the travel time as an objective function.

The results when minimising travel time as an objective function and minimising CO_2 emissions as an objective function revealed that percentage CO_2 emissions is decrease larger than the percentage travel time decrease, when minimising the travel time and when minimising the CO_2 emissions. This means no trading-off is required as the travel time and CO_2 emissions are both decreasing.

6.4 Conclusions

This chapter presented the results of minimising CO_2 emissions applying the CEM-semi framework. The results revealed that applying the CEM-semi framework in disrupted road networks could reduce CO_2 emissions by almost 8%. Therefore, optimising traffic signal control in disrupted road networks could not only reduce the travel time, but also improve the environmental sustainability in the network.

CHAPTER 7

CONCLUSIONS AND FUTURE WORK

7.1 Summary

This study applied a bi-level framework to minimise the travel time or the carbon dioxide emissions in disrupted road networks. This includes three main degradation scenarios (% of capacity reduction and duration). The first degradation investigation involved applying the Cross-Entropy method (CEM), along with the static user equilibrium embedded in SATURN (CEM-static), to optimise the signal settings (i.e. Phase A green times and offsets) in disrupted road networks, to minimise the travel time. The second degradation investigation involved optimising the signal settings, using the CE method, along with the semi-dynamic assignment embedded in SATURN (CEM-semi) to minimise the travel time in disrupted road networks. A comparison between the CEM-static and CEM-semi approaches was then carried out to evaluate the two assignment methods in optimising the signal settings to minimise the travel time in disrupted road networks. Based on this comparison, the third degradation investigation involved applying the CEM-semi approach to optimise the signal settings to minimise the carbon dioxide (CO_2) emissions. These investigations involved modelling a real network (the Cambridge network, UK) applying different capacity reductions (25%, 50%, 75%, 100%) and durations (4 minutes, 20 minutes, 36 minutes, 60 minutes). It is worth noting that the Cambridge network was calibrated and validated by Atkins, and there is no need to calibrate it as part of the research described in this thesis.

The results contribute to current knowledge and bridge some of the gaps in managing

disrupted urban road networks through optimising traffic signals to assist drivers diverting around partial or complete blockages, and appears to be the first to apply the CE method to optimise the signal settings in disrupted road networks to minimise the travel time. Finally, this study appears to be the first to investigate minimising the CO_2 emissions in disrupted road networks by optimising the signal settings. Overall, the results of this research revealed that there is value in optimising traffic signal control to reduce the travel time and CO_2 emissions in disrupted road networks.

7.2 Final conclusions

A number of conclusions can be drawn as follows:

- the results of altering the seed values revealed that while the optimal value of the objective function (the travel time) does not appear to be sensitive to the seed value, the optimal values of the green times and offsets are. This is due to the fact that this problem is not strictly convex (i.e. there is no unique solution).

- in the upper level (the CE algorithm) the value with the of the green times and offsets with the highest probability were chosen. However, this might be not the best solution, due to the bi-level framework as there are two objectives to be considered: the signal settings in the upper level and the shortest route in the lower level.

- the traffic flow at the most congested signalised intersection (node 2010) was degraded by applying several blockage scenarios, which involved various combinations of two main factors: the severity of the blockage (i.e. 25%, 50%, 75%, and 100% capacity reductions) and the duration of the blockage (i.e. 4, 20, 36, and 60 minutes). However, other nodes in the network could be more critical for the network performance (i.e. the nodes in the centre of the network where the network is more dense). Therefore, some other simulations were carried out on another node in the centre of the network (i.e. node 3810) to check the impact of disruptions at this node, in terms of travel time, and compare it to the impact of disruptions at node 2010. The results of simulating a 50% disruption at node 3810 for 4 minutes revealed that the impact of a blockage at node 2010 is greater than the impact of a blockage at node 3810. For instance, the travel time when there is a 50% disruption for 4 minutes at node 3810 is 17,780 hours compared to 17,786 hours

when there is a 50% disruption for 4 minutes at node 2010. This means more delay is expected when there is a blockage at node 2010. This is likely to be due to the greater availability of alternative routes to get around node 3810, than is the case for node 2010.

- the results of applying the CEM-static bi-level framework to optimise the signal settings indicate that optimising traffic signal control to minimise the travel time can assist traffic to divert around blockages. Changes in the optimal signal settings at the node where the disruption occurs can assist in re-routing of drivers around the blockage. Heat maps can be used to demonstrate how a disruption at one node affects the overall network. This representation can be used to gain a better understanding of the impacts of network disruptions network reliability in the case of disruption at one or more nodes.

- small reductions in capacity (i.e. 25%) for small durations have little impact on the road network, as the road network seems to have enough spare capacity to accommodate the flows resulting from small changes in capacities. However, this conclusion could not be generalised as it depends on the topology of the Cambridge network (i.e. the arrangement of the nodes and links) and the demand level. The impact of one node closure depends on the characteristics of the road network and how sparse the network is (i.e. the number and nearness of alternative routes).

- the results show that CO_2 emissions are generally increasing, as the percentage of the capacity reduction increases. It is interesting to note that applying CEM-semi approach in the case of no disruption results in more reduction in CO_2 emissions compared to applying CEM-static approach. For instance, the amount of CO_2 emissions is 10.89 tonnes compared to 10.75 tonnes of CO_2 applying CEM-semi. This could be related to the differences in the simulation approach. The CEM-semi approach results in less travel time as it converges to a better solution. This decreases the amount of CO_2 emissions. However, this is not the case for a complete reduction in capacity. For instance, the amount of CO_2 emissions when applying the CEM-semi is 11.86 tonnes compared to 11.74 tonnes when applying CEM-static. This could be related to the extensive re-routing when applying the semi-dynamic assignment compared to applying the static assignment. For instance, the distance travelled for a complete blockage for 60 minutes applying CEM-semi is 118,256.6 km compared to 117,027.5 km when applying the CEM-static.

- the performance of the CEM-semi bi-level framework demonstrates satisfactory results for simulating short time closures (e.g. 4 minutes). The results showed that the CEM-semi approach gives quicker convergence in the case of disruption than does the CEM-static approach. This means there is value in using the CEM-semi bi-level framework to optimise traffic signal control, to minimise the travel time and to assist traffic by facilitating diversion of traffic around blockages for short-interval disturbances in road networks.

- it was noticed that the level of reduction in capacity (i.e. 25% up to a complete closure) has an impact on the convergence of the Phase A green times and offsets. For instance, the Phase A green time convergence was quicker for a 25% reduction in capacity (i.e. it takes less iterations to converge to a stable value) than a complete reduction in capacity. In addition, the convergence of offsets is hard to achieve when the percentage of the capacity reductions increases.

- the results of the CEM-semi bi-level framework indicate that there is value in using this method to reduce the area of the resilience triangle and to reduce the queue dissipation time.

- the running time for the semi-dynamic (i.e. time slices) approach is higher than the static approach, since 15 time slices for 4-minute interval are generated to complete one run in the semi-dynamic method versus one time slice in the static method. Thus, it takes around 10 days to finish the simulation applying the CEM-semi framework compared to 4 days applying the CEM-static framework. Those simulations were carried out using SATURN multi-core version on a Xeon (R) machine with 32 GB RAM. This multi-threaded application reduced the overall run times up to half that for not using the multi-threaded version of SATURN. However, there is a possibility to reduce the simulation running time when using the semi-dynamic approach. For instance, the Cambridge network consists of a buffer network and a simulation network, and excluding the buffer network will result in reducing the network size, which will reduce the running time. Still, it is important to note that the size of the road network should be large enough to account for the re-routing of drivers. It is worth noting that the results of the computational performance presented in this thesis have not been compared to other studies, as this study is the first applying the semi-dynamic approach in a bi-level framework in degraded networks. However, as discussed in Chapter 2, Section 2.3, Ngoduy and Maher (2011) compared the CE method to the GA method

and concluded that the CE method is better than the GA method in terms of the computational performance .

- the results show that optimising the signal settings applying the CEM-semi bi-level framework can result in a one tonne reduction in CO_2 emissions (about 8% reduction in CO_2 emissions in the case of a complete closure for 60 minutes) compared to not optimising the signal settings. In terms of travel time, the benefits of adjusting signal settings applying the proposed approach can result in at least a 6% reduction in the travel time, in case of a complete closure, compared to not applying the proposed approach. In addition, the results show that minimising travel time gives a reduction in CO_2 emissions, but minimising CO_2 emissions gives a greater reduction in CO_2 emissions.

The study has identified a rigorous tool that could be embedded in traffic simulation packages to simulate disrupted road networks. The bi-level framework suggested in this study will be useful for road controlling authorities, planners and decision makers to test different disruption scenarios in terms of the location, severity and duration of disruption. In addition, this tool can be used to assess the resilience and environmental sustainability of urban road networks, as this study investigated optimising the traffic signal settings to influence drivers to divert around a blockage, considering not only minimising the travel time, but also the CO_2 emissions.

7.3 Further research

Further work is necessary to address the limitations and improve the suggested framework. Recommendations for future work are:

- on the practical level, research to develop a tool to be embedded in traffic software (e.g. SATURN), to optimise signal settings in the case of disruptions could be undertaken.
- Optimising a weighted sum of travel time and emissions could be done, taking account of the value placed on reductions in travel time and reductions in CO_2 emissions.
- it is recommended the model be extended to include other emissions, such as carbon monoxide, nitrogen oxides and hydrocarbons, which are significantly harmful to health and the the environment.

Part III

Appendices

APPENDIX A

THE CONVERGENCE CHARACTERISTICS OF CEM-STATIC FRAMEWORK WHEN MINIMISING TRAVEL TIME

This appendix includes all the convergence results along with the signal settings (Phase A green times and offsets) to check the performance of the CE method as discussed in Chapter 3. This includes the following:

- Testing different combinations of the sample sizes (N) and the number of iterations (t), applying the CE method along with the static assignment approach to minimise the travel time in case of no reduction in capacity;
- Using ten different seed values, applying the CE method along with the static assignment approach to minimise the travel time in case of no reduction in capacity.

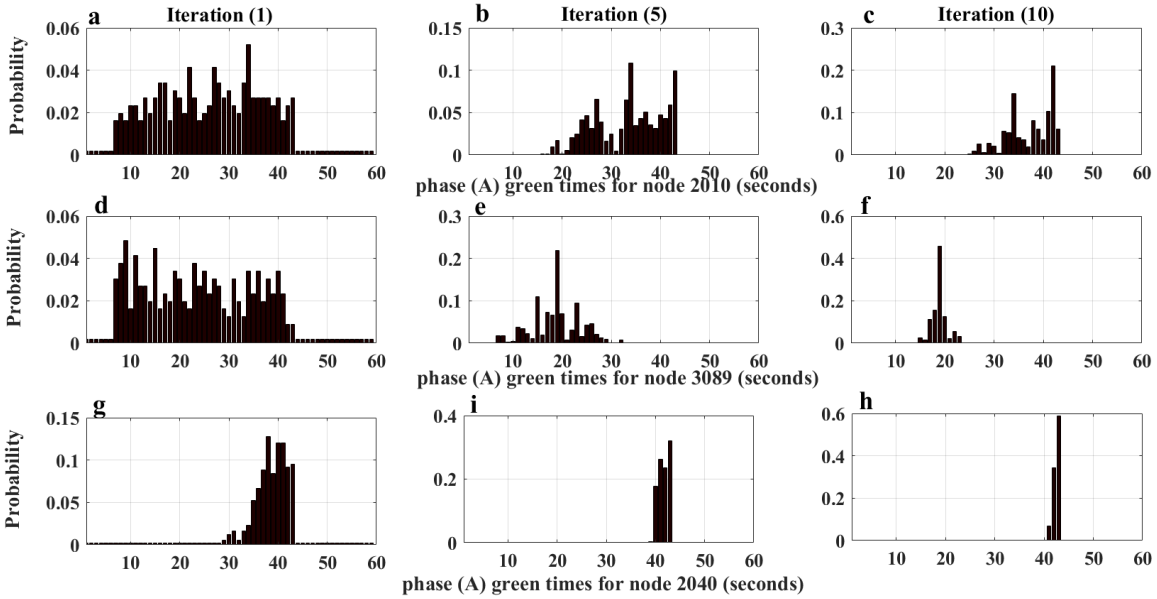

Figure A.1: Phase A green times convergence of N=5,000 and t=10 for nodes 2010, 3089, and 2040

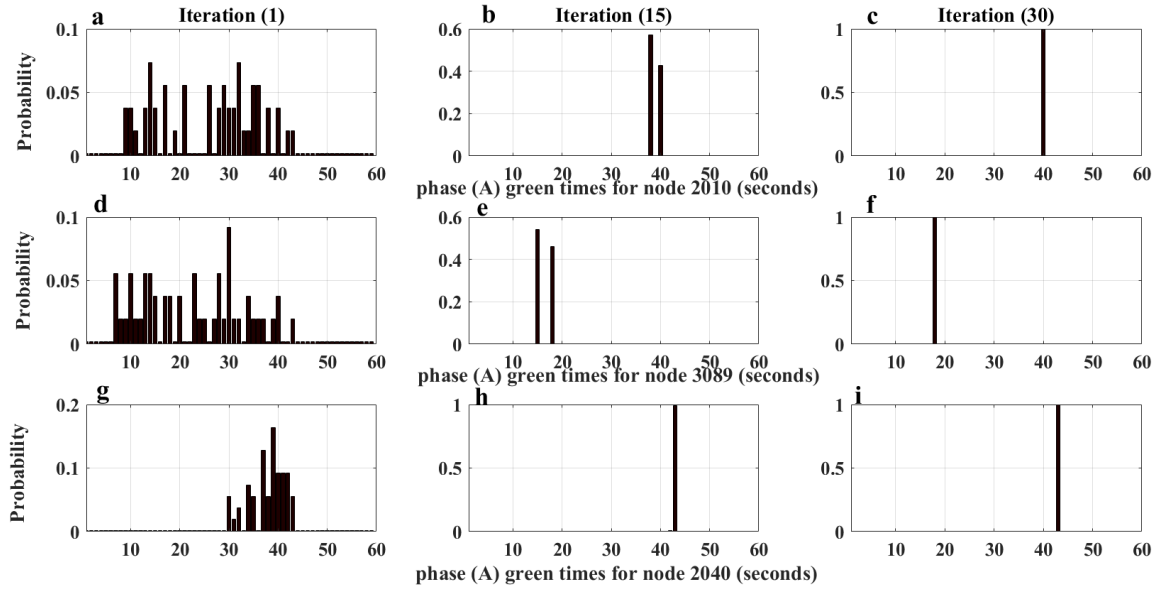

Figure A.2: Phase A green times convergence of N=1,000 and t=30 for nodes 2010, 3089, and 2040

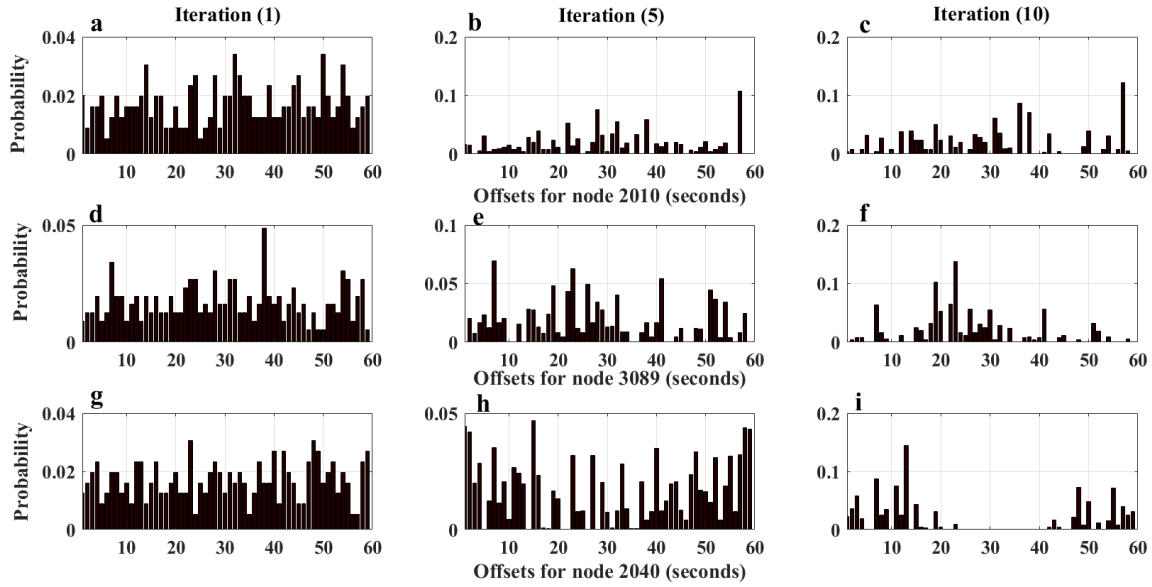

Figure A.3: Offsets convergence of N=5,000 and t=10 for nodes 2010, 3089, and 2040

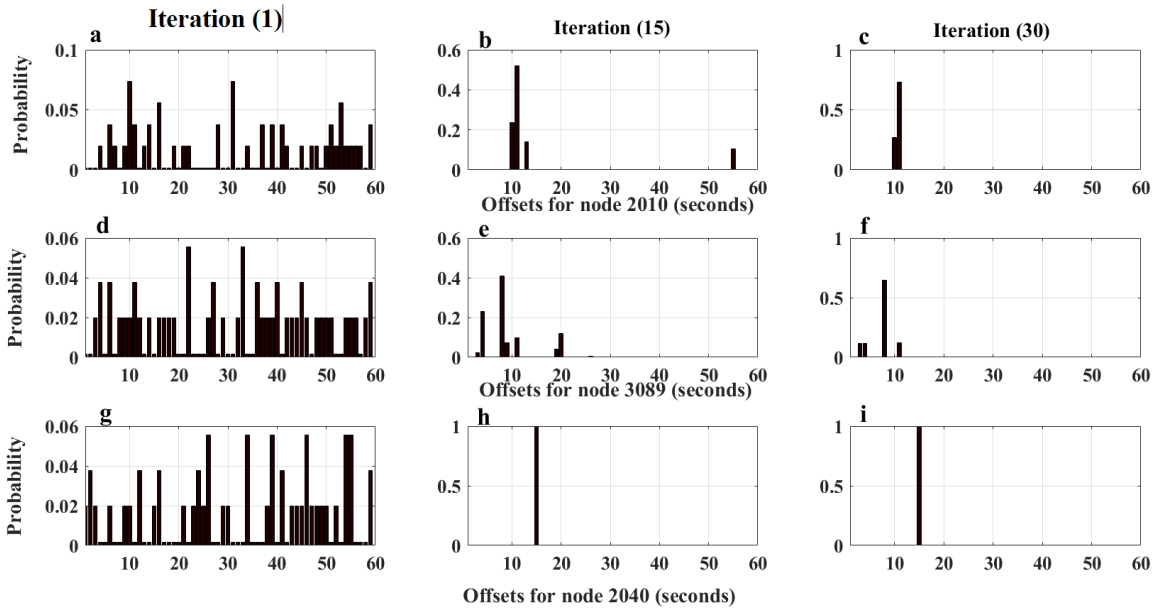

Figure A.4: Offsets convergence of N=1,000 and t=30 for nodes 2010, 3089, and 2040

Table A.1: Phase A green times for the 24 signalised nodes for two different sample sizes and iteration combinations in the case of no capacity reduction, applying the CEM-static framework

No.	Node	N = 1,000 and t=30	N = 5,000 and t=10
1	2010	40	35
2	4740	43	43
3	4580	14	13
4	4500	36	37
5	4550	16	19
6	3070	20	10
7	3080	29	29
8	3089	18	21
9	3810	43	40
10	3560	33	37
11	3900	25	25
12	4360	26	26
13	4190	38	39
14	4350	37	36
15	2620	23	12
16	2680	25	25
17	3740	43	43
18	4700	20	21
19	4400	31	28
20	3330	20	20
21	2410	15	16
22	2500	24	24
23	2040	43	41
24	2045	43	43

Table A.2: Offsets for the 24 signalised nodes for two different sample size and iteration combinations in the case of no capacity reduction, applying the CEM-static framework

No.	Node	N = 1,000 and t=30	N = 5,000 and t=10
1	2010	11	57
2	4740	26	7
3	4580	48	28
4	4500	31	25
5	4550	6	9
6	3070	17	17
7	3080	13	26
8	3089	8	19
9	3810	59	39
10	3560	36	28
11	3900	59	21
12	4360	47	54
13	4190	38	54
14	4350	11	14
15	2620	1	13
16	2680	40	29
17	3740	19	50
18	4700	15	39
19	4400	59	49
20	3330	1	29
21	2410	18	29
22	2500	30	38
23	2040	15	11
24	2045	0	0

Table A.3: Phase A green times for the 24 signalised nodes for random seed values in the case of no capacity reduction, applying the CEM-static framework

No.	Node	Run									
		1	2	3	4	5	6	7	8	9	STD
1	2010	41	42	41	41	30	40	41	42	41	3.76
2	4740	43	43	43	43	43	43	43	43	43	0.00
3	4580	14	14	14	14	7	14	15	15	12	2.49
4	4500	37	35	37	35	36	36	35	36	36	0.78
5	4550	17	18	16	17	17	16	16	16	18	0.83
6	3070	18	8	21	19	21	20	14	10	7	5.70
7	3080	26	26	28	28	27	29	26	28	24	1.54
8	3089	18	20	18	18	18	18	20	17	18	1.00
9	3810	43	43	42	42	41	43	43	43	43	0.73
10	3560	35	36	35	36	38	33	35	36	39	1.76
11	3900	29	28	29	26	28	25	26	27	26	1.45
12	4360	25	24	27	24	29	26	26	25	25	1.58
13	4190	38	38	38	38	39	38	39	39	39	0.53
14	4350	38	37	38	37	40	37	38	37	38	0.97
15	2620	22	10	19	24	11	23	16	23	12	5.65
16	2680	25	26	25	26	27	25	25	25	27	0.87
17	3740	43	41	43	41	43	43	43	43	43	0.88
18	4700	15	16	20	17	21	20	19	19	21	2.18
19	4400	25	31	27	32	27	31	32	26	26	2.88
20	3330	20	20	22	20	21	20	19	23	19	1.33
21	2410	15	16	15	15	15	15	17	14	16	0.87
22	2500	23	22	22	27	23	24	22	21	23	1.73
23	2040	43	43	43	43	43	43	43	43	43	0.00
24	2045	43	43	42	43	42	43	43	43	43	0.44

Table A.4: Offsets for the 24 signalised nodes for random seed values in the case of no capacity reduction, applying the CEM-static framework

No.	Node	Run									
		1	2	3	4	5	6	7	8	9	STD
1	2010	10	13	59	7	37	11	22	40	26	17.41
2	4740	49	16	11	16	5	26	16	10	21	12.85
3	4580	45	28	13	47	9	48	10	29	10	16.83
4	4500	45	19	51	24	18	31	1	48	44	17.01
5	4550	50	8	28	38	59	6	31	22	35	17.51
6	3070	52	50	44	2	58	17	50	27	28	18.90
7	3080	41	47	31	51	6	13	54	22	29	16.93
8	3089	45	41	29	29	1	8	50	15	26	16.73
9	3810	34	3	27	23	17	59	29	41	36	15.70
10	3560	50	41	20	6	53	36	10	56	53	19.46
11	3900	41	22	24	40	37	59	40	1	50	17.09
12	4360	23	8	6	16	23	47	27	48	28	14.85
13	4190	25	3	5	13	24	38	15	46	34	14.86
14	4350	53	32	32	49	48	11	52	22	1	18.95
15	2620	38	29	15	21	49	1	44	6	17	16.72
16	2680	44	12	52	43	43	40	10	45	48	15.38
17	3740	15	38	28	37	35	19	51	25	9	13.12
18	4700	3	36	35	45	51	15	48	15	2	19.27
19	4400	7	55	35	59	43	59	26	27	19	18.63
20	3330	50	56	15	1	6	1	37	27	24	20.44
21	2410	28	6	13	33	11	18	21	28	24	8.97
22	2500	18	5	48	29	7	30	18	21	35	13.63
23	2040	12	12	55	12	52	15	56	7	52	22.34
24	2045	0	0	0	0	0	0	0	0	0	0.00

APPENDIX B

PHASING DIAGRAMS FOR THE 24 SIGNALISED INTERSECTIONS

This appendix includes all the phasing diagrams for the 24 signalised nodes in the Cambridge (UK) network.

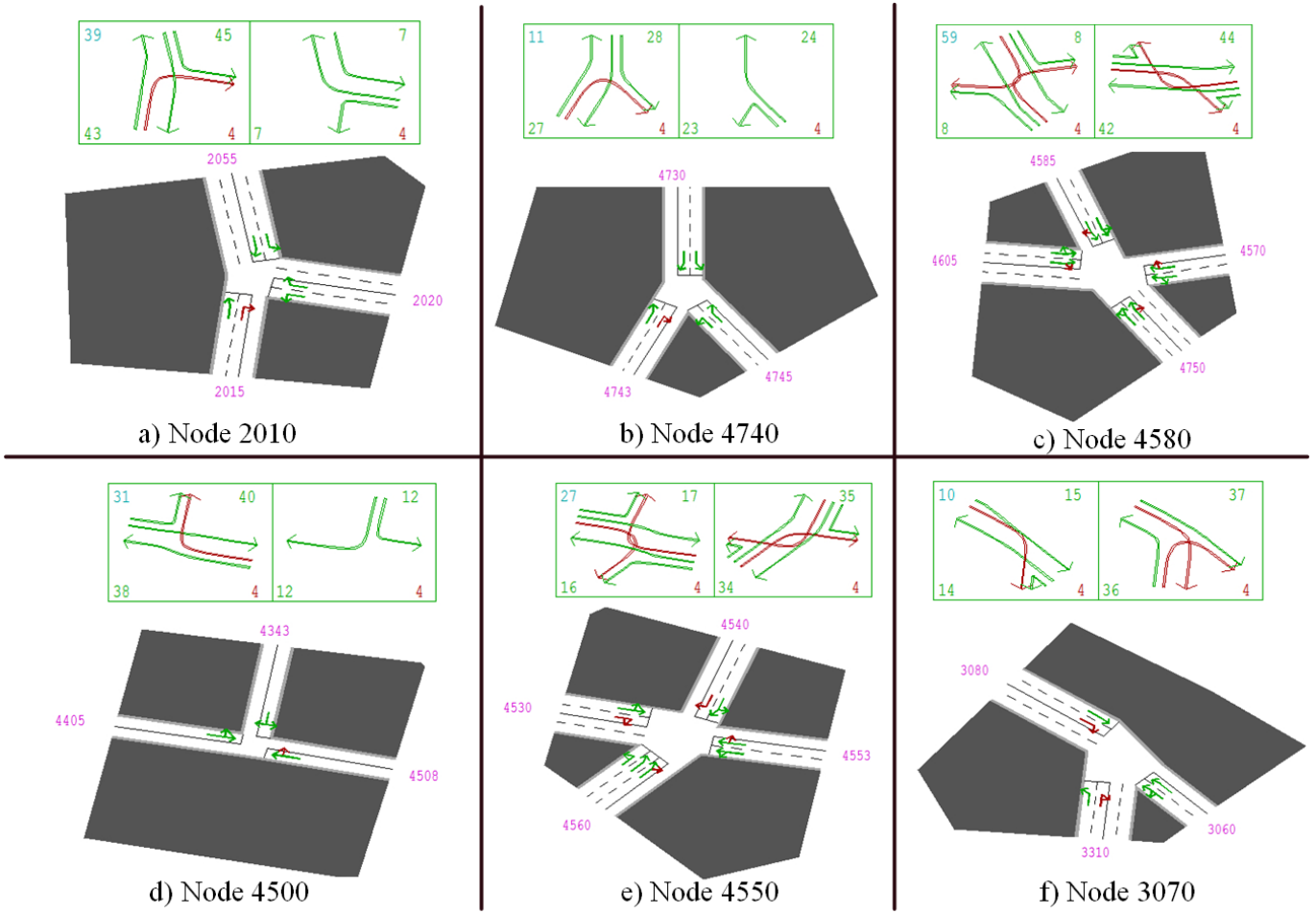

Figure B.1: Phasing arrangements for nodes 2010, 4740, 4580, 4500, 4550, 3070

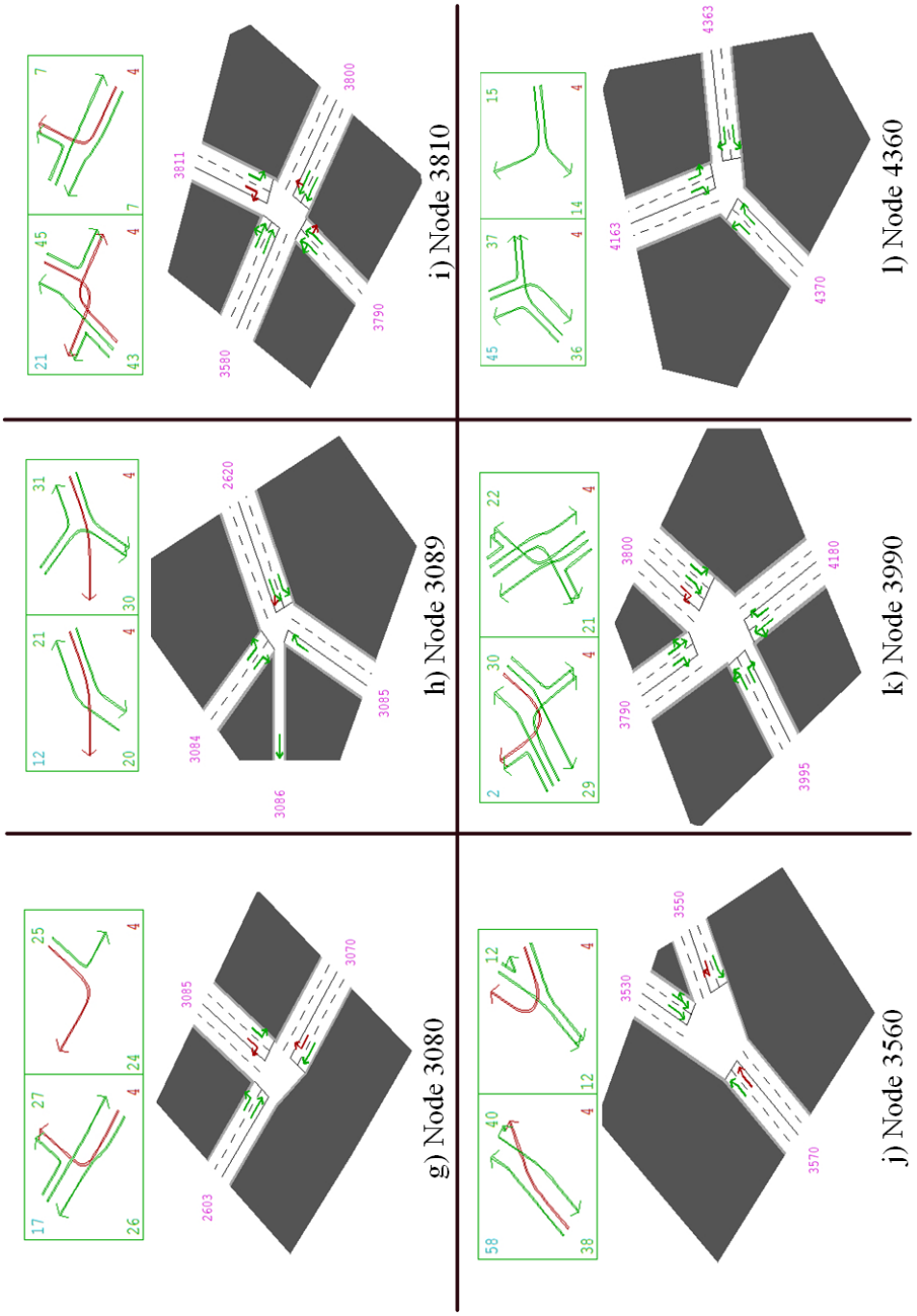

Figure B.2: Phasing arrangements for nodes 3080, 3089, 3810, 3560, 3990, 4360

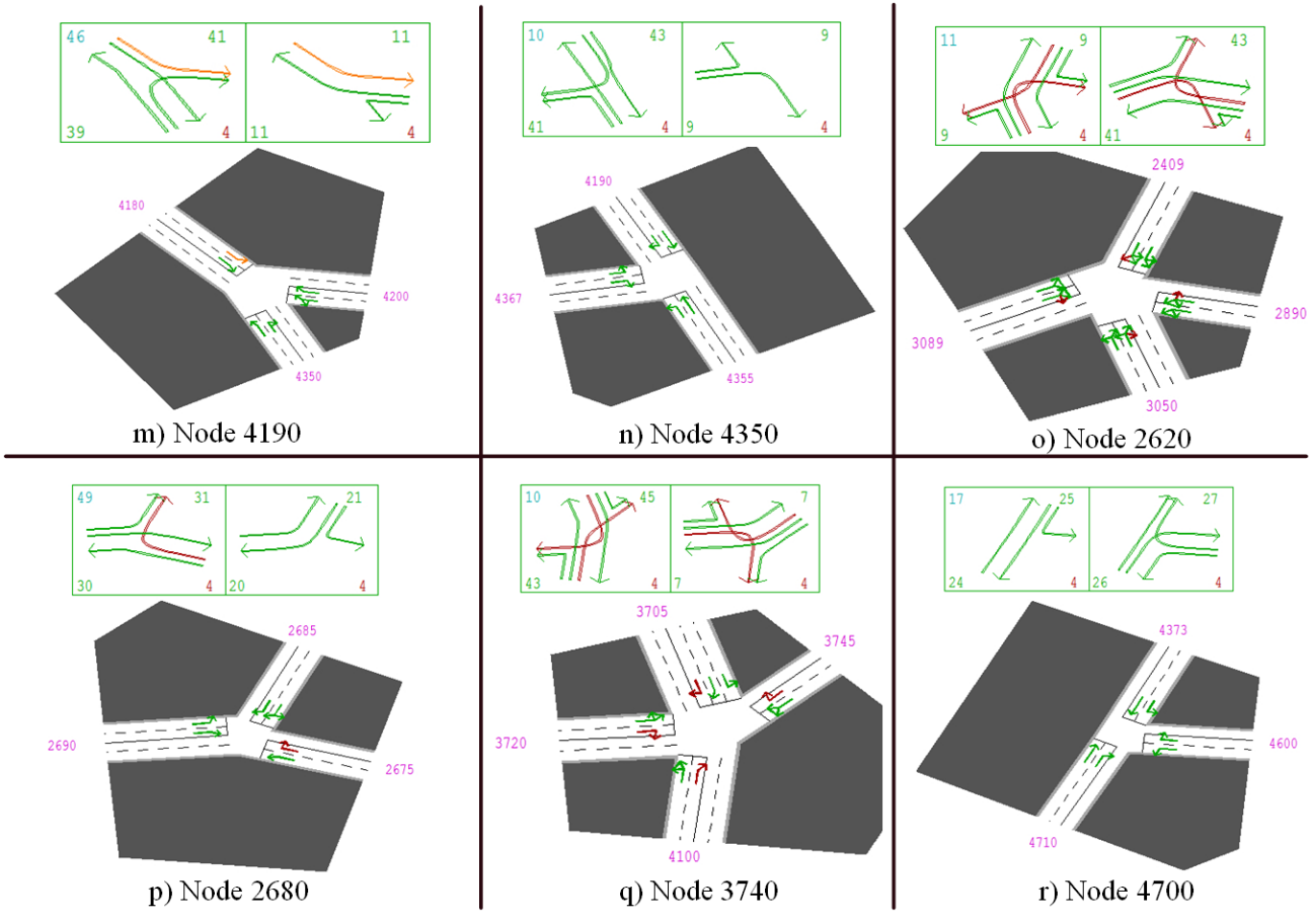

Figure B.3: Phasing arrangements for nodes 4190, 4350, 2620, 2680, 3740, 4700

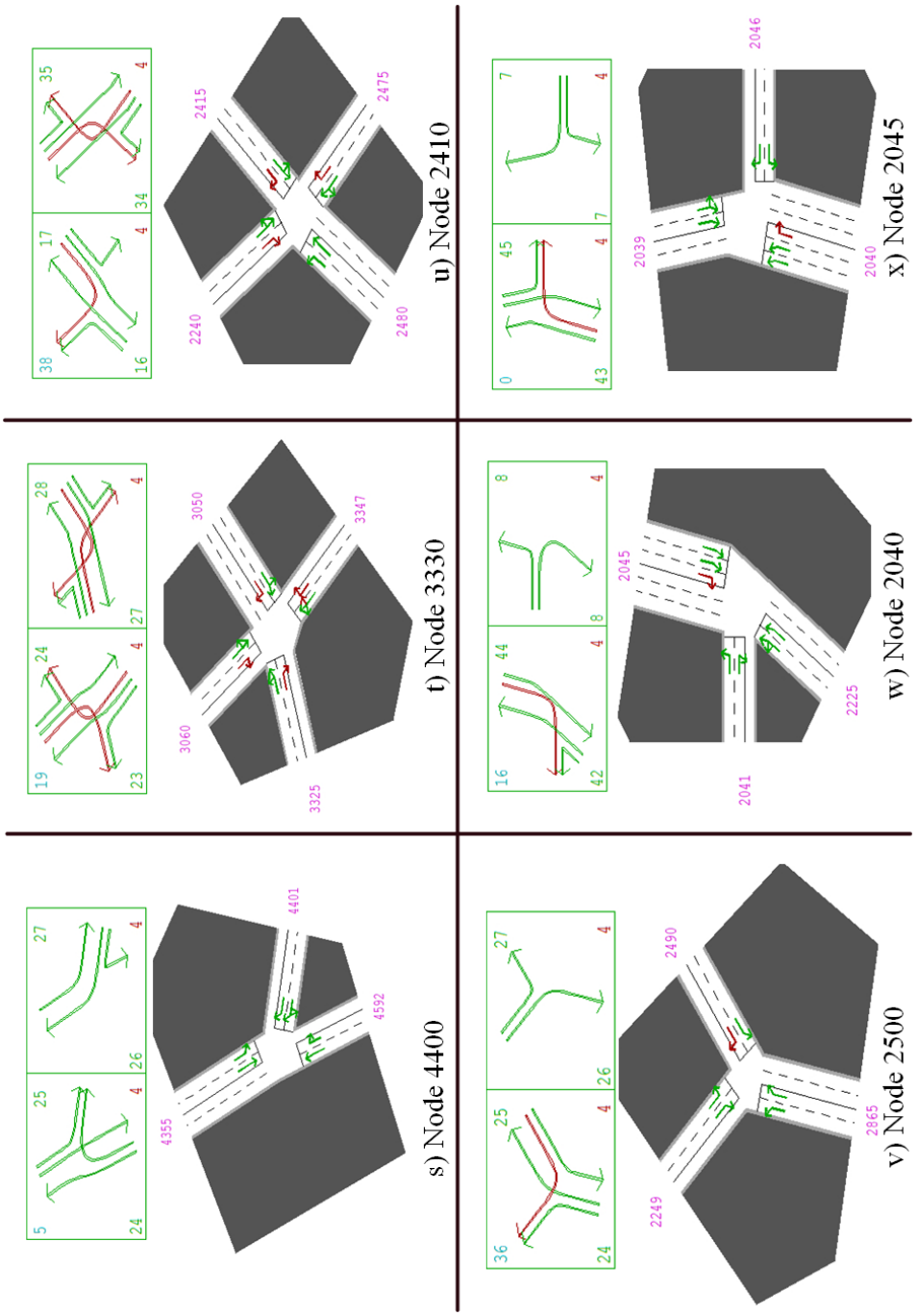

Figure B.4: Phasing arrangements for nodes 4400, 3330, 2410, 2500, 2040, 2045

APPENDIX C

SIGNAL SETTINGS AND CONVERGENCE RESULTS FOR THE CEM-STATIC FRAMEWORK, WHEN MINIMISING TRAVEL TIME

This appendix includes all the signal settings results (i.e. Phase A green times and offsets) and convergence results applying the static approach along with the CE method for no reduction, 25%, 50%, 75%, and 100% capacity reductions at node 2010, as discussed in Chapter 4.

Table C.1: Phase A green times for the 24 signalised nodes for different capacity reductions at node 2010, applying the CEM-static framework

No.	Node	0%	25%	50%	75%	100%
1	2010	40	40	43	43	40
2	4740	43	43	43	43	43
3	4580	14	14	07	13	36
4	4500	36	37	38	36	39
5	4550	16	16	17	39	43
6	3070	20	14	12	08	07
7	3080	29	26	31	37	31
8	3089	18	18	24	26	34
9	3810	43	41	43	43	43
10	3560	33	35	36	28	30
11	3990	25	25	28	29	29
12	4360	26	25	38	23	37
13	4190	38	37	36	40	37
14	4350	37	37	42	35	41
15	2620	23	14	23	12	21
16	2680	25	26	24	18	17
17	3740	43	43	43	43	43
18	4700	20	20	23	12	12
19	4400	31	26	25	33	27
20	3330	20	21	24	24	23
21	2410	15	17	22	29	32
22	2500	24	22	27	27	22
23	2040	43	43	43	43	43
24	2045	43	43	43	43	43

Table C.2: Offset times for the 24 signalised nodes for different capacity reductions at node 2010, applying the CEM-static framework

No.	Node	0%	25%	50%	75%	100%
1	2010	11	16	55	26	33
2	4740	26	27	10	48	48
3	4580	48	59	09	44	29
4	4500	31	42	46	24	24
5	4550	06	12	26	04	55
6	3070	17	18	40	45	14
7	3080	13	17	22	32	06
8	3089	08	11	12	28	07
9	3810	59	59	39	50	51
10	3560	36	21	25	40	01
11	3990	59	58	37	23	01
12	4360	47	46	22	14	32
13	4190	38	40	22	07	40
14	4350	11	10	52	36	14
15	2620	01	03	04	11	25
16	2680	40	45	41	23	55
17	3740	19	15	41	08	27
18	4700	15	09	43	44	08
19	4400	59	15	15	38	33
20	3330	01	20	47	07	51
21	2410	18	26	01	19	24
22	2500	30	39	59	20	18
23	2040	15	06	10	02	05
24	2045	00	00	00	00	00

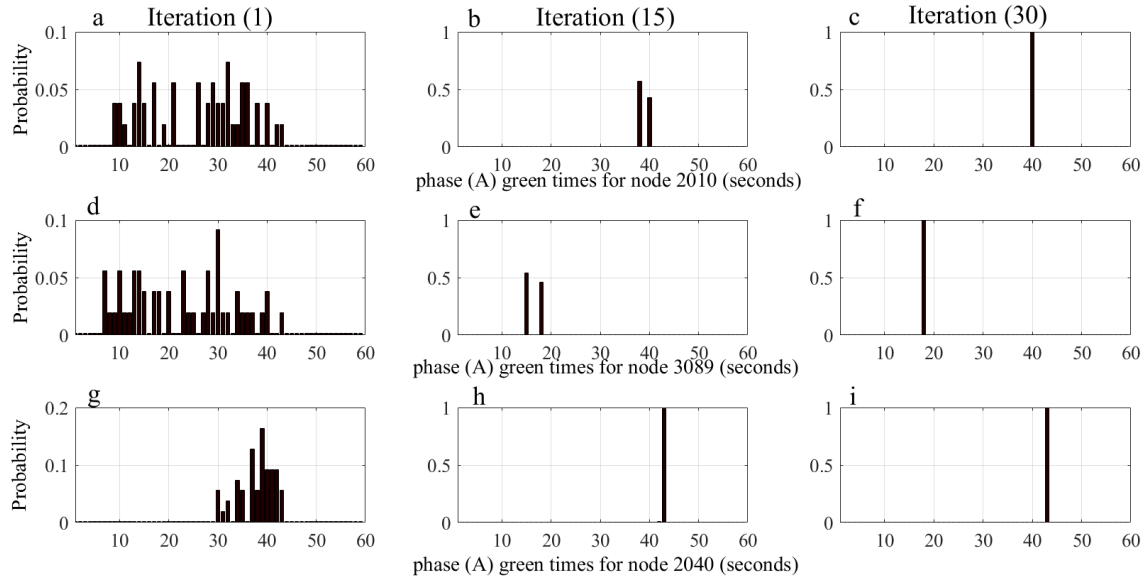

Figure C.1: Convergence of Phase A green times of no capacity reduction at node 2010, for nodes 2010 (a-c), 3089 (d-f), and 2040 (g-i)

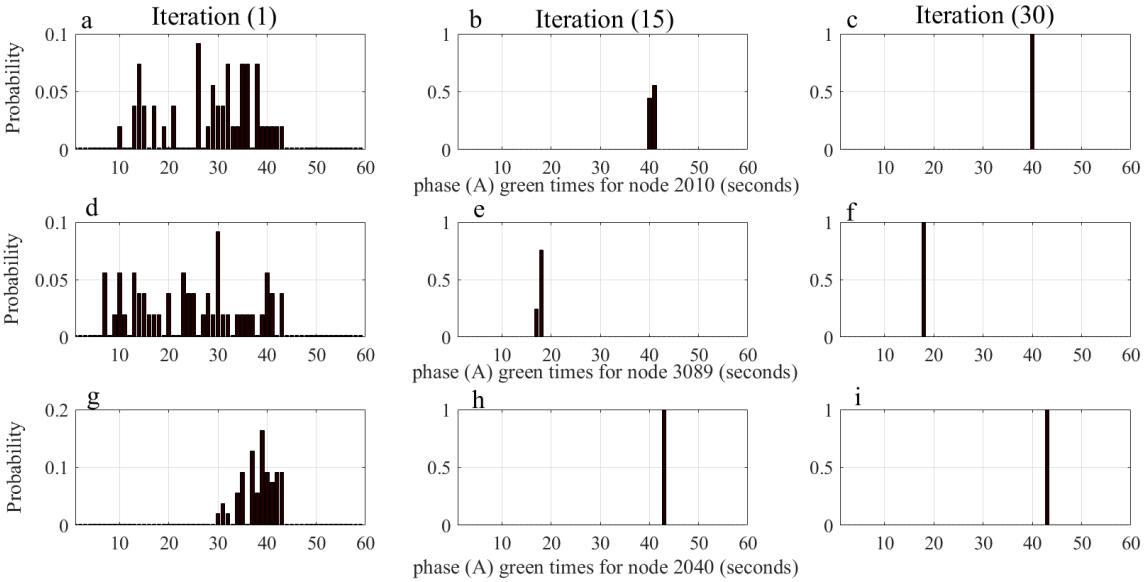

Figure C.2: Convergence of Phase A green times of a 25% capacity reduction at node 2010, for nodes 2010 (a-c), 3089 (d-f), and 2040 (g-i)

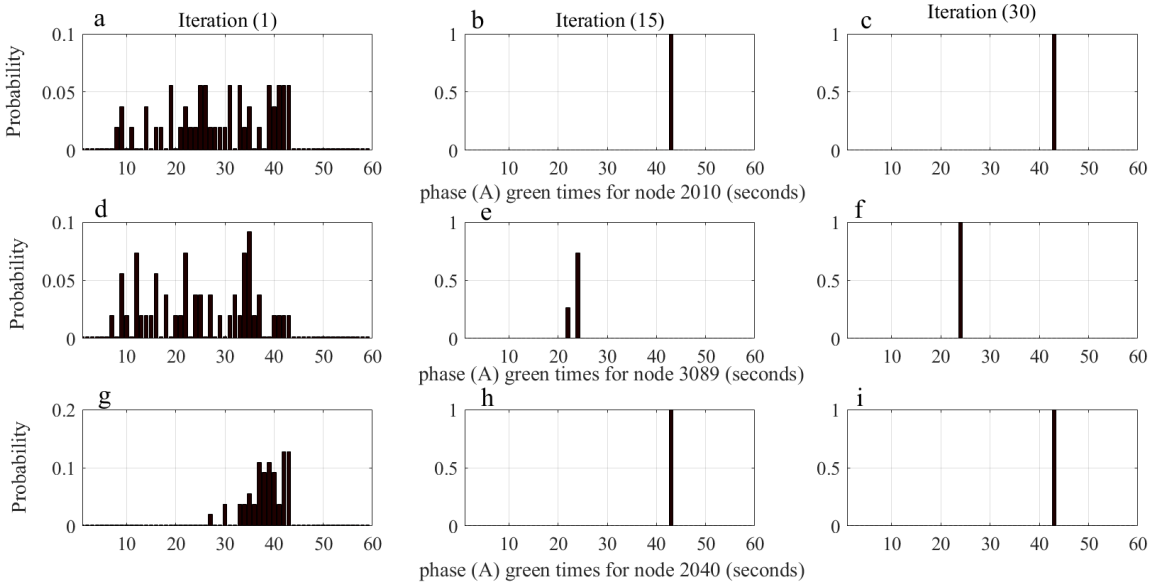

Figure C.3: Convergence of Phase A green times of a 50% capacity reduction at node 2010, for nodes 2010 (a-c), 3089 (d-f), and 2040 (g-i)

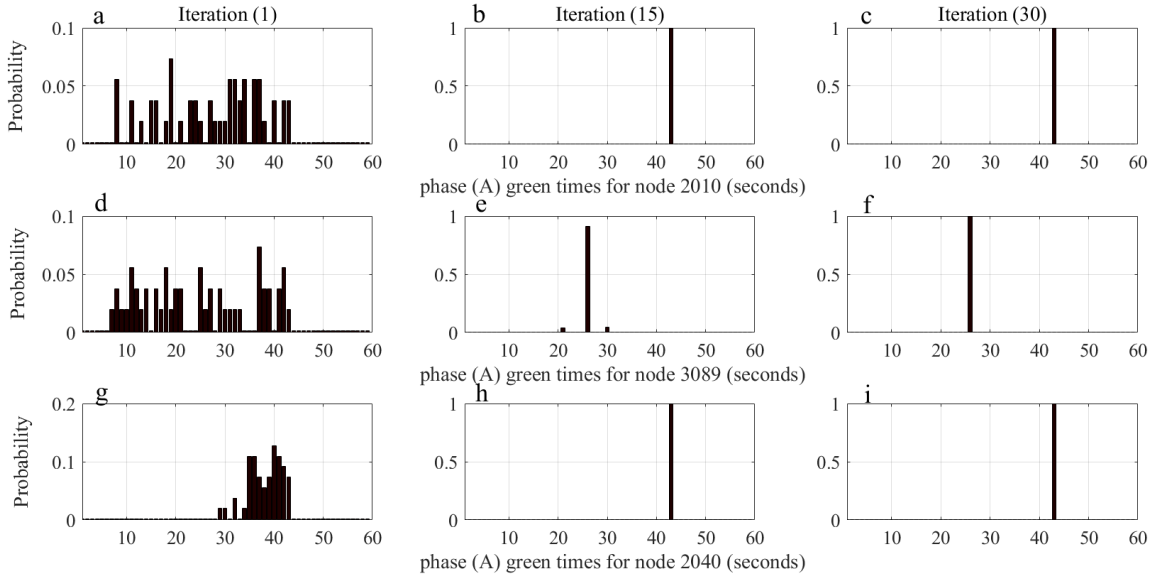

Figure C.4: Convergence of Phase A green times of a 75% capacity reduction at node 2010, for nodes 2010 (a-c), 3089 (d-f), and 2040 (g-i)

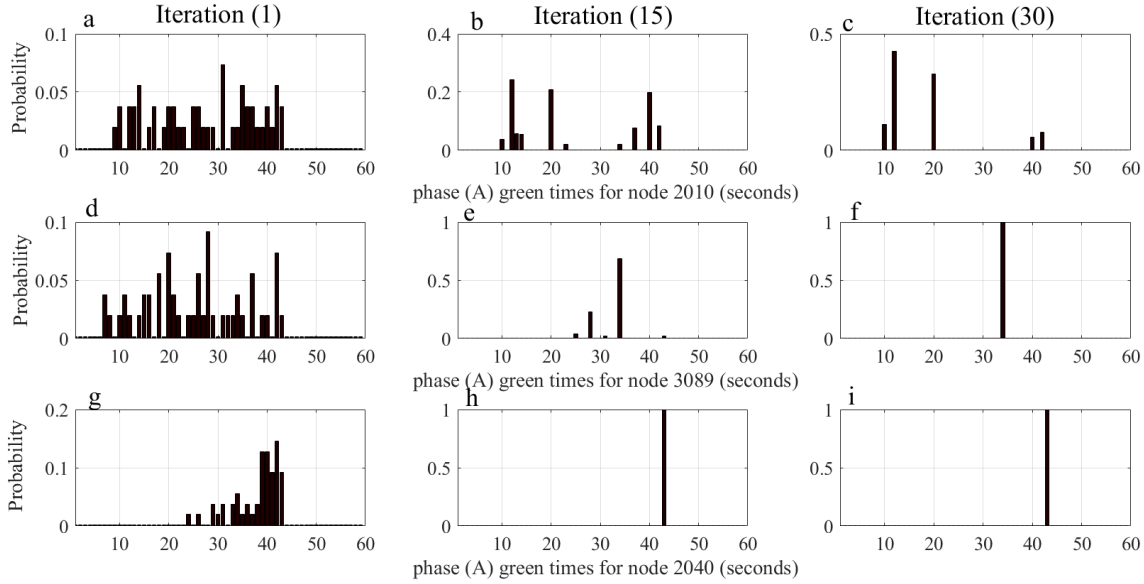

Figure C.5: Convergence of Phase A green times of a 100% capacity reduction at node 2010, for nodes 2010 (a-c), 3089 (d-f), and 2040 (g-i)

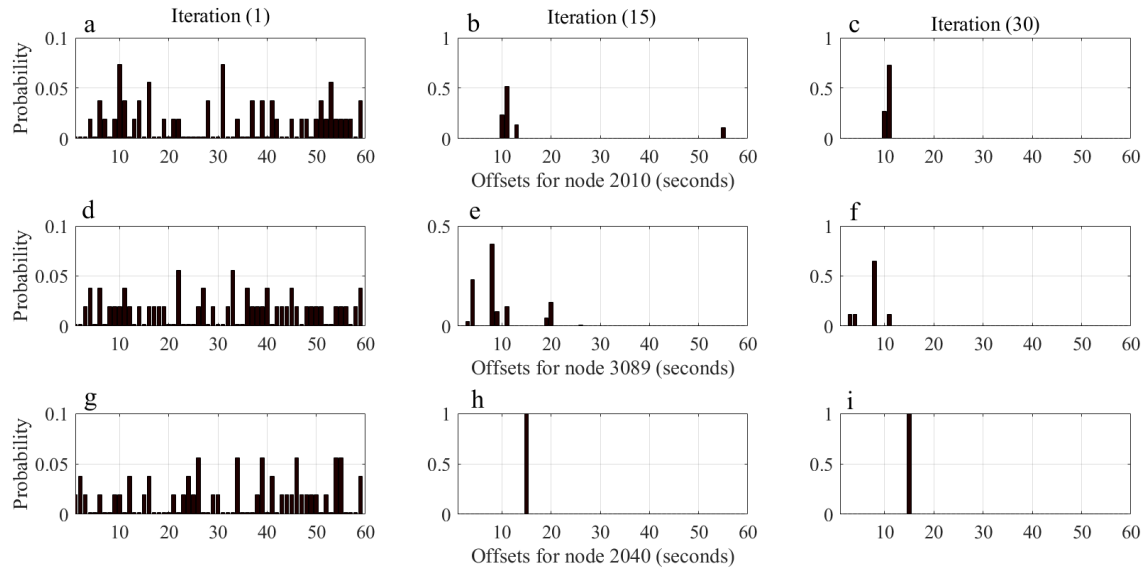

Figure C.6: Convergence of offsets of no capacity reduction at node 2010, for nodes 2010 (a-c), 3089 (d-f), and 2040 (g-i)

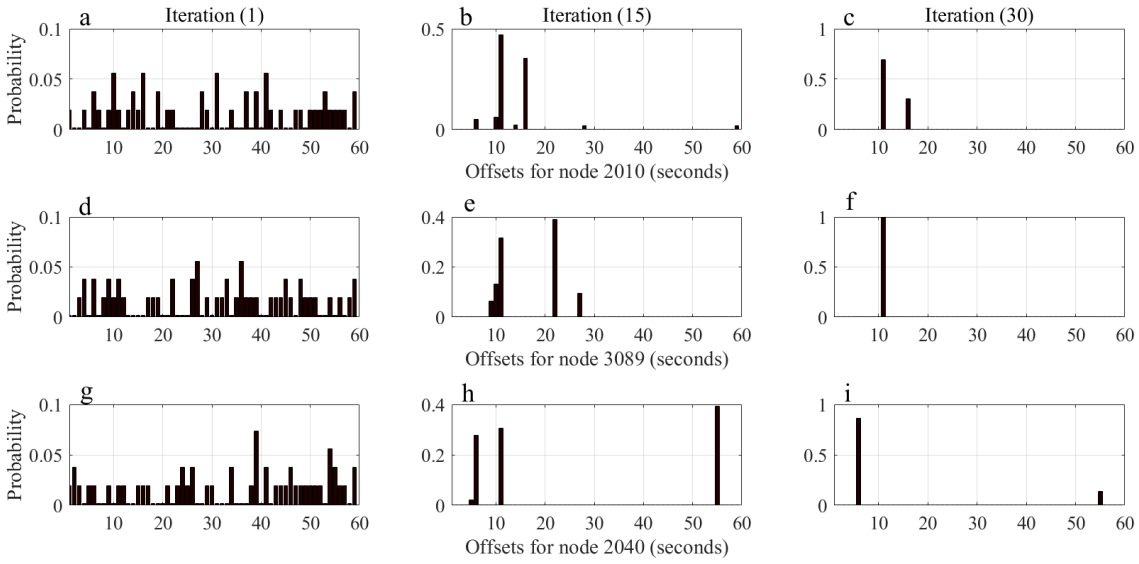

Figure C.7: Convergence of offsets of a 25% capacity reduction at node 2010, for nodes 2010 (a-c), 3089 (d-f), and 2040 (g-i)

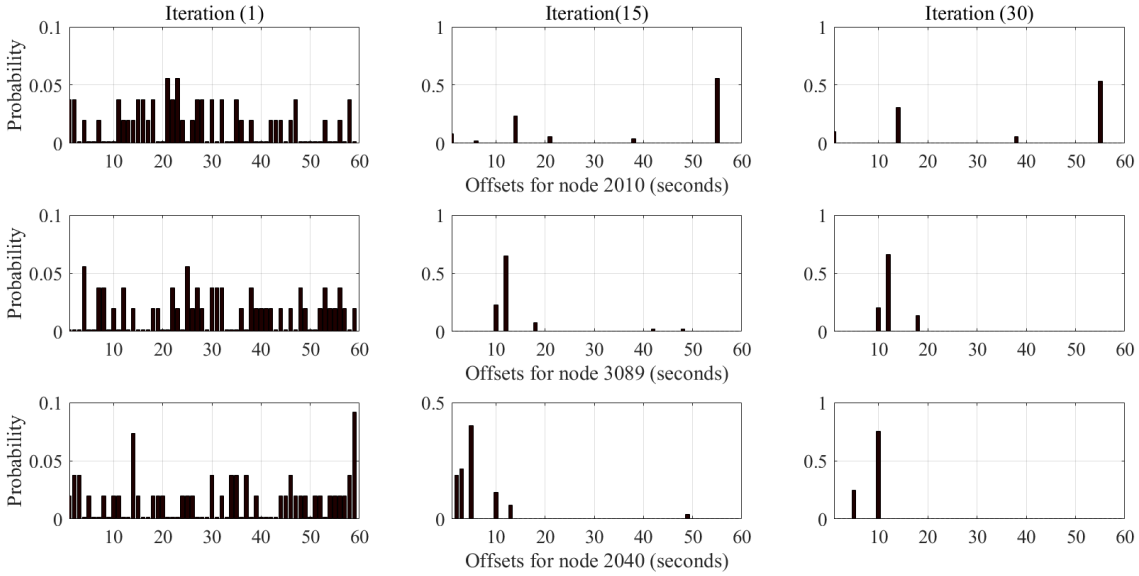

Figure C.8: Convergence of offsets of a 50% capacity reduction at node 2010, for nodes 2010 (a-c), 3089 (d-f), and 2040 (g-i)

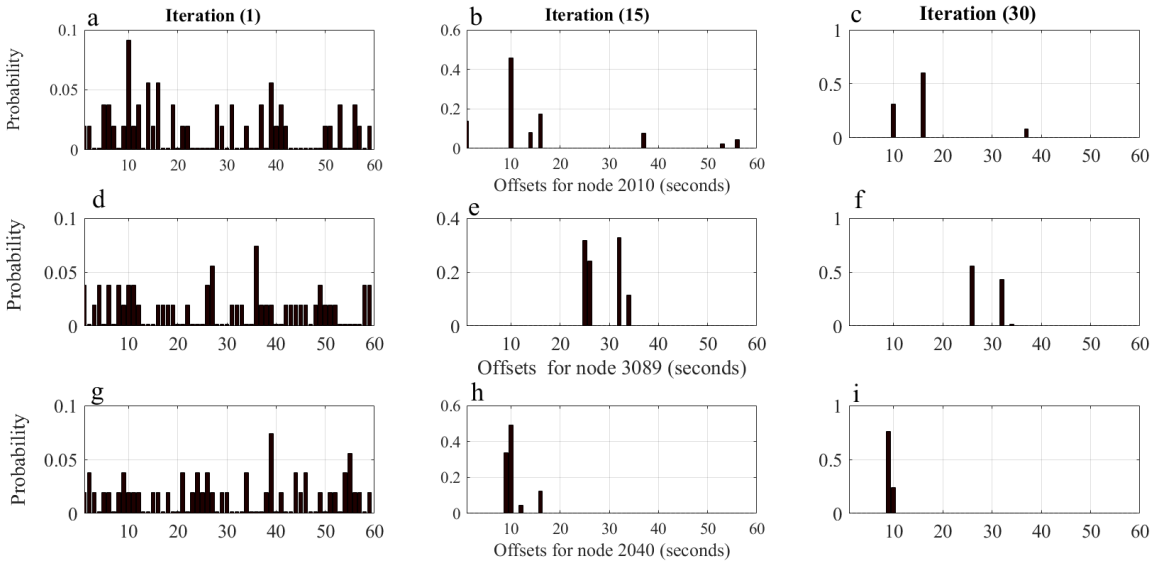

Figure C.9: Convergence of offsets of a 75% capacity reduction at node 2010, for nodes 2010 (a-c), 3089 (d-f), and 2040 (g-i)

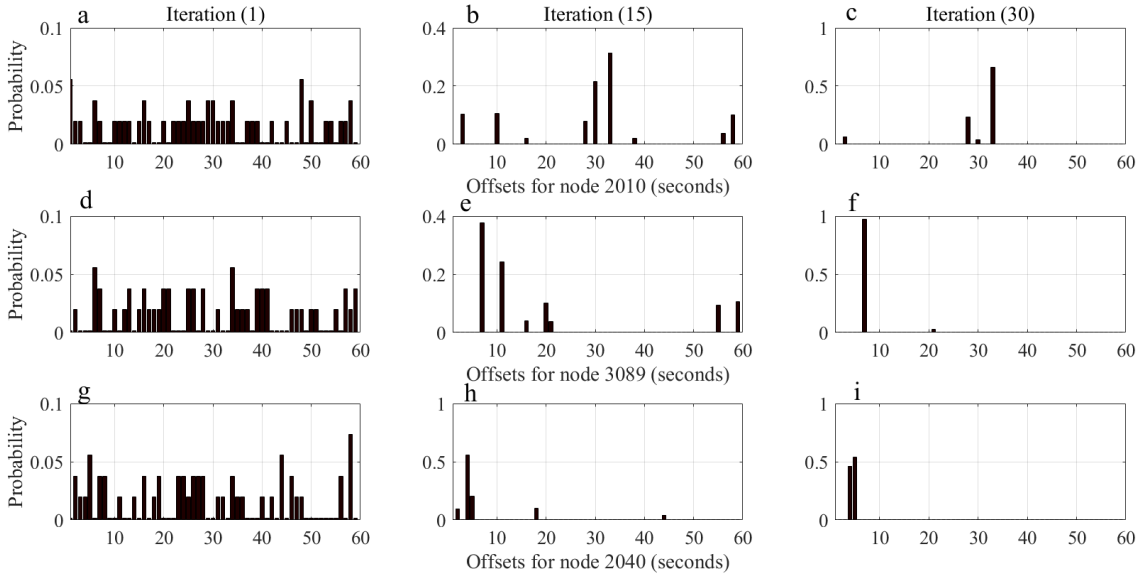

Figure C.10: Convergence of offsets of a 100% capacity reduction at node 2010, for nodes 2010 (a-c), 3089 (d-f), and 2040 (g-i)

APPENDIX D

SIGNAL SETTINGS AND CONVERGENCE RESULTS FOR THE CEM-SEMI FRAMEWORK, WHEN MINIMISING TRAVEL TIME

This appendix includes all the signal settings results (i.e. Phase A green times and offsets) for the 24 signalised nodes and convergence results applying the CE method, along with the semi-dynamic approach (CEM-semi) for a no reduction, 25%, 50%, 75%, and 100% capacity reductions at node 2010, with different capacity reduction durations (i.e. 0 minutes, 4 minutes, 20 minutes, 36, minutes, and 60 minutes), as discussed in Chapter 5.

Table D.1: Phase A green times for the 24 signalised nodes, applying the CEM-semi framework, for a 25% capacity reduction at node 2010

No.	Node	0 minutes	4 minutes	20 minutes	36 minutes	60 minutes
1	2010	42	43	42	42	41
2	4740	27	26	27	26	26
3	4580	8	8	9	8	8
4	4500	37	38	39	38	38
5	4550	15	16	15	15	18
6	3070	29	13	17	12	32
7	3080	27	29	28	29	27
8	3089	20	18	18	18	19
9	3810	43	43	43	43	43
10	3560	39	39	39	39	39
11	3900	30	29	29	29	28
12	4360	35	36	36	36	36
13	4190	36	39	37	37	37
14	4350	39	43	41	41	41
15	2620	16	12	10	17	10
16	2680	29	29	30	29	30
17	3740	43	43	43	43	43
18	4700	25	25	24	25	25
19	4400	24	25	23	24	25
20	3330	21	23	24	24	22
21	2410	16	16	16	19	18
22	2500	23	25	24	23	24
23	2040	42	42	42	42	42
24	2045	43	43	43	43	43

Table D.2: Phase A green times for the 24 signalised nodes, applying the CEM-semi framework, for a 50% capacity reduction at node 2010

No.	Node	0 minutes	4 minutes	20 minutes	36 minutes	60 minutes
1	2010	42	42	43	43	43
2	4740	27	26	27	42	43
3	4580	8	8	9	8	7
4	4500	37	38	37	38	37
5	4550	15	16	15	16	16
6	3070	29	14	10	30	20
7	3080	27	28	29	29	29
8	3089	20	18	23	23	20
9	3810	43	43	43	43	43
10	3560	39	38	39	36	38
11	3900	30	27	25	29	29
12	4360	35	37	36	34	35
13	4190	36	39	39	38	37
14	4350	39	42	41	41	41
15	2620	16	9	14	16	17
16	2680	29	30	29	29	28
17	3740	43	43	43	43	43
18	4700	25	27	25	24	23
19	4400	24	24	25	24	26
20	3330	21	24	31	23	22
21	2410	16	16	19	20	23
22	2500	23	24	23	24	24
23	2040	42	42	43	43	43
24	2045	43	43	43	43	43

Table D.3: Phase A green times for the 24 signalised nodes, applying the CEM-semi framework, for a 75% capacity reduction at node 2010

No.	Node	0 minutes	4 minutes	20 minutes	36 minutes	60 minutes
1	2010	42	42	43	43	43
2	4740	27	26	43	43	43
3	4580	8	8	7	8	3
4	4500	37	38	38	37	35
5	4550	15	16	38	39	40
6	3070	29	30	30	12	10
7	3080	27	28	29	28	22
8	3089	20	20	18	15	21
9	3810	43	43	43	43	43
10	3560	39	38	36	29	32
11	3900	30	28	29	28	26
12	4360	35	37	36	37	38
13	4190	36	37	35	32	32
14	4350	39	42	41	41	43
15	2620	16	14	16	17	9
16	2680	29	30	20	18	18
17	3740	43	43	43	43	43
18	4700	25	25	25	25	26
19	4400	24	24	24	26	27
20	3330	21	23	21	24	28
21	2410	16	19	13	12	28
22	2500	23	23	26	31	27
23	2040	42	43	43	43	43
24	2045	43	43	43	43	42

Table D.4: Phase A green times for the 24 signalised nodes, applying the CEM-semi framework, for a 100% capacity reduction at node 2010

No.	Node	0 minutes	4 minutes	20 minutes	36 minutes	60 minutes
1	2010	42	43	35	32	40
2	4740	27	26	43	42	43
3	4580	8	8	8	8	40
4	4500	37	38	37	37	41
5	4550	15	15	37	39	43
6	3070	29	14	10	10	8
7	3080	27	28	29	29	32
8	3089	20	20	20	23	31
9	3810	43	43	43	43	43
10	3560	39	37	32	32	32
11	3900	30	29	28	28	27
12	4360	35	37	37	38	42
13	4190	36	37	35	35	35
14	4350	39	42	41	42	37
15	2620	16	9	14	16	17
16	2680	29	29	18	16	17
17	3740	43	43	43	43	43
18	4700	25	25	24	25	11
19	4400	24	24	24	26	21
20	3330	21	23	26	22	27
21	2410	16	16	16	31	31
22	2500	23	24	23	22	22
23	2040	42	43	43	43	43
24	2045	43	43	41	39	41

Table D.5: Offsets for the 24 signalised nodes, applying the CEM-semi framework, for a 25% capacity reduction at node 2010

No.	Node	0 minutes	4 minutes	20 minutes	36 minutes	60 minutes
1	2010	24	13	41	39	44
2	4740	49	11	26	23	11
3	4580	56	59	47	29	14
4	4500	5	36	31	46	10
5	4550	53	46	18	6	16
6	3070	35	30	19	1	56
7	3080	53	13	10	21	13
8	3089	46	8	6	19	9
9	3810	31	21	16	59	33
10	3560	59	15	31	22	32
11	3900	28	13	2	58	24
12	4360	3	54	44	47	11
13	4190	57	46	38	41	10
14	4350	27	15	9	6	38
15	2620	37	58	3	12	6
16	2680	43	19	45	46	12
17	3740	38	13	12	10	31
18	4700	22	26	12	5	45
19	4400	41	8	8	23	44
20	3330	49	8	17	2	10
21	2410	40	22	26	28	34
22	2500	48	36	41	43	39
23	2040	16	10	12	12	13
24	2045	0	0	0	0	0

Table D.6: Offsets for the 24 signalised nodes, applying the CEM-semi framework, for a 50% capacity reduction at node 2010

No.	Node	0 minutes	4 minutes	20 minutes	36 minutes	60 minutes
1	2010	24	57	6	39	41
2	4740	49	27	4	11	54
3	4580	56	30	32	45	45
4	4500	5	17	17	40	31
5	4550	53	34	27	35	7
6	3070	35	31	9	23	10
7	3080	53	32	21	6	21
8	3089	46	32	19	58	11
9	3810	31	16	31	33	59
10	3560	59	29	21	7	36
11	3900	28	2	58	56	58
12	4360	3	47	47	45	34
13	4190	57	46	41	40	38
14	4350	27	19	14	12	8
15	2620	37	29	17	52	3
16	2680	43	51	45	52	32
17	3740	38	6	3	12	3
18	4700	22	12	9	14	59
19	4400	41	47	45	9	1
20	3330	49	19	52	41	59
21	2410	40	42	22	19	10
22	2500	48	55	49	26	9
23	2040	16	16	12	12	11
24	2045	0	0	0	0	0

Table D.7: Offsets for the 24 signalised nodes, applying the CEM-semi framework, for a 75% capacity reduction at node 2010

No.	Node	0 minutes	4 minutes	20 minutes	36 minutes	60 minutes
1	2010	24	31	54	19	54
2	4740	49	50	27	11	38
3	4580	56	32	14	50	39
4	4500	5	26	31	41	7
5	4550	53	32	26	15	18
6	3070	35	46	42	10	51
7	3080	53	13	25	15	14
8	3089	46	11	15	9	21
9	3810	31	59	24	44	38
10	3560	59	30	18	31	20
11	3900	28	1	25	7	37
12	4360	3	47	19	40	1
13	4190	57	41	13	21	51
14	4350	27	11	52	6	33
15	2620	37	6	11	59	23
16	2680	43	51	3	51	13
17	3740	38	19	47	5	23
18	4700	22	14	44	12	37
19	4400	41	4	12	10	39
20	3330	49	57	52	17	51
21	2410	40	22	49	44	45
22	2500	48	38	39	19	46
23	2040	16	16	47	42	44
24	2045	0	0	0	0	0

Table D.8: Offsets for the 24 signalised nodes, applying the CEM-semi framework, for a 100% capacity reduction at node 2010

No.	Node	0 minutes	4 minutes	20 minutes	36 minutes	60 minutes
1	2010	24	28	28	7	47
2	4740	49	11	27	44	16
3	4580	56	48	18	59	12
4	4500	5	39	44	15	34
5	4550	53	58	12	5	22
6	3070	35	51	13	10	10
7	3080	53	10	6	13	49
8	3089	46	7	6	11	55
9	3810	31	27	3	37	54
10	3560	59	3	26	24	23
11	3900	28	58	56	36	45
12	4360	03	46	46	58	6
13	4190	57	41	39	41	50
14	4350	27	11	9	23	37
15	2620	37	2	54	44	35
16	2680	43	48	33	55	56
17	3740	38	5	59	24	54
18	4700	22	12	16	26	20
19	4400	41	10	15	49	10
20	3330	49	3	40	3	27
21	2410	40	32	26	26	17
22	2500	48	30	20	25	2
23	2040	16	15	29	23	27
24	2045	0	0	0	0	0

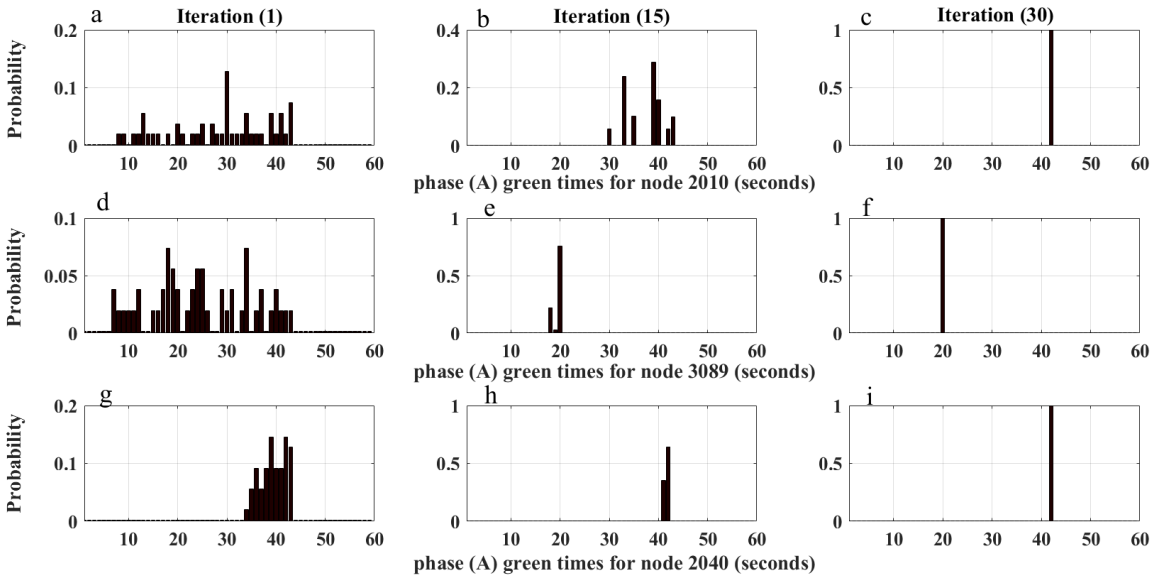

Figure D.1: Convergence of Phase A green times of no capacity reduction for 60 minutes, applying the CEM-semi framework, for nodes 2010 (a-c), 3089 (d-f), and 2040 (g-i)

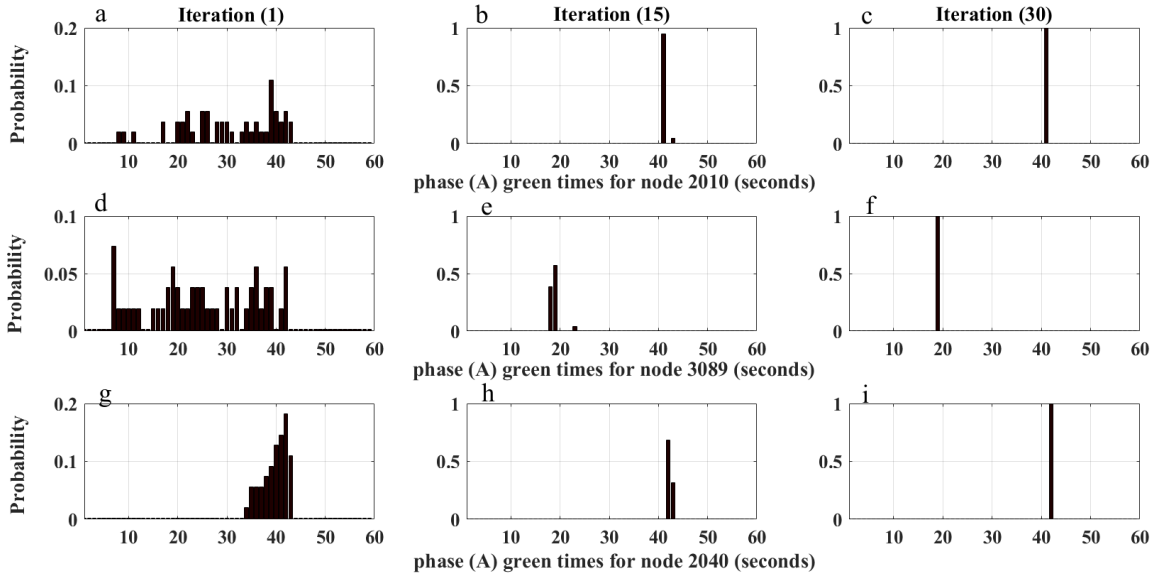

Figure D.2: Convergence of Phase A green times of a 25% capacity reduction at node 2010 for 60 minutes, applying the CEM-semi framework, for nodes 2010 (a-c), 3089 (d-f), and 2040 (g-i)

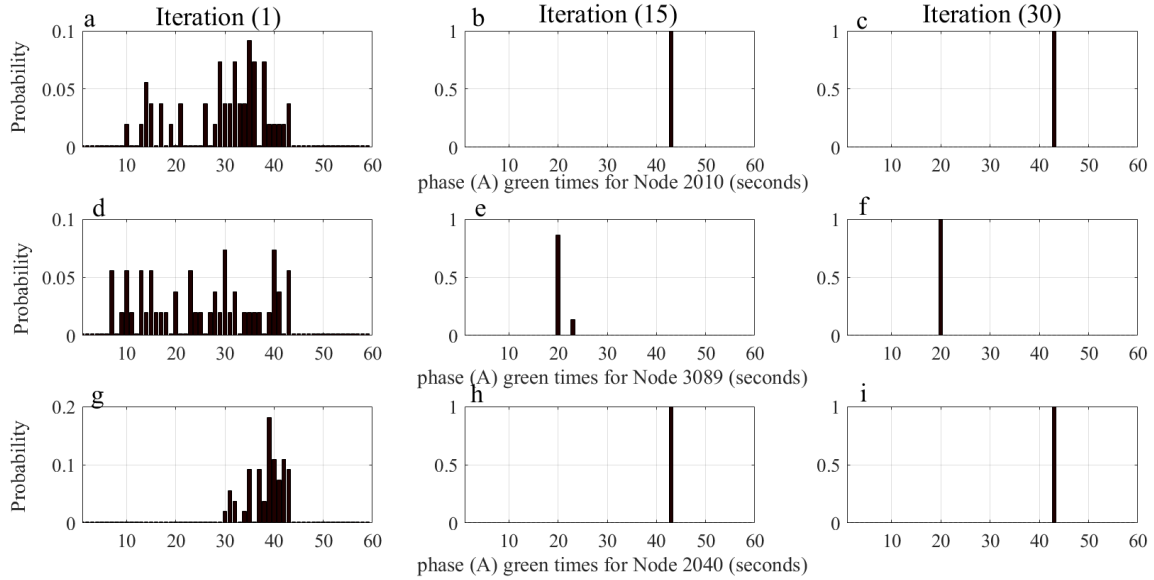

Figure D.3: Convergence of Phase A green times of a 50% capacity reduction at node 2010 for 60 minutes, the CEM-semi framework, for nodes 2010 (a-c), 3089 (d-f), and 2040 (g-i)

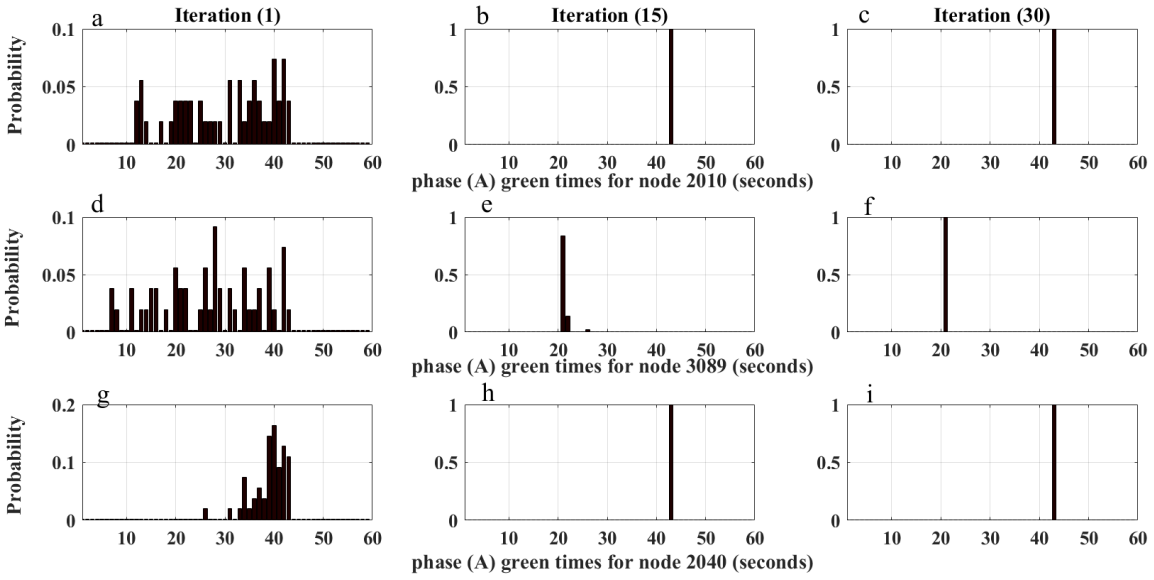

Figure D.4: Convergence of Phase A green times of a 75% capacity reduction at node 2010 for 60 minutes, applying the CEM-semi framework, for nodes 2010 (a-c), 3089 (d-f), and 2040 (g-i)

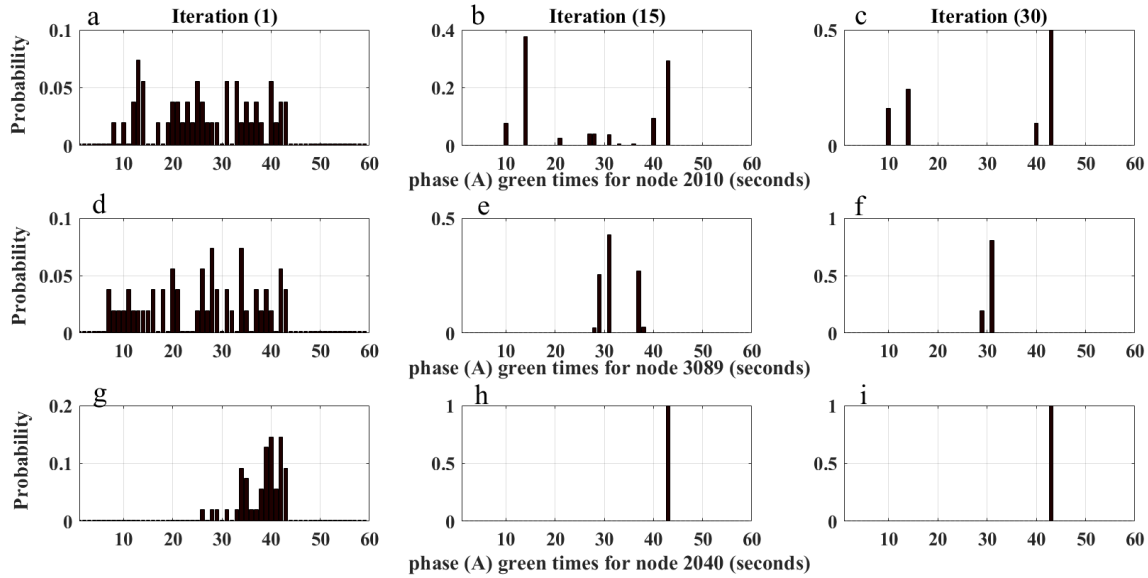

Figure D.5: Convergence of Phase A green times of a 100% capacity reduction at node 2010 for 60 minutes, applying the CEM-semi framework, for nodes 2010 (a-c), 3089 (d-f), and 2040 (g-i)

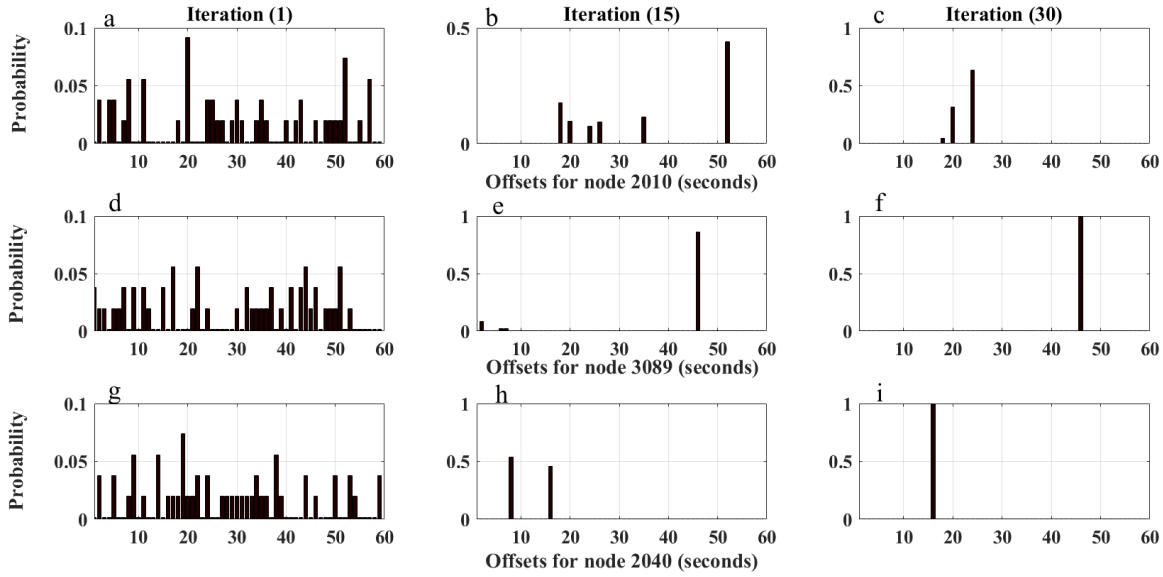

Figure D.6: Convergence of offsets of no capacity reduction for 60 minutes, applying the CEM-semi framework, for nodes 2010 (a-c), 3089 (d-f), and 2040 (g-i)

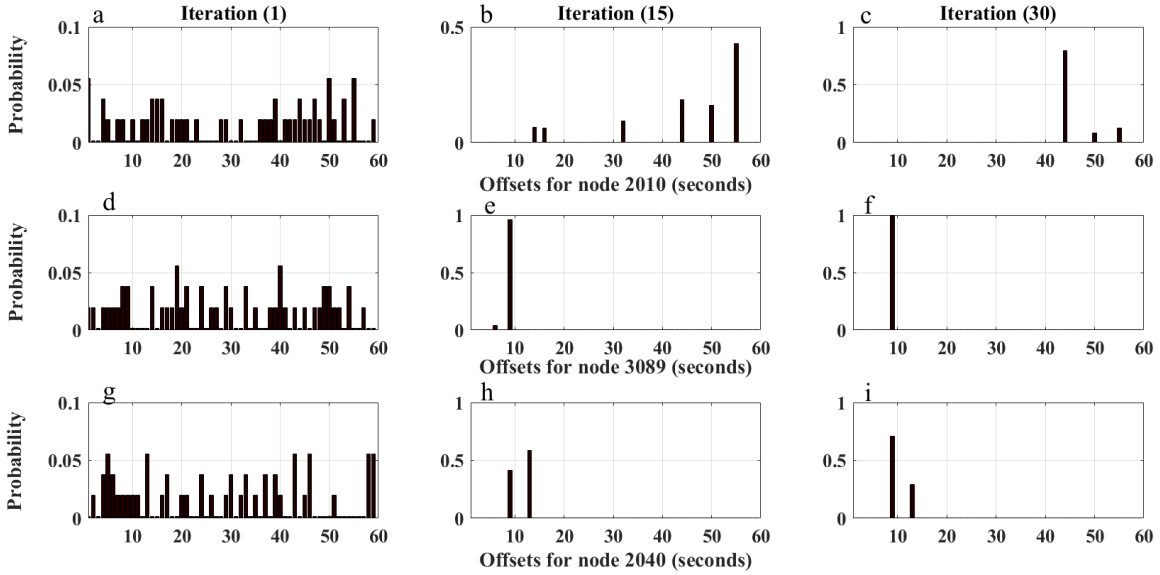

Figure D.7: Convergence of offsets of a 25% capacity reduction at node 2010 for 60 minutes, applying the CEM-semi framework, for nodes 2010 (a-c), 3089 (d-f), and 2040 (g-i)

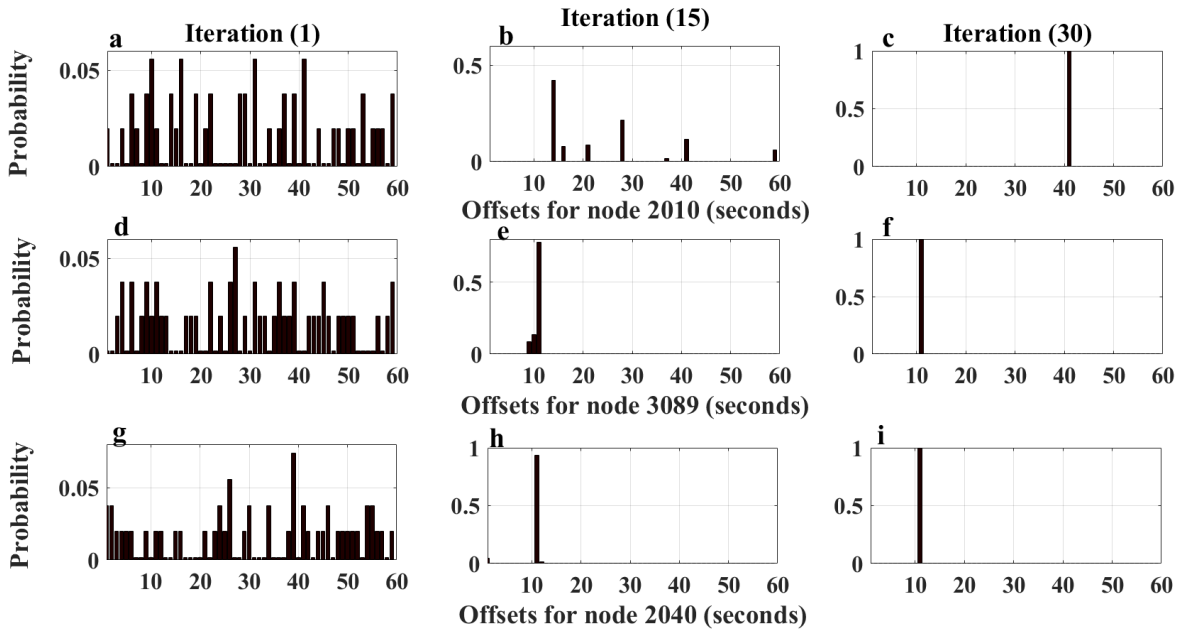

Figure D.8: Convergence of offsets of a 50% capacity reduction at node 2010 for 60 minutes, applying the CEM-semi framework, for nodes 2010 (a-c), 3089 (d-f), and 2040 (g-i)

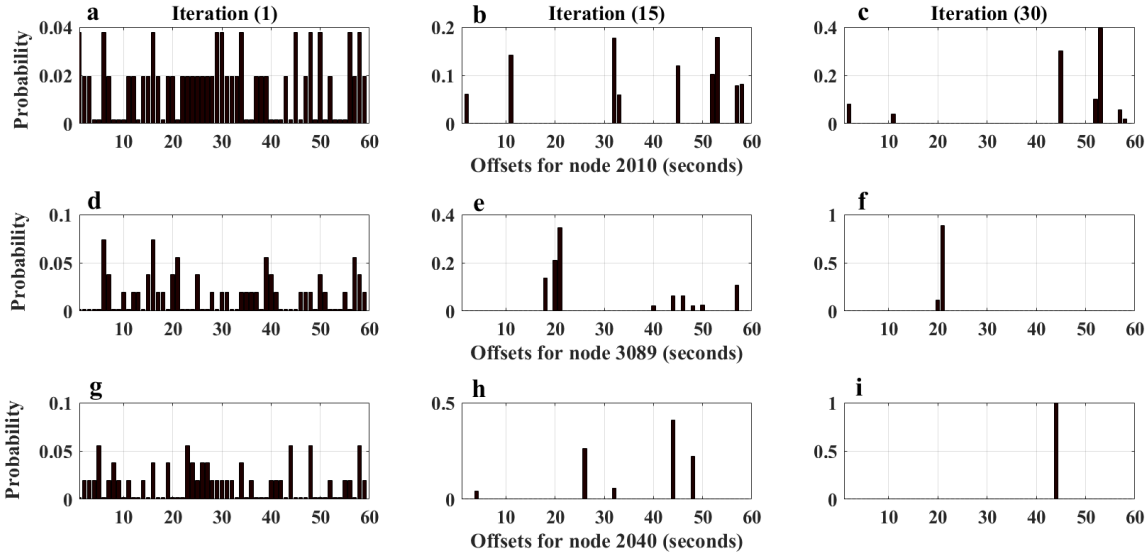

Figure D.9: Convergence of offsets of a 75% capacity reduction at node 2010 for 60 minutes, applying the CEM-semi framework, for nodes 2010 (a-c), 3089 (d-f), and 2040 (g-i)

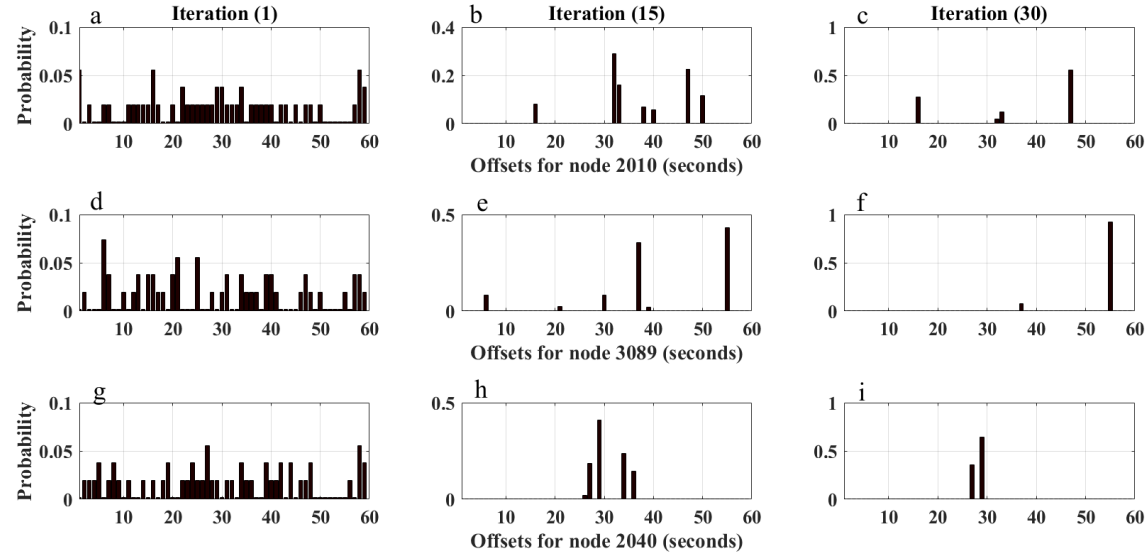

Figure D.10: Convergence of offsets of a 100% capacity reduction at node 2010 for 60 minutes, applying the CEM-semi framework, for nodes 2010 (a-c), 3089 (d-f), and 2040 (g-i)

APPENDIX E

SIGNAL SETTINGS AND CONVERGENCE RESULTS FOR THE CEM-SEMI FRAMEWORK, WHEN MINIMISING CO_2 EMISSIONS

This appendix includes all the signal settings results (i.e. Phase A green times and offsets) for the 24 signalised nodes, along with the convergence results for minimising the CO_2 emissions modelling, applying the semi-dynamic approach.

Table E.1: Phase A green times for a 50% capacity reduction at node 2010, minimising CO_2 emissions

No	Node	0 minutes	20 minutes	36 minutes	60 minutes
1	2010	42	43	43	43
2	4740	7	7	3	3
3	4580	43	13	40	42
4	4500	37	39	38	39
5	4550	15	10	14	16
6	3070	34	19	43	42
7	3080	25	28	39	39
8	3089	11	10	7	10
9	3810	43	43	43	43
10	3560	43	43	41	37
11	3900	35	31	33	33
12	4360	30	43	43	43
13	4190	39	39	39	39
14	4350	33	35	40	38
15	2620	35	36	43	40
16	2680	29	28	28	27
17	3740	43	43	43	43
18	4700	36	26	38	37
19	4400	13	16	16	16
20	3330	43	39	27	27
21	2410	15	15	13	12
22	2500	30	32	28	31
23	2040	43	43	43	43
24	2045	43	43	43	43

Table E.2: Phase A green times for a 75% capacity reduction at node 2010, minimising CO_2 emissions

No	Node	0 minutes	20 minutes	36 minutes	60 minutes
1	2010	42	43	43	43
2	4740	7	7	7	7
3	4580	43	10	43	43
4	4500	37	38	37	40
5	4550	15	19	10	14
6	3070	34	8	9	7
7	3080	25	39	43	43
8	3089	11	5	33	16
9	3810	43	43	43	43
10	3560	43	38	41	40
11	3900	35	37	15	27
12	4360	30	41	42	40
13	4190	39	37	38	23
14	4350	33	36	27	43
15	2620	35	43	41	43
16	2680	29	27	27	27
17	3740	43	43	43	43
18	4700	36	28	18	31
19	4400	13	27	16	17
20	3330	43	25	34	34
21	2410	15	15	9	43
22	2500	30	32	17	31
23	2040	43	43	43	43
24	2045	43	43	43	43

Table E.3: Phase A green times for a 100% capacity reduction at node 2010, minimising CO_2 emissions

No	Node	0 minutes	20 minutes	36 minutes	60 minutes
1	2010	42	26	16	43
2	4740	7	7	4	5
3	4580	43	43	19	43
4	4500	37	42	36	38
5	4550	15	9	9	10
6	3070	34	43	10	6
7	3080	25	38	37	43
8	3089	11	11	10	17
9	3810	43	43	43	43
10	3560	43	40	41	39
11	3900	35	31	17	21
12	4360	30	43	42	42
13	4190	39	39	39	39
14	4350	33	39	27	30
15	2620	35	41	43	20
16	2680	29	32	32	31
17	3740	43	43	43	43
18	4700	36	34	18	32
19	4400	13	16	31	18
20	3330	43	27	29	31
21	2410	15	12	30	34
22	2500	30	23	30	23
23	2040	43	43	43	43
24	2045	43	43	43	43

Table E.4: Offsets for a 50% capacity reduction at node 2010, minimising CO_2 emissions

No	Node	0 minutes	20 minutes	36 minutes	60 minutes
1	2010	42	54	53	53
2	4740	51	20	26	14
3	4580	8	45	7	14
4	4500	15	26	26	26
5	4550	17	19	13	31
6	3070	17	45	14	58
7	3080	53	19	4	45
8	3089	3	22	36	33
9	3810	47	44	59	42
10	3560	18	27	16	10
11	3900	16	1	16	10
12	4360	48	27	46	41
13	4190	46	32	42	42
14	4350	22	6	17	19
15	2620	30	54	17	9
16	2680	52	39	52	40
17	3740	34	48	14	55
18	4700	4	12	10	58
19	4400	47	54	53	53
20	3330	18	33	42	34
21	2410	34	32	28	14
22	2500	13	7	56	53
23	2040	7	6	8	8
24	2045	0	0	0	0

Table E.5: Offsets for a 75% capacity reduction at node 2010, minimising CO_2 emissions

No	Node	0 minutes	20 minutes	36 minutes	60 minutes
1	2010	42	1	54	22
2	4740	51	26	37	31
3	4580	8	13	24	20
4	4500	15	38	32	14
5	4550	17	18	54	17
6	3070	17	54	58	11
7	3080	53	42	37	5
8	3089	3	33	34	40
9	3810	47	46	8	57
10	3560	18	28	10	6
11	3900	16	16	3	39
12	4360	48	53	47	29
13	4190	46	41	41	46
14	4350	22	21	26	11
15	2620	30	19	30	1
16	2680	52	2	58	17
17	3740	34	49	10	12
18	4700	4	42	13	54
19	4400	47	54	59	47
20	3330	18	32	16	2
21	2410	34	14	15	8
22	2500	13	7	47	33
23	2040	7	8	5	6
24	2045	0	0	0	0

Table E.6: Offsets for a 100% capacity reduction at node 2010, minimising CO_2 emissions

No	Node	0 minutes	20 minutes	36 minutes	60 minutes
1	2010	42	22	55	57
2	4740	7	16	16	44
3	4580	43	27	14	14
4	4500	37	31	26	5
5	4550	15	15	18	13
6	3070	34	35	45	1
7	3080	25	23	21	48
8	3089	11	27	19	24
9	3810	43	28	7	12
10	3560	43	15	14	30
11	3900	35	5	1	3
12	4360	30	31	32	40
13	4190	39	32	38	39
14	4350	33	11	11	21
15	2620	35	18	43	16
16	2680	29	56	51	56
17	3740	43	12	59	36
18	4700	36	57	56	23
19	4400	13	54	34	35
20	3330	43	58	32	16
21	2410	15	42	3	12
22	2500	30	11	56	24
23	2040	43	8	8	8
24	2045	43	0	0	0

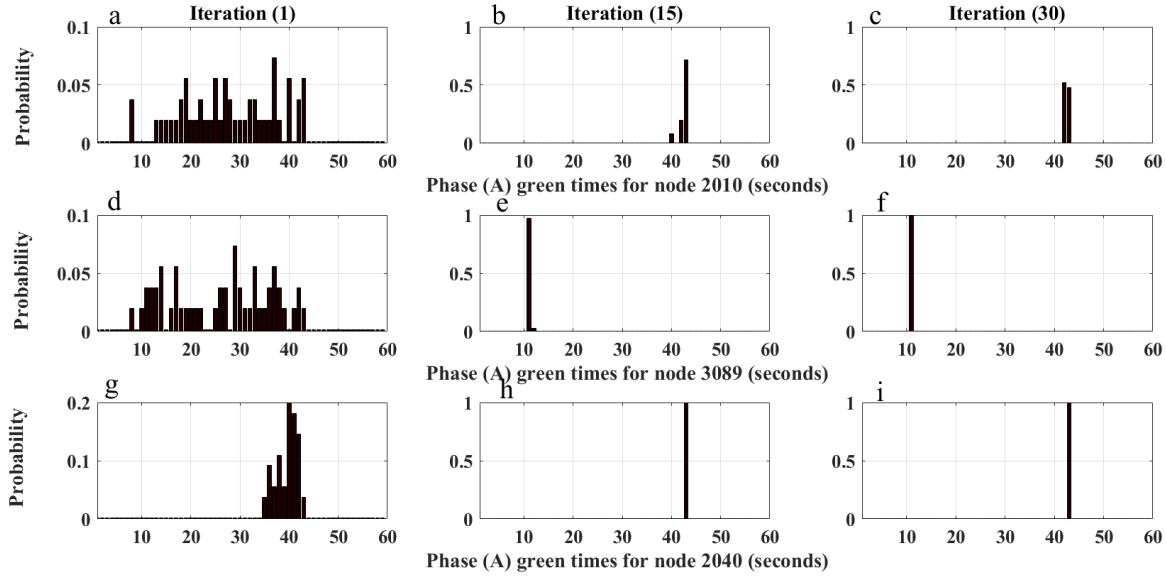

Figure E.1: Convergence of Phase A green times of a 0% capacity reduction at node 2010 for 60 minutes, for nodes 2010 (a-c), 3089 (d-f), and 2040 (g-i)

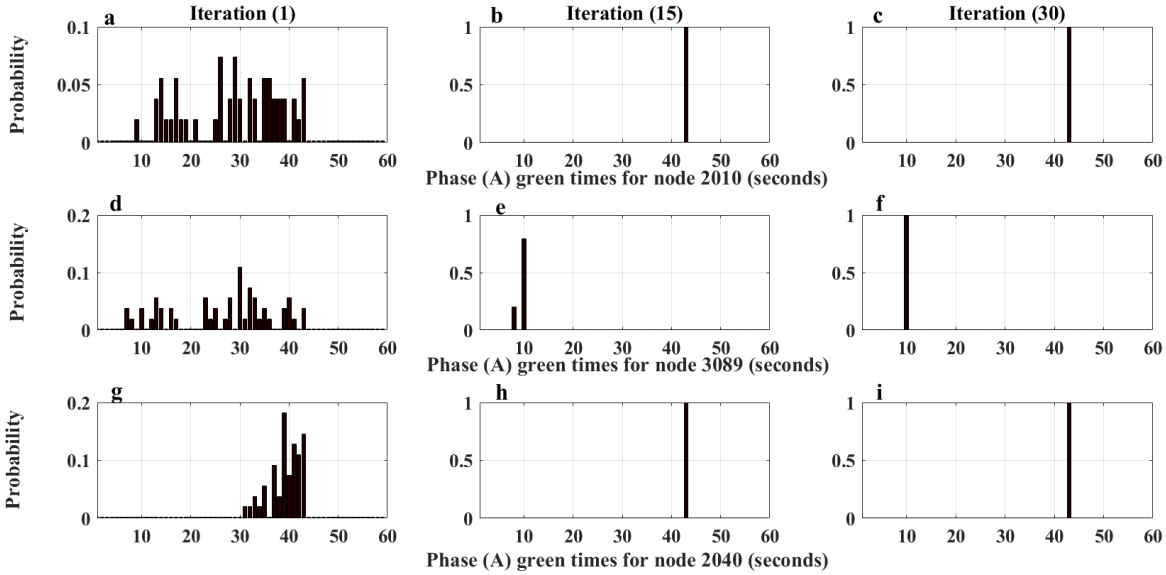

Figure E.2: Convergence of Phase A green times of a 50% capacity reduction at node 2010 for 60 minutes, for nodes 2010 (a-c), 3089 (d-f), and 2040 (g-i)

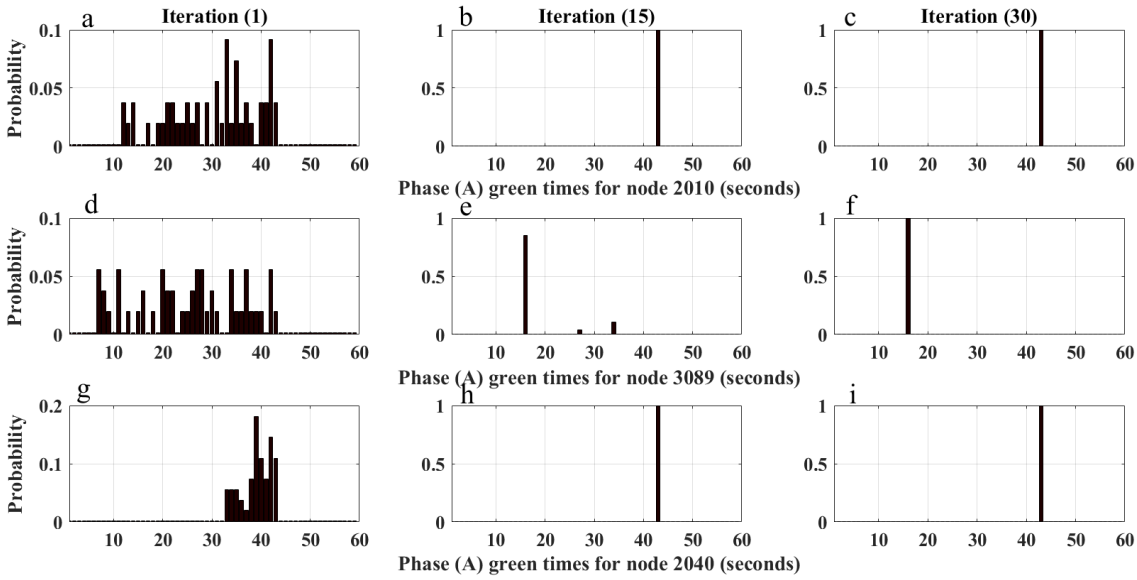

Figure E.3: Convergence of Phase A green times of a 75% capacity reduction at node 2010 for 60 minutes, for nodes 2010 (a-c), 3089 (d-f), and 2040 (g-i)

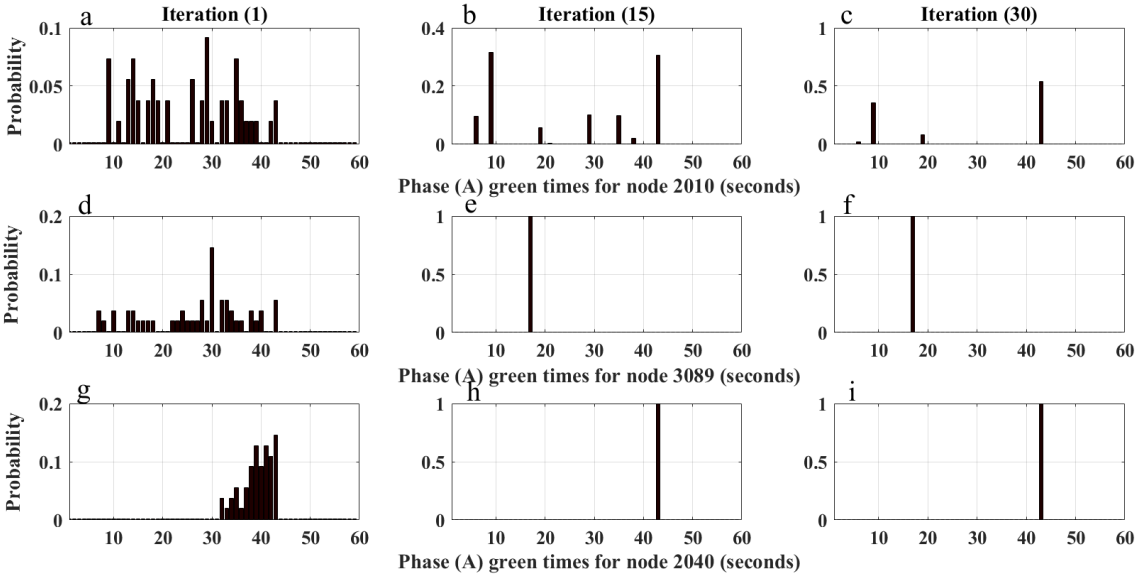

Figure E.4: Convergence of Phase A green times of a 100% capacity reduction at node 2010 for 60 minutes, for nodes 2010 (a-c), 3089 (d-f), and 2040 (g-i)

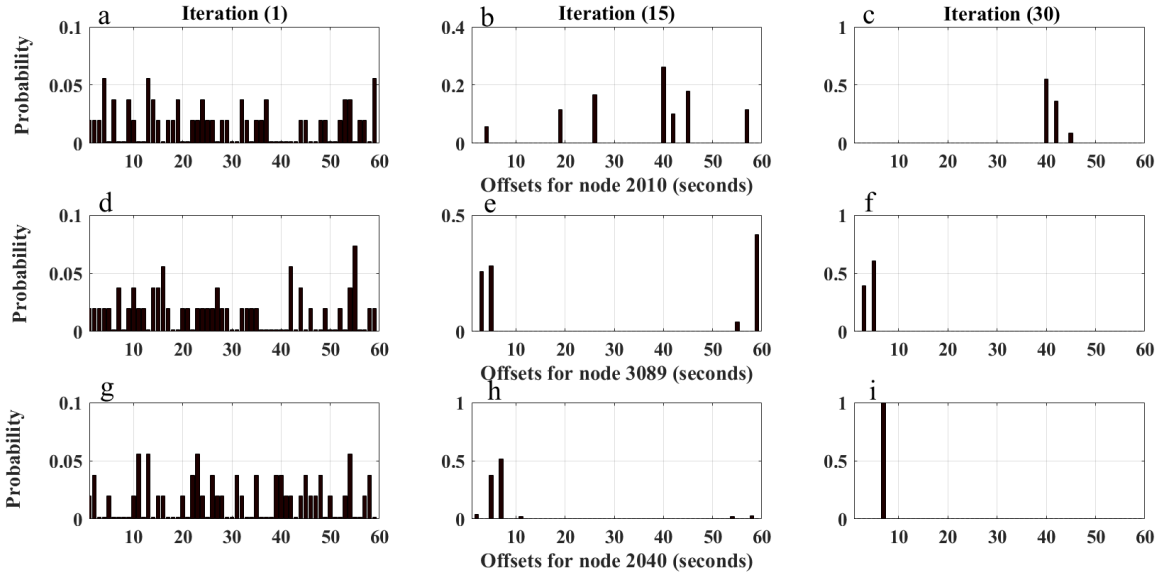

Figure E.5: Convergence of offsets of a 0% capacity reduction at node 2010 for 60 minutes, for nodes 2010 (a-c), 3089 (d-f), and 2040 (g-i)

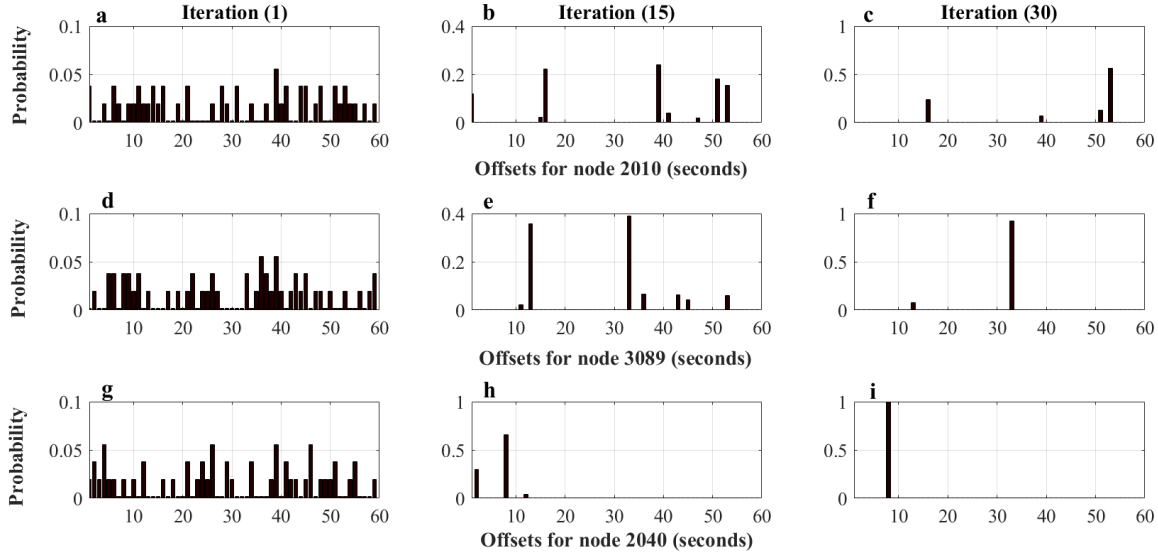

Figure E.6: Convergence of offsets of a 50% capacity reduction at node 2010 for 60 minutes, for nodes 2010 (a-c), 3089 (d-f), and 2040 (g-i)

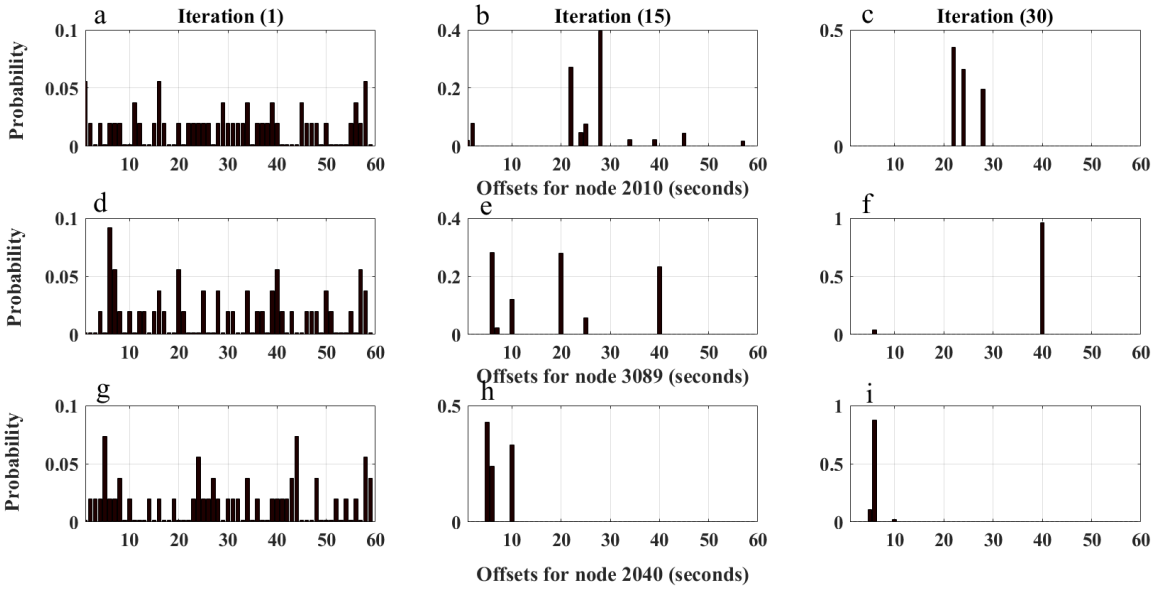

Figure E.7: Convergence of offsets of a 75% capacity reduction at node 2010 for 60 minutes, for nodes 2010 (a-c), 3089 (d-f), and 2040 (g-i)

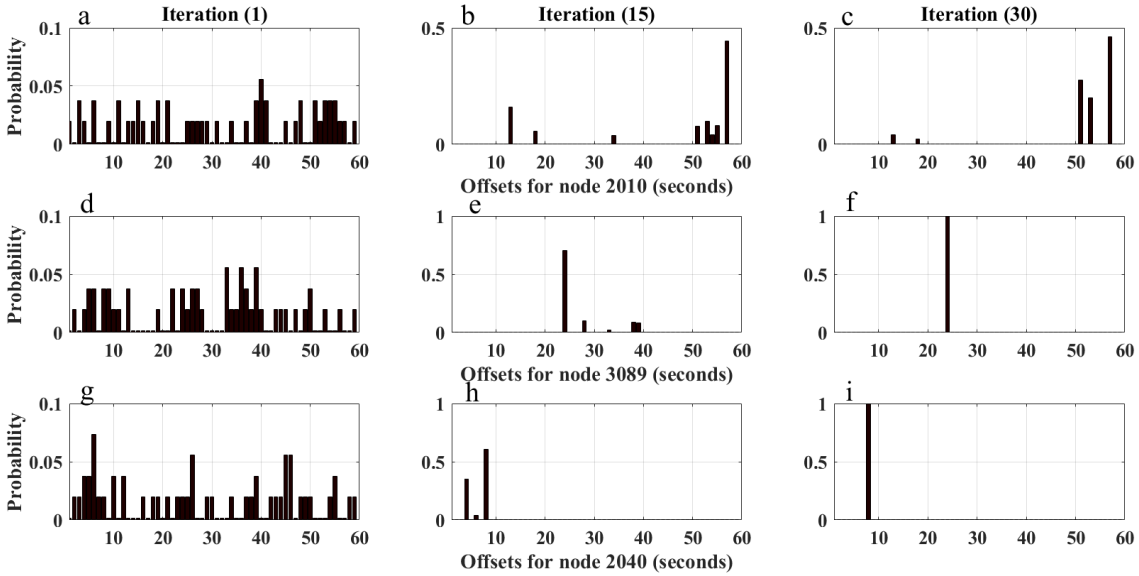

Figure E.8: Convergence of offsets of a 100% capacity reduction, at node 2010 for 60 minutes, for nodes 2010 (a-c), 3089 (d-f), and 2040 (g-i)

APPENDIX F

PUBLICATIONS AND AWARDS RELATED TO THESIS

This appendix includes a list of published and submitted papers, along with the received awards related to this thesis, as listed below:

- **Conference publications**
  - **Abudayyeh, D.** 2018. Modelling disrupted networks: A literature review of modelling simulators. IPENZ Transportation Group conference. Queenstown, New Zealand. **(Parts of Chapter 2)**.
  - **Abudayyeh, D.**, Ngoduy, D. Nicholson, A. 2018. Traffic Signal Optimisation in Disrupted Networks with Re-routing. Proceedings of the 6th International Symposium on Transport Simulation, Matsuyama, Japan. **(Parts of Chapter 3 and 4)**.
  - **Abudayyeh, D.**, Nicholson, A. Ngoduy, D. 2018. Traffic Signal Optimisation in Disrupted Networks Using a Semi-dynamic Assignment. Proceedings of the 40th Australasian Transport Research Forum (ATRF), Darwin, Australia. **(Parts of Chapter 5)**.
  - **Abudayyeh, D.**, Nicholson, A. Ngoduy, D. 2018. Traffic Signal Optimisation in Disrupted Networks Using a Semi-dynamic Assignment. Accepted for publication in the IEEE-ITSC 2019 conference, Auckland, New Zealand. **(Parts of Chapter 5 and 6)**.

- **Journal publications**
  - **Abudayyeh, D.**, Ngoduy, D. Nicholson, A. 2018. Traffic Signal Optimisation in Disrupted Networks with Re-routing. Transportation Research Procedia 34 (2018), 195-202. **(Parts of Chapter 1, 3, and 4)**.
  - **Abudayyeh D.**, Nicholson, A., Ngoduy, D. 2019. Traffic signal optimisation in disrupted road networks; a means of improving the resilience and sustainability. Prepared to be submitted to Transport Sustainability Journal. **(Parts of Chapter 5 and 6)**.
- **Awards**
  - University of Canterbury Publication Scholarship, 2019.
  - The ITE-ANZ travel grant, 2018, Austraffic Worldwide Learning Opportunity Award, to attend the ISTS conference in Japan.
  - The "Best Student Paper" Award, the 2018 IPENZ Transportation Group conference.
  - The 2018 IPENZ Transportation Group Tertiary Study Award.
  - The NZ Modelling User Group's Young Professional/Student Award to attend the 2017 NZMUGS conference.
- **Seminars related to thesis**
  - Christchurch City Council, Christchurch, New Zealand, (May, 2018).
  - Kyoto University, Kyoto, Japan (August, 2018).
  - Monash University, Melbourne, Australia (September, 2018).
- **Co-supervising the below final year graduation project at UC**
  - Tan O., Gaona C., " Optimising Signal Timings in Urban Traffic Networks", 2017

References

Akçelik, R. (1983), Progress in fuel consumption modelling for urban traffic management, Technical Report ARR Report 124, Australian Road Research Board.

Akcelik, R. (1991), 'Sidra 4.0 software status', *Traffic engineering & control* **32**(12), 585–589.

Akcelik, R. (1998), Traffic signals: Capacity and timing analysis, Technical Report ARR No. 123, Australian Road Research Board, Melbourne, Australia.

Akçelik, R. and Besley, M. (2007), Microsimulation and analytical models for traffic engineering, *in* 'Presentation at the ARRB-AUSTROADS Microsimulation Forum', California, USA.

Allsop, R. E. (1972), 'Estimating the traffic capacity of a signalized road junction', *Transportation Research* **6**(3), 245–255.

Asbjornslett, B. E. (1999), 'Assess the vulnerability of your production system', *Production Planning & Control* **10**(3), 219–229.

Astarita, V. (1996), A continuous time link model for dynamic network loading based on travel time function, *in* 'Proceedings of the 13th international symposium on transportation and traffic theory', Lyon, France.

Barceló, J., Codina, E., Casas, J., Ferrer, J. and García, D. (2005), 'Microscopic traffic simulation: A tool for the design, analysis and evaluation of intelligent transport systems', *Journal of Intelligent and Robotic Systems* **41**(2-3), 173–203.

Barceló, J., ed. (2010), *Fundamentals of traffic simulation*, Springer, New York, USA.

Beckmann, M., McGuire, C. B. and Winsten, C. B. (1956), *Studies in the Economics of Transportation*, Yale University Press, New Haven, USA.

Bektaş, T. and Laporte, G. (2011), 'The pollution-routing problem', *Transportation Research Part B: Methodological* **45**(8), 1232–1250.

Bell, M. G. and Iida, Y. (1997), *Transportation network analysis*, John Wiley Sons Ltd, Chichester, England.

Bell, M. G. and Iida, Y., eds (2003), *The network reliability of transport: proceedings of the 1st International Symposium on Transportation Network Reliability (INSTR)*, Emerald Group Publishing Limited, Bingley, United Kingdom.

Ben-Akiva, M. E., Gao, S., Wei, Z. and Wen, Y. (2012), 'A dynamic traffic assignment model for highly congested urban networks', *Transportation research part C: emerging technologies* **24**, 62–82.

Berdica, K. (2002*a*), 'An introduction to road vulnerability: what has been done, is done and should be done', *Transport policy* **9**(2), 117–127.

Berdica, K. (2002*b*), TraVIS for Roads-Examples of Road Transport Vulnerability Impact Studies, PhD thesis, Royal Institute of Technology, Stockholm, Sweden.

Berdica, K., Andjic, Z. and Nicholson, A. J. (2003), Simulating road traffic interruptions–does it matter what model we use?, *in* 'The Network Reliability of Transport: Proceedings of the 1st International Symposium on Transportation Network Reliability (INSTR)', Emerald Group Publishing Limited, pp. 353–368.

Bliemer, M. C., Raadsen, M. P., Brederode, L. J., Bell, M. G., Wismans, L. J. and Smith, M. J. (2017), 'Genetics of traffic assignment models for strategic transport planning', *Transport reviews* **37**(1), 56–78.

Bliemer, M. C., Raadsen, M. P., Smits, E.-S., Zhou, B. and Bell, M. G. (2014), 'Quasi-dynamic traffic assignment with residual point queues incorporating a first order node model', *Transportation Research Part B: Methodological* **68**, 363–384.

Bruneau, M., Chang, S. E., Eguchi, R. T., Lee, G. C., O'Rourke, T. D., Reinhorn, A. M., Shinozuka, M., Tierney, K., Wallace, W. A. and Von Winterfeldt, D. (2003), 'A framework to quantitatively assess and enhance the seismic resilience of communities', *Earthquake spectra* **19**(4), 733–752.

Burghout, W. and Wahlstedt, J. (2007), 'Hybrid traffic simulation with adaptive signal control', *Transportation Research Record* **1999**, 191–197.

Calvert, S. C. and Snelder, M. (2018), 'A methodology for road traffic resilience analysis and review of related concepts', *Transportmetrica A: transport science* **14**(1-2), 130–154.

Cantarella, G. E., Pavone, G. and Vitetta, A. (2006), 'Heuristics for urban road network design: lane layout and signal settings', *European Journal of Operational Research* **175**(3), 1682–1695.

Černỳ, V. (1985), 'Thermodynamical approach to the traveling salesman problem: An efficient simulation algorithm', *Journal of optimization theory and applications* **45**(1), 41–51.

Ceylan, H. and Bell, M. G. (2004), 'Traffic signal timing optimisation based on genetic algorithm approach, including drivers' routing', *Transportation Research Part B: Methodological* **38**(4), 329–342.

Chepuri, K. and Homem-de Mello, T. (2005), 'Solving the vehicle routing problem with stochastic demands using the cross-entropy method', *Annals of Operations Research* **134**(1), 153–181.

DBEIS (2018), 2017 uk greenhouse gas emissions, provisional figures, Technical report, Department for Business, Energy and Industrial Strategy, UK.

de Boer, P.-T., Kroese, D. P., Mannor, S. and Rubinstein, R. Y. (2005), 'A tutorial on the cross-entropy method', *Annals of operations research* **134**(1), 19–67.

de Dios Ortuzar, J. and Willumsen, L. G. (2011), *Modelling transport*, John Wiley & Sons, New Jersey, USA.

D'este, G., and Taylor, M. (2003), Network vulnerability: an approach to reliability analysis at the level of national strategic transport networks, *in* 'The Network Reliability of Transport: Proceedings of the 1st International Symposium on Transportation Network Reliability (INSTR)', Emerald Group Publishing Limited, pp. 23–44.

Elmqvist, T., Andersson, E., Frantzeskaki, N., McPhearson, T., Olsson, P., Gaffney, O., Takeuchi, K. and Folke, C. (2019), 'Sustainability and resilience for transformation in the urban century', *Nature Sustainability* **2**(4), 267.

EPA (2018), Inventory of u.s. greenhouse gas emissions and sinks:1990-2016, Technical report, Environmental Protection Agency, USA.

Everall, P. (1968), *The effects of road and traffic conditions on fuel consumption*, Road Research Laboratory.

Faturechi, R. and Miller-Hooks, E. (2014), 'Measuring the performance of transportation infrastructure systems in disasters: A comprehensive review', *Journal of infrastructure systems* **21**(1), 04014025:1–15.

Ferreira, L. (1982), 'Car fuel consumption in urban traffic. the results of a survey in leeds using instrumented vehicles.', *Institute of Transport Studies, University of Leeds* **Working Paper 162**.

Florian, M., Mahut, M. and Tremblay, N. (2001), A hybrid optimization-mesoscopic simulation dynamic traffic assignment model, *in* '2001 IEEE Intelligent Transportation Systems. Proceedings (Cat. No. 01TH8585). ITSC 2001.', IEEE, Oakland, USA, pp. 118–121.

Freeman, S., Taylor, M. A. and Holyoak (2008), Vulnerability analysis of road networks, *in* 'the Australasian Transport Research Forum', Auckland, New Zealand.

Fusco, G., Colombaroni, C. and Sardo, S. L. (2012), 'Modeling road traffic congestion by quasi-dynamic traffic assignment', *Advances in Mathematical and Computational Methods* pp. 219–224.

Ganin, A. A., Mersky, A. C., Jin, A. S., Kitsak, M., Keisler, J. M. and Linkov, I. (2019), 'Resilience in intelligent transportation systems (its)', *Transportation Research Part C: Emerging Technologies* **100**, 318–329.

Gill, D. and Zuccollo, J. (2012), Roles and limits of performance measures, Technical report, NZIER, New Zealand.

Glover, F. (1986), 'Future paths for integer programming and links to artificial intelligence', *Computers & operations research* **13**(5), 533–549.

Golberg, D. E. (1989), *Genetic algorithms in search, optimization, and machine learning*, Addison-Wesley Longman Publishing Co., Boston, USA.

Google (2019), 'attribution: Imagery@2019 the geoinformation group, google, getmapping plc, imagery ©2019 getmapping plc, infoterra ltd bluesky, landsat/ copernicus, maxar technologies, the geoinformation group, map data © 2019.', https://goo.gl/maps/tYNbAoLrUzf32iWY6.

Grubb, M., Vrolijk, C. and Brack, D. (1997), *The Kyoto Protocol: a guide and assessment*, Royal Institute of International Affairs-Chatham House, London, UK.

Hadi, M. A. and Wallace, C. E. (1992), *Progression-based optimization model in TRANSYT-7F*, number 1360.

Hadi, M. A. and Wallace, C. E. (1994), 'Optimization of signal phasing and timing using cauchy simulated annealing', *Transportation Research Record* (1456).

Hadi, M., Sinha, P. and Wang, A. (2007), 'Modeling reductions in freeway capacity due to incidents in microscopic simulation models', *Transportation Research Record* **1999**(1), 62–68.

Hall, M. and Willumsen, L. (1980), 'Saturn-a simulation-assignment model for the evaluation of traffic management schemes', *Traffic Engineering & Control* **21**(4).

Herman, R. and Lam, T. (1974), 'Trip time characteristics of journeys to and from work', *Transportation and traffic theory* **6**, 57–86.

Hickman, J., Hassel, D., Joumard, R., Samaras, Z. and Sorenson, S. (1999), Methodology for calculating transport emissions and energy consumption, Technical Report SE/491/98, European Commission / DG VII.

Holland, J. H. (1992), *Adaptation in natural and artificial systems: an introductory analysis with applications to biology, control, and artificial intelligence*, MIT press, Massachusetts, USA.

Homem-de Mello, T. and Rubinstein, R. Y. (2002), Rare event estimation for static models via cross-entropy and importance sampling.

Janson, B. N. (1991), 'Dynamic traffic assignment for urban road networks', *Transportation Research Part B: Methodological* **25**(2-3), 143–161.

Jayakrishnan, R. and Mahmassani, H. S. (1991), Dynamic modelling framework of real-time guidance systems in general urban traffic networks, *in* 'Proceedings of the 2nd International Conference on Applications of Advanced Technologies in Transportation Engineering', ASCE, Minneapolis, USA.

Jeannotte, K., Chandra, A., Alexiadis, V. and Skabardonis, A. (2004), Traffic analysis toolbox volume ii: Decision support methodology for selecting traffic analysis tools, Technical Report FHWA-HRT-04-039, Federal Highway Administration, USA.

Jenelius, E., Petersen, T. and Mattsson, L.-G. (2006), 'Importance and exposure in road network vulnerability analysis', *Transportation Research Part A: Policy and Practice* **40**(7), 537–560.

Kaviani, A., Thompson, R. G. and Rajabifard, A. (2017), 'Improving regional road network resilience by optimised traffic guidance', *Transportmetrica A: Transport Science* **13**(9), 794–828.

Kheifits, L. and Gur, Y. J. (1997), 'Traffic assignment which considers queue formation', *IFAC Proceedings Volumes* **30**(8), 1253–1258.

Kirkpatrick, S., Gelatt, C. D. and Vecchi, M. P. (1983), 'Optimization by simulated annealing', *science* **220**(4598), 671–680.

Kontorinaki, M., Spiliopoulou, A., Papamichail, I., Papageorgiou, M., Tyrinopoulos, Y. and Chrysoulakis, J. (2015), 'Overview of nonlinear programming methods suitable for calibration of traffic flow models', *Operational Research* **15**(3), 327–336.

Koorey, G., McMillan, S. and Nicholson, A. (2014), The effectiveness of incident management on network reliability: Stage 2, Technical Report LTR-118, NZ Transport Agency research report, Wellington, NZ.

Koorey, G., McMillan, S. and Nicholson, A. (2015), 'Incident management and network performance', *Transportation research procedia* **6**, 3–16.

Laguna, M., Duarte, A. and Martí, R. (2009), 'Hybridizing the cross-entropy method: An application to the max-cut problem', *Computers & Operations Research* **36**(2), 487–498.

Liao, T.-Y., Hu, T.-Y. and Ko, Y.-N. (2018), 'A resilience optimization model for transportation networks under disasters', *Natural hazards* **93**(1), 469–489.

Little, J. D. (1966), 'The synchronization of traffic signals by mixed-integer linear programming', *Operations Research* **14**(4), 568–594.

Lu, L., Xu, Y., Antoniou, C. and Ben-Akiva, M. (2015), 'An enhanced spsa algorithm for the calibration of dynamic traffic assignment models', *Transportation Research Part C: Emerging Technologies* **51**, 149–166.

Maher, M. (2008), 'The optimization of signal settings on a signalized roundabout using the cross-entropy method', *Computer-Aided Civil and Infrastructure Engineering* **23**(2), 76–85.

Maher, M., Liu, R. and Ngoduy, D. (2013), 'Signal optimisation using the cross entropy method', *Transportation Research Part C: Emerging Technologies* **27**, 76–88.

Mattsson, L.-G. and Jenelius, E. (2015), 'Vulnerability and resilience of transport systems–a discussion of recent research', *Transportation Research Part A: Policy and Practice* **81**, 16–34.

Matzoros, A. and van Vliet, D. (1992), 'A model of air pollution from road traffic, based on the characteristics of interrupted flow and junction control: Part i—model description', *Transportation Research Part A: Policy and Practice* **26**(4), 315–330.

MBIE (2017), New zealand energy sector greenhouse gas emissions, Technical report, Ministry of Business, Innovation and Employment, New Zealand.

Nanduri, K. (2013), Mitigating emissions and energy consumption for urban transportation networks: simulation-based signal control strategies, Master's thesis, Massachusetts Institute of Technology, USA.

Ngoduy, D. and Maher, M. (2011), Cross entropy method for a deterministic optimal signalization in an urban network, *in* 'Proceedings of the Transportation Research Board 90th Annual Meeting', Washington, DC, USA.

Ngoduy, D. and Maher, M. (2012), 'Calibration of second order traffic models using continuous cross entropy method', *Transportation Research Part C: Emerging Technologies* **24**, 102–121.

Nicholson, A. and Dalziell, E. (2003), *Risk evaluation and management: a road network reliability study*, pp. 45–60.

Nicholson, A. and Du, Z. (1994), Improving transportation system reliability: a framework, *in* 'Proceedings of the 17TH ARRB Conference', Queensland, Australia.

Papageorgiou, M. (1990), 'Dynamic modeling, assignment, and route guidance in traffic networks', *Transportation Research Part B: Methodological* **24**(6), 471–495.

Pearce, V. (2000), Incident management successful practices: a cross-cutting study: improving mobility and saving lives, Technical Report FHWA-JPO-99-018;FTA-TRI-11-99-09, Federal Highway Administration and Federal Transit Administration, USA. Joint Program Office for Intelligent Transportation Systems.

Ran, B., Hall, R. W. and Boyce, D. E. (1996), 'A link-based variational inequality model for dynamic departure time/route choice', *Transportation Research Part B: Methodological* **30**(1), 31–46.

Rashidy, E. and Hassan, R. A. (2014), The resilience of road transport networks redundancy, vulnerability and mobility characteristics, PhD thesis, University of Leeds.

Richardson, A. and Taylor, M. (1978), 'Travel time variability on commuter journeys', *High Speed Ground Transportation Journal* **12**(1), 77–99.

Rubinstein, R. Y. (1997), 'Optimization of computer simulation models with rare events', *European Journal of Operational Research* **99**(1), 89–112.

Rubinstein, R. Y. and Kroese, D. P. (2004), *The cross-entropy method: a unified approach to combinatorial optimization, Monte-Carlo simulation and machine learning*, Springer Science & Business Media, Berlin, Germany.

Sands, P. (1992), 'The united nations framework convention on climate change', *Review of European Community & International Environmental Law* **1**(3), 270–277.

Schmöcker, J.-D., Bell, M. G. and Kurauchi, F. (2008), 'A quasi-dynamic capacity constrained frequency-based transit assignment model', *Transportation Research Part B: Methodological* **42**(10), 925–945.

Schrank, D., Lomax, T. and Turner, S. (2009), Urban mobility report texas transportation institute, Technical report, Texas Transportation Institute, Texas, USA.

Sharda, R., Vob, S., Woodruff, D. and Fink, A. (2003), 'Optimization software class libraries'.

Sharma, S. and Mathew, T. V. (2011), 'Multiobjective network design for emission and travel-time trade-off for a sustainable large urban transportation network', *Environment and Planning B: Planning and Design* **38**(3), 520–538.

Sheffi, Y. (2005), *The resilient enterprise: overcoming vulnerability for competitive advantage*, The MIT Press books, Massachusetts, USA.

Sheffi, Y. and Powell, W. (1981), 'A comparison of stochastic and deterministic traffic assignment over congested networks', *Transportation Research Part B: Methodological* **15**(1), 53–64.

Snelder, M. and Calvert, S. (2016), 'Quantifying the impact of adverse weather conditions on road network performance', *European Journal of Transport and Infrastructure Research* **16**(1), 128–149.

Snelder, M., Van Zuylen, H. and Immers, L. (2012), 'A framework for robustness analysis of road networks for short term variations in supply', *Transportation Research Part A: Policy and Practice* **46**(5), 828–842.

Sugawara, S. and Niemeier, D. (2002), 'How much can vehicle emissions be reduced?: Exploratory analysis of an upper boundary using an emissions-optimized trip assignment', *Transportation Research Record* **1815**(1), 29–37.

Swidan, H. et al. (2011), Integrating aimsun micro simulation model with portable emissions measurement system (pems): Calibration and validation case study., Master's thesis, North Carolina State University, North Carolina, USA.

Taale, H. and Pel, A. (2015), 'Better convergence for dynamic traffic assignment methods', *Transportation Research Procedia* **10**, 197–206.

Tajtehranifard, H. (2017), Incident duration modelling and system optimal traffic rerouting, PhD thesis, Queensland University of Technology.

Tan, O. and Gaona, C. (2017), 'Optimising signal timings in urban traffic networks', *Final year undergraduate project, University of Canterbury* .

Taylor, M. (2017), *Vulnerability analysis for transportation networks*, Elsevier, Amsterdam, Netherlands.

Teklu, F., Sumalee, A. and Watling, D. (2007), 'A genetic algorithm approach for optimizing traffic control signals considering routing', *Computer-Aided Civil and Infrastructure Engineering* **22**(1), 31–43.

Turner, J. and Wardrop, J. (1951), The variation of journey time in central london, Technical Report Note. RN/1511/JKT. JGW, Road Research Laboratory, UK.

van Vliet, D. (1982), 'Saturn-a modern assignment model', *Traffic Engineering & Control* **23**(12), 578–581.

van Vliet, D. (2004), *SATURN manual*, UK.

van Vliet, D. (2018), *SATURN manual*, 11.4 edn, UK.

Wakabayashi, H. and Iida, Y. (1992), 'Upper and lower bounds of terminal reliability of road networks: an efficient method with boolean algebra', *Journal of Natural Disaster Science* **14**(1), 29–44.

Wardrop, J. G. (1952), 'Road paper. some theoretical aspects of road traffic research.', *Proceedings of the institution of civil engineers* **1**(3), 325–362.

Webster, F. V. (1958), Traffic signal settings, Technical Report No 39, Road Research Lab Tech Papers, UK.

Wilmshurst, B., W. I. K. P. (2015), Demonstrating the benefit of network operations activities, Technical Report No. 594, NZ Transport Agency, New Zealand.

Zhang, H., Cai, H., Oh, J.-S. and Yang, C. D. (2010), Development of a microscopic traffic simulation model using transims: A case study in the southeast michigan area, *in* 'The 10th International Conference of Chinese Transportation Professionals (ICCTP): Integrated Transportation Systems: Green, Intelligent, Reliable', Beijing, China, pp. 3552–3563.

Zhilinskas, A., Dzemyda, G. and Šaltenis, V. (2002), *Stochastic and Global Optimization*, Kluwer Academic.

Zhong, R., Fu, K., Sumalee, A., Ngoduy, D. and Lam, W. (2016), 'A cross-entropy method and probabilistic sensitivity analysis framework for calibrating microscopic traffic models', *Transportation Research Part C: Emerging Technologies* **63**, 147–169.

Zhou, Y., Wang, J. and Yang, H. (2019), 'Resilience of transportation systems: Concepts and comprehensive review', *IEEE Transactions on Intelligent Transportation Systems* pp. 1–15.